

Tectonophysics

Elsevier Editorial System(tm) for

Manuscript Draft

Manuscript Number: TECTO10726R1

Title: The role of continental margins in the final stages of arc formation: Constraints from teleseismic tomography of the Gibraltar and Calabrian Arc (Western Mediterranean)

Article Type: Research Paper

Keywords: teleseismic tomography; upper mantle; Gibraltar Arc; Calabrian Arc; subduction zone

Corresponding Author: Dr. Giovanni Battista Cimini,

Corresponding Author's Institution: Istituto Nazionale di Geofisica e Vulcanologia

First Author: Andrea Argnani

Order of Authors: Andrea Argnani; Giovanni Battista Cimini; francesco frugoni; Stephen Monna; Caterina Montuori

Abstract: The deep seismicity and lateral distribution of seismic velocity in the Central Western Mediterranean, point to the existence under the Alboran and Tyrrhenian Seas of two lithospheric slabs reaching the mantle transition zone. Gibraltar and Calabrian narrow arcs correspond to the slabs. Similarities in the tectonic and mantle structure of the two areas have been explained by a common subduction and roll-back mechanism, in which the two arcs are symmetrical end members. We present a new 3-D tomographic model at mantle scale for the Calabrian Arc and compare it with a recently published model for the Gibraltar Arc by Monna et al. (2013a). The two models, calculated with inversion of teleseismic phase arrivals, have a scale and parametrization that allow for a direct comparison. The inclusion in both inversions of ocean bottom seismometer broadband data improves the resolution of the areas underlying the seafloor networks. This additional information is used to resolve the deep structure and constrain the reconstruction of the Central Western Mediterranean geodynamic evolution. The Gibraltar tomography model suggests that the slab is separated from the Atlantic oceanic domain by a portion of African continental margin, whereas the Calabrian model displays a continuous oceanic slab that is connected, via a narrow passage (~350 km), to the Ionian basin oceanic domain. Starting from the comparison of the two models we propose the following interpretation: within the Mediterranean geodynamic regime (dominated by slab rollback) the geometry of the African continental margin, located on the lower plate, represents a critical control on the evolution of subduction. As buoyant continental lithosphere entered the subduction zones, slab pull caused tears in the subducted lithosphere. This tectonic response in the final stages of arc evolution, strongly controlled by the paleogeography of the subducted plates, explains the observed differences between the Gibraltar and Calabrian Arcs.

Suggested Reviewers: Gideon Rosenbaum

g.rosenbaum@aug.edu.au
Expert of Mediterranean geodynamics

Antonio Villaseñor
antonio@ija.csic.es
Expert of Mediterranean region. Expert in seismic tomography.

Rome, 21 March 2016

Paper: TECTO10726

Title: "The role of continental margins in the final stages of arc formation: Constraints from teleseismic tomography of the Gibraltar and Calabrian Arc (Western Mediterranean)"

Authors: A. Argnani, G.B. Cimini, F. Frugoni, S. Monna, C. Montuori

Dear Editor,

We are pleased to resubmit our revised paper to Tectonophysics. We have followed the reviewer's suggestions and modified the paper accordingly. We have also submitted our point-to-point answer (in italics) to the reviewer's comments (in bold). We thank the reviewer for the useful comments.

The submitting author certifies that all co-authors know of and concur with the submission of the manuscript.

Thank you very much for your attention.

Sincerely,

Andrea Argnani

The deep seismicity and lateral distribution of seismic velocity in the Central Western Mediterranean, point to the existence under the Alboran and Tyrrhenian Seas of two lithospheric slabs reaching the mantle transition zone. Gibraltar and Calabrian narrow arcs correspond to the slabs. Similarities in the tectonic and mantle structure of the two areas have been explained by a common subduction and roll-back mechanism, in which the two arcs are symmetrical end members. We present a new 3-D tomographic model at mantle scale for the Calabrian Arc and compare it with a recently published model for the Gibraltar Arc by Monna et al. (2013a). The two models, calculated with inversion of teleseismic phase arrivals, have a scale and parametrization that allow for a direct comparison. The inclusion in both inversions of ocean bottom seismometer broadband data improves the resolution of the areas underlying the seafloor networks. This additional information is used to resolve the deep structure and constrain the reconstruction of the Central Western Mediterranean geodynamic evolution. The Gibraltar tomography model suggests that the slab is separated from the Atlantic oceanic domain by a portion of African continental margin, whereas the Calabrian model displays a continuous oceanic slab that is connected, via a narrow passage (~350 km), to the Ionian basin oceanic domain. Starting from the comparison of the two models we propose the following interpretation: within the Mediterranean geodynamic regime (dominated by slab rollback) the geometry of the African continental margin, located on the lower plate, represents a critical control on the evolution of subduction. As buoyant continental lithosphere entered the subduction zones, slab pull caused tears in the subducted lithosphere. This tectonic response in the final stages of arc evolution, strongly controlled by the paleogeography of the subducted plates, explains the observed differences between the Gibraltar and Calabrian Arcs.

Paper: TECTO10726

Title: "The role of continental margins in the final stages of arc formation: Constraints from teleseismic tomography of the Gibraltar and Calabrian Arc (Western Mediterranean)"

Authors: A. Argnani, G.B. Cimini, F. Frugoni, S. Monna, C. Montuori

Please note that the **reviewer's comments** are in bold while *our answer* are in italics. The parts of the text that are highlighted in yellow have been added in response to the Reviewers' requirements. We re sending a text with tracked changes (Argnani_et_al_Revisions) and a version without visible changes (Argnani_et_al_clean).

We thank the reviewers for the useful comments.

Reviewer #1: The is an interesting paper that compares the seismic velocity structure of the upper mantle beneath the Gibraltar and the Calabrian arcs and interprets them tectonically.

The paper makes use of tomography models from both regions that incorporate data from ocean bottom seismographs, giving the models better offshore resolution than previous models. The Gibraltar arc model has been published elsewhere recently, whereas the Calabrian arc model has not been previously published as far as I can tell. Given the large amount of recent work on the Gibraltar arc region and the western Mediterranean generally the paper is timely, and the addition of Atlantic OBS data is important and unique.

I was a bit disappointed that the authors did not include at least part of the large volume of land data for this region that is now available in their inversions, but that may have been beyond the scope of the project. The author's have done a reasonably good job of citing the relevant literature.

We agree with the reviewer. For the Gibraltar arc 3D model we used the data that was available to us at the time. We hope to improve our model by adding the new permanent network data and, if available, data from recent large experiments in the area, such as IberArray and PICASSO.

The paper's chief shortcoming is that it tends to be somewhat redundant, and the English needs to be reviewed by a native speaker. In a number of places it is difficult to understand the authors' meaning. It is for this reason that I recommend moderate revision. The author's should look to tightening the manuscript by removing redundancies and clarifying the English. I ended up with so many grammatical corrections and revised phrasing that it is not feasible to list them here, after a short while I quit attempting to keep track of suggested revisions Part of the paper's structural problem is that the authors are repeatedly skipping back and forth between the two arcs, which gets a bit tedious, and also results in some of the redundancy.

Yes, we agree. We have made several changes to make the paper more readable.

Various parts of the paper have been restructured (to see which parts please see version with annotated changes)

In particular:

1) We have deleted redundant parts

2) Section 2 has been shortend, leaving only the parts that are more relevant to our work.

2) We have included section 3.1 and 3.2 in sections 2.1 and 2.2, respectively, to (hopefully) make the paper more readable.

3) Some akward and possibly obscure phrases have been corrected/clarified.

Please be aware that with the changes old Section 4 is now Section 3 and so on.

Specific comments: Section 3: introduction: I would call the smallest scale tomography models regional rather than local, as they are still examining multiple tectonic domains. Local, as in local earthquake normally means on the scale of 100km.

We agree and have applied the reviewer's suggestion.

Line 418: The authors say that the intermediate-depth earthquakes provide information on the subjected slab beneath the Alboran basin, but then make only a vague statement about exactly what information it is they provide. I find this section to be a little vague. I think that the authors could make much more of the seismicity in both arcs, actually.

We have added more information in Sections 2.1 and 2.2 on the seismicity, in particular on the focal mechanisms and stress regime in the two slabs, and a new citation (Bufo et al., 2011).

All of the labels on my versions of figures 6 and 7 are unclear. As the authors base their interpretations on these two figures and several cross sections, they should make the labels larger and clearer.

We have enlarged the labels so that they are visible also in the pdf version

I don't quite understand their interpretation of the Gulf of Cadiz low velocity anomaly (GC-LVA) as thinned continental lithosphere. If the lithosphere was thinned by extension during the opening of the Atlantic then it should have re-equilibrated to a normal TBL lithosphere of ~100km thickness by now, similar to Atlantic oceanic lithosphere. If it thinned more recently due to the local GA tectonics, then I missed the explanation somehow. Please explain this.

The thinning of the continental lithosphere is related to the Mesozoic oceanic opening. We agree that the lithosphere has likely re-equilibrated to ca. 100 km thickness, but the crustal part of it remains thin and has a slower Vp with respect to the adjacent oceanic lithosphere. The lithospheric velocity structure just offshore Gibraltar appears different from that of the adjacent oceanic lithosphere in the Gulf of Cadiz, and, most important, it interrupts the continuity between the slab subducted underneath Alboran and the Atlantic oceanic lithosphere.

I think the authors should discuss their figures 11 and 12 in comparison to the results of van Hinsbergen et al 2013 G3, which in my opinion is the clearest exposition on development of the Gibraltar Arc.

The focus of our paper was not to present a long-term evolution of the Gibraltar and Clabrian arcs, but rather to show how the nature of the crust and lithosphere in the subducting plate affected the finale stage of arc formation. To illustrate this aspect we used a couple of snapshots at Tortonian and present-day (figures 11 and 12). Nevertheless, we did mention that our results are more compatible with the model presented by Rosenbaum et al., 2002, Chertova et al. 2014, and now we have also taken into consideration van Hinsbergen et al 2014.

The author's have overlooked a paper by Thurner et al, 2014, G3, which to my eye most clearly shows the Alboran slab delamination under the Betics and Rif. I'm sure this was just an oversight, as the literature on the GA and CA is extensive.

Our paper suffered from a long gestation, during which several papers on the Alboran-Gibraltar region were published; it happened that we missed some references. However, the paper of Thurner et al, that we now acknowledge, is in line with many studies published more or less at the same time and resulting from the massive work carried out within the PICASSO and IberArray projects; we tried to take advantage of these recent results in our interpretation.

Reviewer #2: This paper contrasts the seismic structure of two present-day subducted slabs that bracket the western-central Mediterranean and that are widely thought to have originated from what was initially a single slab. These are the Alboran and the Calabrian slabs. The analysis is centered on recent tomography models carried out using the same technique which facilitates the comparison. The main point that comes across is that the Alboran and Calabrian slabs are different in that further Alboran subduction was impeded by the entrance into the trench of African continental margin lithosphere.

The paper is generally well written and illustrated although in my opinion it could be shortened without loss of clarity. More importantly, I think some of the literature is not referenced appropriately (see below).

There is, in my view, an issue that is very relevant to the central point of this paper that the authors do not

address: the role of the continental lithosphere of the Alboran domain. In some models [Faccenna et al., 2004; Bezada et al., 2013] the Alboran loses its lithospheric mantle by delamination as part of the Alboran slab. That is, the slab includes the Alboran mantle. These hybrid rollback/delamination models are not discussed in the introduction. More importantly, in this scenario the entrance into the trench of continental lithosphere did not stop subduction from proceeding, but rather resulted in delamination of the continental lithosphere and transfer of the crust to the overriding plate. If this was the case, then it would be interesting to sort out why the entrance of the Alboran into the trench was not able to stop rollback, but the arrival of the African continental margin was. Of course, the authors could argue that those models are wrong, and that this kind of delamination doesn't happen, but I think the possibility should be discussed. In any case, delamination of continental mantle lithosphere when a continental block enters the trench has been shown to be possible by numerical [e.g. Faccenna et al., 2009] and analog [e.g. Bialas et al., 2011] modeling. It is my opinion that the authors should engage with this issue in one way or another.

Perhaps the Reviewer is adopting a concept of Alboran as a continental microplate, which we believe is not likely (see for instance the reconstructions of Platt et al and van Hinsbergen et al where the Alboran domain is seen as an accretionary complex, floating above a retreating oceanic subduction zone. Delamination has affected the Iberian and African continental margin when the continental crust entered subduction, that is, in the final stage of arc formation.

Also with regards to this central point, a crucial aspect is the non-continuity of the subducted Alboran lithosphere with the Atlantic. A number of papers have been published suggesting that such a continuity does exist and exploring the implications. I don't think the authors currently engage sufficiently with those arguments [e.g. Gutscher et al., 2002; Duarte et al., 2013]. Note that even though these papers are cited, the arguments are not really addressed. At least this should be addressed in the introduction to provide necessary context.

The continuity of the slab inferred in published papers [e.g. Gutscher et al., 2002; Duarte et al., 2013] is not supported by evidence as there is a gap in geophysical data in the critical region between the Gulf of Cadiz and Gibraltar; this is the region from which we obtain good tomographic images thanks to the offshore OBS stations.

These guys seem to be in direct contraposition to Gutscher and those guys who talk of ongoing subduction of Atlantic beneath Gibraltar. They better address those papers.

We have extensively cited the papers by Gutscher and co-authors and we have clearly pointed out that our view is different.

Regarding the referencing of previous work, I noticed that some papers that present seismic tomography models as well as tectonic evolution [Spakman and Wortel, 2004; Bezada et al., 2013] models were only considered insofar as the tomography model is concerned, but the ideas about tectonic evolution that are presented were not included in the discussion. Also, citing Levander et al. [2014] Along with Platt and Vissers and Calvert et al. is not appropriate. The Levander et al. paper discusses a fundamentally different model for the tectonic evolution of the region. Finally, there are a couple of tomography models of the Gibraltar area that came out after the Bezada et al. model and should probably be referenced: [Bonnin et al., 2014; Villaseñor et al., 2015]

We mention that Wortel and Spakman proposed subduction rollback followed, in the final stage, by lithospheric tearing. In general we mentioned models that propose different solutions with respect to the removal of thickened continental crust/lithosphere in the Alboran region, and we acknowledged the point of Levander et al. on the role of these processes on recycling of continental material into the mantle. We also now consider the papers by Bonnin et al. (2014) and Villaseñor et al., 2015.

Other comments:

The variance reduction for the Calabrian Arc is fair, but for the Gibraltar Arc is poor. The authors should comment on why that may be.

While the method and parameterization for both arcs is the same, the ray density is not. The authors should comment on how this may affect the imaging in each case and the comparison of the two arcs.

These two questions are linked. The GA dataset contains a large percentage of bulletin arrival times, while the larger CA dataset has a small percentage of bulletin data. The difference in data quality is already evident in the starting RMS values of the two datasets, for CA 0.6 s^{-1} on 8600 arrival times, against 0.7 s^{-1} for GA on 6238 arrival times. The errors in the bulletin arrival times limit the amount of RMS reduction. The differences in resolution between the two datasets is proved by the checkerboard resolution test. This test shows that the synthetic anomalies are better reconstructed by the CA dataset than with the GA dataset. In fact, the CA model could be parametrized with a smaller grid ($\sim 80 \text{ km}$), but we have chosen the same parametrization as for GA (100 km) to better compare them. In any case, in both cases the parts that we interpret are in volumes of the models that are reliably reconstructed in the synthetic tests. We have added more information on this aspect in the text.

L135 states that the GA model resolves previously undetected features, but does not specify which features these are. Models that came shortly after this one [Bezada et al., 2013; Bonnin et al., 2014; Villaseñor et al., 2015] have the advantage of much greater station coverage in Spain in Morocco.

We have clarified this part in the text. The features that are better resolved in our model (with respect to other models) are the ones resolved by the OBS data, particularly the lithosphere-upper mantle structure of the Gibraltar Strait-Atlantic sector.

L154: in the Algerian sector,

We have implemented the suggestion.

L163: It would probably be appropriate to cite Spakman and Wortel 2004 here as well.

We agree, the reference was added.

L182: At least in American English, "sketchy" has a negative connotation. I understand the authors mean "oversimplified" or something like that.

Yes, we have changed "sketchy" into "oversimplified".

L195: The authors should consider justifying their judgement that the evidence is "rather poor".

The occurrence of a so called Alkapeca microcontinent is used in some palaeogeographic reconstructions, where a continental domain much wider than the Corsica-Sardina microcontinent is represented. This continental domain would be located in the upper plate with respect to the African and Betic subductions and it is difficult to envisage how it can be completely destroyed during the opening of the Western Mediterranean backarc basins. So far, the evidence for the occurrence of thinned continental crust (not belonging to the Iberia and African margins) is lacking within the Western Mediterranean basins. In any case, we have deleted this part of Section 2 trying to comply to the Reviewers' suggestion to shorten the paper.

I think section two in general could be shortened without leaving out anything that is crucially relevant to this paper.

We agree. We have tried to apply this suggestion.

L351: What did you use to correct for the crustal structure.

This aspect is later described in Sections 4.1 and 4.2 (now 3.1 and 3.2), we have inserted this reference at this point.

L440: "mentioned at the beginning of this section" is confusing. The variance reduction is actually mentioned in the following paragraph.

We agree and we have deleted this misleading information.

L444-446: the regularization weights are generally relative to the number of observations. More observations require higher regularization to obtain the same amount of damping/smoothing because the relative weight of the data in the objective function is larger. Without some knowledge of the specifics of the implementation of regularization these numbers have very little meaning to the reader.

We have deleted this confusing sentence in L444-446 and added a reference (in the beginning of Section 4, now Section 3) to the governing equation where the damping and smoothing parameters are defined. The regularization is due to the ill-posed mathematical inversion problem. In the case of seismic tomography the amount of regularization is strongly dependent on the event-station geometry and the chosen Earth parametrization.

L499: An important point is whether these low velocities could actually be produced by unaccounted-for low velocities in the crust; for example, a very thick sedimentary package.

The crustal correction used for the Gulf of Cadiz includes a 6 km thick low-velocity (3.5 km/s) sedimentary layer (see Table 1 in Monna et al., 2013a). In spite of this strong correction we still observe the strong low-velocity anomaly GC-LVA. We have added this information in the text.

L520-523: There is some intermediate-depth seismicity occurring in the slab, that much is clear. I think a more accurate statment is that seismicity is not restricted to the Slab or not even concentrated in the slab. Locally it does closely follow the slab.

We agree, this sentence can be confusing. We have rephrased this concept and linked the distribution of the overall seismicity to the diffuse plate margin. We are referring to crustal seismicity; this point has been rephrased.

Regarding Fig. 12: Why is the Tortonian particularly important? Is this figure really necessary?

Perhaps the reviewer is referring to Figure 11 (referring Tortonian time) ? Tortonian time is particularly important because at this time the GA subduction is finished while the CA subduction is just on its way. The reconstruction of Figure 11 complements the present-day setting illustrated in Figure 12, as we are comparing the two time slices, Tortonian and Present, that represent the completion of arc formation in Gibraltar and Calabria, respectively.

In the figure captions (at least in Fig 8) if not defining the HVA, LVA on the figure, plaase say "look in the text for the definition of the HVA, LVA" or something to that effect.

We agree. Now we have added an explanation of all acronyms in the figure captions captions.

References cited:

We have added most of the missing references suggested by the Reviewer.

Bezada, M. J., E. D. Humphreys, D. R. Toomey, M. Harnafi, J. M. Dávila, and J. Gallart (2013), Evidence for slab rollback in westernmost Mediterranean from improved upper mantle imaging, *Earth Planet. Sci. Lett.*, 368, 51-60, doi:10.1016/j.epsl.2013.02.024.

Bialas, R. W., F. Funiciello, and C. Faccenna (2011), Subduction and exhumation of continental crust: insights from laboratory models, *Geophys. J. Int.*, 184(1), 43-64.

Bonnin, M., G. Nolet, A. Villaseñor, J. Gallart, and C. Thomas (2014), Multiple-frequency tomography of the upper mantle beneath the African/Iberian collision zone, *Geophys. J. Int.*, 198(3), 1458-1473, doi:10.1093/gji/ggu214.

Duarte, J. C., F. M. Rosas, P. Terrinha, W. P. Schellart, D. Boutelier, M.-A. Gutscher, and A. Ribeiro (2013), Are subduction zones invading the Atlantic? Evidence from the southwest Iberia margin, *Geology*, 41(8), 839-842, doi:10.1130/G34100.1.

Faccenna, M., G. Minelli, and T. V. Gerya (2009), Coupled and decoupled regimes of continental collision: Numerical modeling, *Earth Planet. Sci. Lett.*, 278(3-4), 337-349, doi:10.1016/j.epsl.2008.12.021.

Faccenna, C., C. Piromallo, A. Crespo-Blanc, L. Jolivet, and F. Rossetti (2004), Lateral slab deformation and the origin of the western Mediterranean arcs, *Tectonics*, 23(1), TC1012, doi:10.1029/2002TC001488.

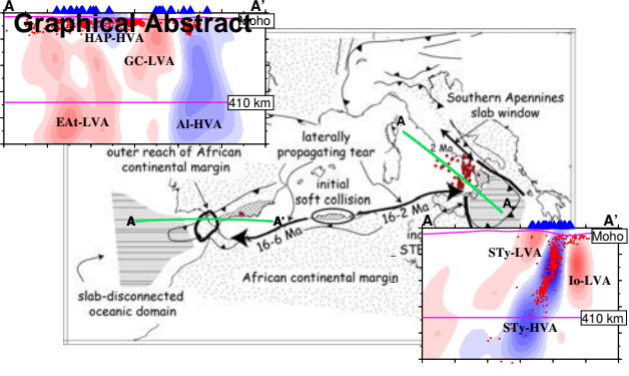
Gutscher, M. A., J. Malod, J. P. Rehault, I. Contrucci, F. Klingelhoefer, L. Mendes-Victor, and W. Spakman (2002), Evidence for active subduction beneath Gibraltar, *Geology*, 30(12), 1071-1074, doi:10.1130/0091-7613(2002)030<1071:EFASBG>2.0.CO;2.

Levander, A. et al. (2014), Subduction-driven recycling of continental margin lithosphere, *Nature*, 515(7526), 253-256, doi:10.1038/nature13878.

Spakman, W., and R. Wortel (2004), A tomographic view on Western Mediterranean geodynamics, *TRANSMED Atlas Mediterr. Reg. Crust Mantle*, 31-52.

Villaseñor, A., S. Chevrot, M. Harnafi, J. Gallart, A. Pazos, I. Serrano, D. Córdoba, J. A. Pulgar, and P. Ibarra (2015), Subduction and volcanism in the Iberia-North Africa collision zone from tomographic images of the upper mantle, *Tectonophysics*, 663, 238-249, doi:10.1016/j.tecto.2015.08.042.

Graphical Abstract



Highlights

- OBS data improve the resolution of mantle tomography in the Mediterranean region
- Comparison of lithosphere-asthenosphere structure under Calabrian and Gibraltar arcs
- Geometry of continental margin can influence subduction and tectonic arc evolution

1 Title

2 **The role of continental margins in the final stages of arc formation: Constraints from**
3 **teleseismic tomography of the Gibraltar and Calabrian Arc (Western Mediterranean)**

4

5 **Authors**

6 Andrea Argnani ^a

7 a Istituto di Scienze Marine – Consiglio Nazionale delle Ricerche

8 Via Gobetti, 101

9 Bologna, 40129, Italy

10 andrea.argnani@bo.ismar.cnr.it

11 Telephone +39 051 6398886

12

13 Giovanni Battista Cimini ^b

14 b Istituto Nazionale di Geofisica e Vulcanologia

15 Via di Vigna Murata, 605

16 Rome, 00143, Italy

17 giovannibattista.cimini@ingv.it

18 Telephone: +39-06-51860-407

19

20 Francesco Frugoni ^b

21 b Istituto Nazionale di Geofisica e Vulcanologia

22 Via di Vigna Murata, 605

23 Rome, 00143, Italy

24 francesco.frugoni@ingv.it

25 Telephone: +39-06-51860-547

26

27 Stephen Monna ^b

28 b Istituto Nazionale di Geofisica e Vulcanologia

29 Via di Vigna Murata, 605

30 Rome, 00143, Italy

31 stephen.monna@ingv.it

32 Telephone: +39-06-51860-404

33

34 Caterina Montuori ^b

35 b Istituto Nazionale di Geofisica e Vulcanologia

36 Via di Vigna Murata, 605
37 Rome, 00143, Italy
38 caterina.montuori@ingv.it
39 Telephone: +39-06-51860-496

40

41

42 Corresponding author

43 Giovanni Battista Cimini

44 giovannibattista.cimini@ingv.it

45

46

47 **Abstract**

48 The deep seismicity and lateral distribution of seismic velocity in the Central Western
49 Mediterranean, point to the existence under the Alboran and Tyrrhenian Seas of two lithospheric
50 slabs reaching the mantle transition zone. Gibraltar and Calabrian narrow arcs correspond to the
51 slabs. Similarities in the tectonic and mantle structure of the two areas have been explained by a
52 common subduction and roll-back mechanism, in which the two arcs are symmetrical end members.
53 We present a new 3-D tomographic model at mantle scale for the Calabrian Arc and compare it
54 with a recently published model for the Gibraltar Arc by Monna et al. (2013a). The two models,
55 calculated with inversion of teleseismic phase arrivals, have a scale and parametrization that allow
56 for a direct comparison. The inclusion in both inversions of ocean bottom seismometer broadband
57 data improves the resolution of the areas underlying the seafloor networks. This additional
58 information is used to resolve the deep structure and constrain the reconstruction of the Central
59 Western Mediterranean geodynamic evolution. The Gibraltar tomography model suggests that the
60 slab is separated from the Atlantic oceanic domain by a portion of African continental margin,
61 whereas the Calabrian model displays a continuous oceanic slab that is connected, via a narrow
62 passage (~350 km), to the Ionian basin oceanic domain. Starting from the comparison of the two
63 models we propose the following interpretation: within the Mediterranean geodynamic regime
64 (dominated by slab rollback) the geometry of the African continental margin, located on the lower
65 plate, represents a critical control on the evolution of subduction. As buoyant continental
66 lithosphere entered the subduction zones, slab pull caused tears in the subducted lithosphere. This
67 tectonic response in the final stages of arc evolution, strongly controlled by the paleogeography of
68 the subducted plates, explains the observed differences between the Gibraltar and Calabrian Arcs.

69

70 **Key words:** teleseismic tomography, upper mantle, Gibraltar Arc, Calabrian Arc, subduction zone

72 **1. Introduction**

73 One of the outstanding and controversial features of the Mediterranean region is the presence of
74 large-scale extensional basins within a convergent domain located between the African and
75 European plates. Early studies recognized that the Central Western Mediterranean (CWM)
76 extensional basins (Fig. 1) developed in a backarc setting (Dewey et al., 1973, 1989; Horvath and
77 Berckhemer, 1982; Rehault et al., 1984), and also hypothesized that outward migration of
78 subduction, due to slab sinking and retreat, was the most likely explanation for the observables
79 (Malinverno and Ryan, 1986). Several papers stemmed from these early concepts, with progressive
80 refinement of the timing and kinematics of backarc extensional and outward migration of the fold-
81 and-thrust belt (e.g., Royden, 1993; Lonergan and White, 1997; Seranne, 1999; Argnani and
82 Savelli, 1999).

83 A remarkable lateral variability in the character of the fold-and-thrust belts, timing of extension of
84 backarc basins, and so on, is present in the Mediterranean orogen. Two main factors contributed to
85 this result: i) non linear continental margins of the converging plates; and ii) gravitational instability
86 of the subducted lithosphere.

87 The land-locked condition of the Mediterranean plate boundary, due to the presence of the Adriatic
88 promontory, enhanced the effects of slab rollback (Le Pichon, 1982; Mascle et al., 1988). In fact,
89 the collision of the Adriatic promontory with Eurasia around the Paleocene caused a slowdown in
90 the Africa–Eurasia plate convergence, particularly for the N-ward component (Le Pichon et al.,
91 1988; Dewey et al., 1989). This, in turn, promoted the activation of processes operating within the
92 orogen, such as lithospheric root detachment, lithosphere delamination, lateral escape towards areas
93 of depressed topography and rollback of dense oceanic slab, which are responsible for the origin of
94 the Mediterranean extensional basins (i.e. Le Pichon, 1982; Dewey, 1988; Le Pichon et al., 1988;
95 Otsuki, 1989; Argnani, 2000; Jolivet and Faccenna, 2000).

96 An additional important aspect is the interaction between lithospheric slabs and asthenosphere
97 which could possibly result into slab breakoff or detachment and delamination of continental
98 lithosphere. Lateral migration of slab breakoff has been proposed as a key factor for lithosphere
99 dynamics in this region in the last 20-30 Ma, especially in the final stage of subduction (Wortel and
100 Spakman, 1992, 2000; Carminati et al., 1998; Faccenna et al., 2004; Rosenbaum et al., 2008;
101 Argnani, 2009). Within this setting, mantle flow possibly played a role in the deformation of the
102 Gibraltar and Calabrian slabs (Gvirtzman and Nur, 1999; Faccenna et al., 2004; Baccheschi et al.,
103 2008). Delamination of continental lithosphere is a process that likely operated within the
104 Mediterranean orogens, following the subductional consumption of oceanic lithosphere (e.
105 g., Serri et al., 1993; Fillerup et al., 2010; Argnani, 2012; Levander et al., 2014). Although it is

106 known that continental rocks can experience subduction to depth over 100 km, before returning to
107 shallow depth and becoming exhumed to the surface (e.g., Hacker et al., 2010; Butler et al., 2014),
108 continental subduction is likely to be limited, both in extent and rate of subduction, as suggested by
109 the overall stability of continents (Cloos, 1993). The tectonic evolution of the Mediterranean type
110 orogen suggests that when a continental margin enters a retreating subduction zone (soft collision),
111 the processes of subduction and slab retreat get to the end (e.g., Burchfiel and Royden 1991; Wortel
112 and Spakman, 2000; Argnani, 2009).

113 The present structure and origin of the Gibraltar Arc-Alboran Basin system (GA) (Fig. 1) does not
114 fit well in this unifying picture based on slab subduction and rollback, and alternative evolution
115 scenarios have been proposed. Several authors do suggest that subduction of oceanic lithosphere
116 (active or extinct) caused extension within the Alboran Basin in the Miocene by slab rollback
117 (Royden, 1993; Lonergan and White 1997; Bijward and Spakman, 2000; Gutscher et al., 2002) or
118 by slab detachment (Zeck, 1996). Alternatively, another group of authors presents an evolution for
119 the Alboran basin initiating with lithospheric thickening during the Paleogene caused by the
120 collision of Europe and Africa. The thickened continental lithosphere was later (ca. 25 Ma)
121 detached by convective removal (Platt and Vissers, 1989) or by delamination (Calvert et al., 2000),
122 leading to recycling of continental material (Levander et al., 2014). The collapse of this lithosphere
123 caused extension of the Alboran and Algerian basins and uplift around the margin, edge
124 delamination under the Betics and Rif margins and mixed continental-oceanic subduction (Booth-
125 Rea et al., 2007; Duggen et al., 2005; Medaouri et al., 2014).

126 On the other hand, there is a general consensus that the Calabrian Arc-Tyrrhenian Basin system
127 (CA) (Fig. 1) does fit well in the unifying picture: subduction with slab rollback has been the main
128 factor in the opening of the Tyrrhenian Sea (Malinverno and Ryan, 1986), a well defined Wadati-
129 Benioff zone is contained in a high seismic velocity body (Cimini and Marchetti, 2006, and
130 references therein), and subduction-related magmatism is active under the CA (Barberi et al., 1974;
131 De Astis et al., 2003).

132 Several tomography studies have concentrated on the Mediterranean mantle at different scales.
133 They range from the global (e.g., Bijwaard and Spakman, 2000), to the European (e.g., Koulakov et
134 al., 2009), to the Mediterranean scale (e.g., Piromallo and Morelli, 2003), down to a more regional
135 scale (e.g., Cimini and Marchetti, 2006; Montuori et al., 2007; Bezada et al., 2013).

136 In this paper we focus on two tomographic P-wave velocity models of the upper mantle beneath the
137 GA and CA regions, which give , with respect to previous models, a more resolved 3-D picture of
138 the two subduction zones and surrounding asthenospheric mantle. Both tomographies take
139 advantage of improved teleseismic-phase arrivals datasets obtained by integrating recordings from
140 permanent national networks with recordings from recent dense deployments of temporary land and

141 marine (Ocean Bottom Seismometers - OBS) broad band arrays (Dahm et al., 2002; Monna et al.,
142 2005; NEAREST project, <http://nearest.bo.ismar.cnr.it>). The teleseismic inversions were performed
143 using a modern iterative technique (Rawlinson et al., 2006), by employing the same grid
144 parametrization and depth extension (600 km) of the target volume, which allows for a direct
145 comparison of the images. The GA tomography has been recently published (Monna et al., 2013a,
146 2015), while for the CA we present a new tomography model. Regarding the deep structure of GA
147 the model shows features that were previously undetected or poorly resolved, in particular the
148 lithosphere-upper mantle structure of the Gibraltar Strait-Atlantic sector, whereas for the CA the
149 slab geometry and the surrounding asthenosphere are more accurately defined with respect to a
150 previous models based on OBS data (Montuori et al., 2007). The inversion results are the starting
151 point for a discussion and comparison of the two subduction systems within the geodynamic and
152 tectonic framework of the Western Mediterranean region.

153

154 **2 Geodynamic and tectonic evolution of the Central Western Mediterranean**

155 Africa moved several 100's km towards Europe from the Cenomanian to the Chattian, and 200-300
156 km of convergence occurred in the Eocene-Oligocene time interval. Average N-S convergence
157 between Africa and Europe slowed down since the Chattian, following the Alpine collision, and, as
158 a result, rollback of subducted lithosphere initiated the opening of the backarc basins and the
159 concomitant outward migration of the fold-and-thrust belts, that characterize the Western
160 Mediterranean (Fig. 2) (Le Pichon, 1982; Dewey, 1988; Le Pichon et al., 1988; Argnani, 2000;
161 Jolivet and Faccenna, 2000). The concomitant presence of calc-alkaline volcanism along the
162 European margin (Sardinia, offshore western Corsica, Provence) is an evidence that subduction of
163 oceanic lithosphere occurred during the formation of these backarc basins (Argnani and Savelli,
164 1999).

165 The Balearic backarc basin was the first to open (Fig. 1) from late Oligocene to early-middle
166 Miocene (Rehault et al., 1984; Chamot-Rooke et al., 1997; Faccenna et al., 1997) and extend to the
167 western end of the Mediterranean, up to the Alboran basin (Watts et al., 1993; Booth-Rea et al.,
168 2007). In the Algerian sector, the opening of the basin continued until late Miocene, possibly with
169 oceanic crust emplacement in late Miocene (Mauffret et al., 2004; Booth-Rea et al., 2007; Medaouri
170 et al., 2014). The Tyrrhenian backarc basin opened from Late Miocene to Pleistocene above the
171 NW-dipping subduction of the Ionian lithosphere (Malinverno and Ryan, 1986; Kastens et al.,
172 1988; Argnani and Savelli, 1999). Evidence from regional geophysics, arguments from plate
173 kinematics and palaeo-reconstructions, suggest that the oceanic lithosphere, that subducted during
174 the Tyrrhenian opening, belonged to a Triassic seaway (Argnani, 2005; Speranza et al., 2012).

175 The most striking feature in this process of backarc basin opening is the formation of the two tightly

176 arcuate features: the Gibraltar and Calabrian arcs (Fig. 1) (Horvath and Berckhemer, 1982;
177 Faccenna et al., 2004; Rosenbaum and Lister 2004). The foreland of the Calabrian Arc fold-and-
178 thrust belt faces the African plate (s.l.), although the nature of the lithosphere varies from oceanic in
179 the apex of the arc to continental on either side. The foreland of the Gibraltar Arc fold-and-thrust
180 belt, instead, covers both the African and Iberian plates; this plate boundary location contributes to
181 additional tectonic complexity.

182 The large-scale models, that explain the Gibraltar and Calabrian arc subduction as coming from a
183 single slab SE-ward retreat of the western Mediterranean (Faccenna et al., 2004; Carminati et al.,
184 2012), may be too oversimplified to account for the geological complexity of the Alboran region.
185 Other evolutionary models start with a shorter subduction zone, that is initially limited to the
186 Balearic region (e.g., Lonergan and White, 1997; Rosenbaum et al., 2002; van Hinsbergen et al.,
187 2014); this class of models seem to explain more satisfactorily the geological evolution of the
188 Alboran region (Platt et al., 2013; Chertova et al., 2014).

189

190 **2.1 Gibraltar Arc-Alboran Basin**

191 The Atlantic sea-floor magnetic anomalies (Srivastava et al., 1990) indicate that the Iberia plate
192 experienced a complex kinematics within the Africa-Eurasia convergence. Iberia was part of Africa
193 from Late Cretaceous to Early Oligocene, whereas from Late Oligocene to present it became part of
194 Europe, following the Pyrenean collision. As an alternative, recent reviews of the magnetic
195 anomalies (Vissers and Meijer, 2012) allow for some 50-70 km convergence between Africa and
196 Iberia for the Late Cretaceous-Middle Eocene time span. The west-ward arc propagation of the
197 Betic-Rif fold-and-thrust belt is larger than the 200-250 km N-S convergence between Africa and
198 Iberia, as suggested by the length of the east-dipping subducted slab imaged by high-resolution
199 seismic tomography (e.g., Bezada et al., 2013; Palomeras et al., 2014). This propagation has been
200 modelled with a substantial westward slab rollback (e.g., Royden, 1993; Lonergan and White, 1997;
201 Gutscher et al., 2002; Rosenbaum et al., 2002). The internal Betics and Rif units (Fig. 2a) have a
202 continental substrate of Palaeozoic age with a Mesozoic-Cenozoic sedimentary cover, and have
203 been affected by Palaeogene HP/LT metamorphism (Platt et al., 2013). These internal units have
204 been also recovered in the Alboran Sea, defining the so-called Alboran Domain. The external Betics
205 and Rif units are characterized by successions derived from the Iberian and African passive
206 continental margins that were emplaced during the opening of the Alboran basin (e.g., Blankenship,
207 1992; Wildi, 1983). The sediments of the Flysch basin were thrust by the Alboran Domain units
208 that were moving west-southwest-ward during the Oligocene-Early Miocene (Fig. 2a; Wildi, 1983).
209 The basement of the Flysch basin domain was likely oceanic and could correspond to the oceanic
210 slab imaged by tomography under the Alboran basin. Most of the vertical-axis rotation and arc

211 formation in the Rif and western Betics was accomplished by the early Pliocene, as indicated by
212 paleomagnetic data (e.g., Platt et al., 1995; Platzman et al., 1993; Krijgsman and Garces, 2004;
213 Cifelli et al., 2008; Fig. 2a).

214 The Alboran Sea basin, which was formed in the Neogene as a result of extensional tectonics, is
215 currently floored by thinned continental crust, 13-20 km thick (Watts et al., 1993), and by
216 magmatically accreted arc-type crust in its eastern sector (Booth-Rea et al., 2007).

217 Recent tectonic models try to account for the details of the geological evolution of the Alboran
218 region. Platt et al. (2013), following their previous work, propose a NW-ward Paleogene subduction
219 that originated the Alboran Domain, followed (during the Early Miocene) by orogenic collapse and
220 a new subduction on the Iberian side of the Alboran Domain. As an alternative explanation, Vergés
221 and Fernandez (2012) propose a continuous southward subduction of the Iberian plate, with slab
222 rollback and slab break-off, that would account for both the Paleogene and Miocene subduction
223 events. This reconstruction which describes the evolution of the Betics, requires the occurrence of a
224 major transform boundary that separates the Betics (northward polarity) from the eastern
225 Maghrebides (southward polarity) subduction segments, and implies some difference in the tectonic
226 evolution of the Maghrebian belt of north Africa, for which there is not much evidence in the field.
227 Finally, a recent reconstruction (Van Hinsbergen et al., 2014) assumes that the Alboran terranes
228 mostly formed along an oblique subduction zone located south of the Balearic islands, partly
229 building on the reconstruction of Rosenbaum and Lister (2004). Here, the early Miocene heating
230 and exhumation affecting the peridotite mantle and overlaying Alboran terranes occurred within a
231 forearc setting, with the Alboran terranes subsequently dispersed across the western Mediterranean
232 during backarc opening.

233 A number of tomographic studies have been performed in the last decade to image the deep seismic
234 velocity structure of the GA. These studies agree on the presence of a high-velocity body under the
235 Alboran Sea, down to mantle depths (Blanco and Spakman, 1993; Bijwaard and Spakman, 2000;
236 Calvert et al., 2000). Very recent high-resolution tomography studies (Bezada et al., 2013;
237 Palomeras et al., 2014; Thurner et al., 2014; Bonnín et al., 2014; Villaseñor et al., 2015) confirm the
238 presence of a slab-shaped high velocity body, seen from the surface down to the bottom of the
239 transition zone. The GA slab has a small curvature radius, similarly to the CA, but it does not show
240 a Wadati-Benioff plane. In fact, sub-crustal seismicity (Figs. 3 and 8) is mostly located near the
241 Strait of Gibraltar within 120 km depth and distributed in a very narrow north-south oriented
242 vertical band (Seber et al., 1996), with a mixture of focal mechanisms showing both compression
243 and extension (Buforn et al., 2004). Deep earthquakes (depth > 300km) are rare and occur at the
244 bottom of the transition zone (~630 km depth) under southern Spain in the Granada area, and show
245 dip-slip motion with a vertical north-south plane and a nearly horizontal plane with the pressure

246 axis dipping 45° to the east (Buforn et al., 2004, 2011).

247 The large amount of geophysical and geological data for this area confirms a complex geodynamic
248 evolution, and in fact the high velocity anomaly below the Alboran has been interpreted as a
249 continuous subducting slab (Gutscher et al., 2002; Piromallo and Morelli, 2003), as a broken-off
250 slab (Blanco and Spakman, 1993), and as lithosphere which has undergone delamination (Calvert et
251 al., 2000), or convective removal of the root (Platt and Vissers, 1989).

252 One of the open problems for the GA has been the interaction between the Atlantic and Alboran
253 domains, west and east of the Gibraltar Strait. Although global scale tomography studies cover both
254 regions, they do not have the capability to resolve the finer details. On the other hand, in spite of the
255 increase in available data, the great majority of the higher resolution (regional scale) tomography
256 models do not image the mantle below the Atlantic region west of the Gibraltar Strait due to a lack
257 of station coverage at sea. A recent regional scale tomography model (WMGC-OBS) based on OBS
258 data which includes both domains, has been proposed by Monna et al. (2013a). A relevant aspect of
259 model WMGC-OBS is that there is a separation of the two lithospheres of the two domains, thus
260 excluding the existence of a single continuous slab coming from the Atlantic side and subducting
261 eastward below the Alboran.

262

263 **2.2 Calabrian Arc-Tyrrhenian Basin**

264 The Calabrian Arc connects the Sicilian Maghrebides and Southern Apennines and is characterized
265 by a stack of basement units, coming from different levels of a Hercinian continental crust (Fig. 2b)
266 (Bonardi et al., 2001). A thick forearc sedimentary succession crops out in the Ionian side of
267 Calabria, supporting the accretion of the Calabrian Arc terranes within a subduction system
268 (Bonardi et al., 2001). The wide accretionary complex of the External Calabrian Arc extends into
269 the Ionian Sea and is confined to the NE and SW by the Apulian and Malta Escarpments,
270 respectively (e.g., Biju Duval et al., 1982; Argnani and Bonazzi, 2005; Argnani, 2006).

271 The evolution of the Calabrian Arc is strictly related to the opening of the Tyrrhenian backarc basin
272 (Malinverno and Ryan, 1986; Patacca et al., 1993) and is marked by a progressive narrowing of the
273 subducted slab. Palaeomagnetic data support the saloon-door opening of the Tyrrhenian basin
274 (Cifelli et al., 2007), as the structural units of the Southern Apennines experienced a counter-
275 clockwise rotation of 60° during Middle-Late Miocene (Gattacceca and Speranza, 2002), whereas
276 the structural units of the Sicilian Maghrebides show a large clockwise rotation of ca. 70° between
277 Langhian and Late Tortonian (Channell et al., 1990; Speranza et al., 1999).

278 The Tyrrhenian Basin is located on the wake of the Apennines and Sicilian Maghrebides. The
279 amount of extension is greater in the southern basin which, in fact, is characterized by a thin crust
280 (less than 10 km) and high heat flow (Kastens et al., 1988), with possibly wide stretches of

281 exhumed mantle (Prada et al., 2014). A girdle of volcanic islands, the Aeolian Islands, located north
282 of Sicily represents the volcanic arc of the Tyrrhenian subduction, with calc-alkaline activity that
283 spans from 1 Ma to the Present (Fig. 2b) (Barberi et al., 1974; De Astis et al., 2003). The rocks of
284 the Campania Magmatic Province (Fig. 2b), that includes the Campi Flegrei high potassium
285 calcalkaline (2.0 - 1.6 Ma), the Campi Flegrei, Ischia and Procida shoshonites (100 ka - Present),
286 and the Vesuvio leucitite and leucitite basanite (1 Ma - Present), also show affinity with island arc
287 magmatism. Magmatic rocks from Campania and the Aeolian volcanic arc have comparable
288 geochemical features, suggesting a similar Oceanic Island Basalt mantle source, enriched by
289 components derived from subducted oceanic lithosphere (Serri, 1990).

290 The onshore Calabrian Arc has been affected by major uplift in the last 0.8 Ma, with rates up to 2.0
291 mm/yr (Westaway, 1993; Bordoni and Valensise, 1998), and presents extensional grabens filled by
292 Late Pliocene-Quaternary sediments, trending both parallel and perpendicular to the arc (Tortorici
293 et al., 1995). This active tectonic regime is supported by extensional focal mechanisms (e.g.,
294 Vannucci et al., 2004). To the west of the central Aeolian Islands, earthquake focal mechanisms
295 indicate that active compressional deformation occurs offshore northern Sicily (Pondrelli et al.,
296 2004; Argnani et al., 2007; Serpelloni et al., 2007), although the seismogenic structures have not
297 been properly identified. This compressional boundary has been considered as part of a kinematic
298 rearrangement that occurred about 2 Myr ago (Jenny et al., 2006).

299 For the CA there is a wide consensus that subduction of oceanic lithosphere below the southern
300 Tyrrhenian is taking place. In the tomographic images the subduction is represented as a narrow
301 arc-shaped high velocity body which flattens in the transition zone at the 660 km discontinuity
302 between upper and lower mantle (Cimini, 1999; Piromallo and Morelli, 2003; Spakman and Wortel,
303 2004; Montuori et al., 2007). The existence of subduction and overlying mantle wedge for the CA
304 is confirmed by other geophysical and geochemical observations, such as, for example, the presence
305 of a volcanic arc (Barberi et al., 1974; De Astis et al., 2003). Furthermore, the spatial distribution of
306 the deep events (Figs. 3 and 9) (Frepoli et al., 1996) shows a Wadati-Benioff zone dipping $\sim 70^\circ$
307 NW beneath the southern Tyrrhenian, down to about 600 km depth (Cimini and Marchetti, 2006,
308 and references therein). **The focal mechanism P-axes show steep down-dip compression at
309 intermediate depths (between 160 and 370 km). The deepest events (below 370 km) have P-axes
310 with shallower dip (Frepoli et al., 1996).**

311 The tomographic models have been interpreted as representing the final result of a subduction with
312 rollback process which has caused the opening of the Tyrrhenian Sea in the last ~ 13 Ma (Wortel
313 and Spakman, 2000; Piromallo and Morelli, 2003).

314 The tomographic images show that there is not a continuous slab under the Italian peninsula, as it is
315 interrupted by a low-average velocity volume below the central-southern Apennines at lithospheric

316 depths. Other distinct high velocity bodies are found below the Northern Apennines and the Alps
317 (Spakman and Wortel, 2004; Piromallo and Morelli, 2003; Giacomuzzi et al., 2012). This
318 distribution in space of the high velocity bodies, prompted several authors to hypothesize the
319 existence of an original single slab which had undergone one or more slab tears and/or detachment
320 (e.g., Wortel and Spakman, 1992; 2000; Amato et al., 1993; Spakman and Wortel, 2004).

321 In recent years, thanks to the improvement of the Italian National Seismic Network, regional
322 tomography studies could resolve finer details of the CA lithosphere-asthenosphere structure (e.g.,
323 Chiarabba et al., 2008). Furthermore, inversion of the 3-D attenuation structure (Chiarabba et al.,
324 2008; Monna and Dahm, 2009) has added independent constraints, which are especially helpful in
325 distinguishing the role of chemical composition and temperature as causes for seismic velocity
326 anomalies.

327

328 **3. Teleseismic tomography models of GA and CA based on OBS data**

329 In this section we describe 3-D P-wave velocity models computed for the upper mantle of GA and
330 CA. The CA images are derived from the new tomographic model presented in this work The GA
331 images are derived from model WMGC-OBS presented in two recent papers (Monna et al., 2013a,
332 2015). To calculate both models we used accurate time picks of teleseismic waveforms recorded by
333 the integrated arrays shown in Fig. 4 at epicentral distances between 25° and 95° (P phases) from
334 worldwide $M_w \geq 5.5$ earthquakes. The time picks were corrected for station elevation/bathymetry,
335 Earth's ellipticity, local crustal structure (see sections 3.1 and 3.2), and then reduced to relative
336 arrival time residuals using the ak135 global velocity model (Kennett et al., 1995). We applied the
337 iterative nonlinear tomography method developed by Rawlinson et al. (2006) to map these residuals
338 into 3-D P wave velocity anomalies. We note that inversion of relative traveltimes residuals
339 produces only 3-D velocity perturbations with respect to an average (usually 1-D) Earth model
340 modified for the appropriate crustal structure. In the inversion scheme, the calculation of teleseismic
341 wavefronts and the traveltimes from the base of the model volume to the array of receivers on the
342 surface is performed with the fast marching method (FMM) (Sethian and Popovici, 1999). For both
343 study regions, the bottom of the 3-D model was set at 600 km depth and the grid spacing used for
344 the parametrization of mantle structure was 60 km. Outside the model volume the Earth is assumed
345 to be spherically symmetric, which allows the use of a 1-D global reference model to rapidly
346 compute the traveltimes from the distant sources to all grid nodes at the bottom. For a detailed
347 description of the technique and the inversion equation we refer the reader to Rawlinson et al.
348 (2006). In both cases, the nonlinear inversion was performed by testing different values of the
349 maximum iteration number, to check the overall stability and performance in modeling the residual
350 data. The tomographic images displayed in the following subsections describe the velocity field

351 computed at the third iteration, as only minor improvements in the data fit (<1%) and small
352 structural changes in the velocity patterns were observed, for both cases, with successive inversion
353 steps. Since the parametrization for the two models is the same, their direct comparison is possible.
354 In general, the images for the CA show stronger anomalies, which explains the different scale of the
355 color palettes in Figs. 6-10, +/- 0.2 km/s for the GA and +/- 0.3 km/s for the CA, in spite of the
356 stronger regularization applied in the CA inversion. The difference in the amplitude of the
357 anomalies could be explained by differences in accuracy of the two datasets and in the RMS
358 reduction, but also by a greater heterogeneity of the CA upper mantle with respect to GA. With
359 respect to previous tomographic studies at the same scale (e.g., Montuori et al., 2007; Giacomuzzi
360 et al., 2011) the CA inversion we present has greater resolution and coverage of the oceanic areas.
361 A comparison between the resolution of the GA and CA models is performed using the
362 “checkerboard tests” displayed in Fig. 5. In this test the input velocity model is formed by
363 alternating regions of fast and slow anomalies (with added gaussian noise to account for errors in
364 the data; Monna et al., 2013a). The recovered pattern provides information on the well resolved
365 areas of the models. We note that the CA model could be parametrized with a smaller grid (~80
366 km), but we have chosen the same parametrization as for GA (100 km) to better compare them. In
367 any case, in both cases the parts that we interpret are in volumes of the models that are reliably
368 reconstructed in the synthetic tests. We have clarified this aspect in the text.

369

370 **3.1 Gibraltar Arc (GA) model**

371 The information on the GA model that we present in the following is an updated summary of the
372 results presented in Monna et al. (2013a, 2015). The teleseismic data set for the GA model is
373 composed by 152 events recorded in the period 2007-2009 by the permanent networks of Spain,
374 Portugal, and Morocco, and by the NEAREST OBS array (Carrara et al., 2008) deployed in the
375 Gulf of Cadiz from August 2007 to August 2008 (in total 111 seismic stations; Fig. 4; left). This
376 data set provided 6238 residuals for the tomography. The OBS array (25 seafloor broad band
377 stations) recorded waveforms from 67 events. Other waveforms were collected from two land
378 stations operating in SW Portugal installed during the experiment, and from the European
379 Integrated Data Archive (EIDA; <http://eida.rm.ingv.it>). To improve ray coverage, arrival times
380 extracted from the ISC bulletin (<http://www.isc.ac.uk>) were also added. The average time pick error
381 was estimated in 0.43s. A crustal correction was applied based on four models which take into
382 account up-to-date information available from published studies. These four models represent the
383 Atlantic Ocean Domain, the Iberian Peninsula, Betics and Rif, and Atlas (see Table 1 in Monna et
384 al., 2013a).

385 The GA-Alboran Basin model lateral extension (Fig. 3; left) spans 12.0° in latitude (from 31.0°N to

386 43.0°N), and 16.0° in longitude (from 15.0°W to 1.0°E). The 3-D velocity grid comprises 5544
387 nodes at 60 km spacing in all three dimensions (depth, latitude, longitude). The tomographic
388 inversion was carried out with damping and smoothing parameters of 5.0 and 2.5, respectively. The
389 three-step inversion reduced the data variance by 26% from 0.53 to 0.39 s² (Monna et al., 2013a).

390 We now briefly describe the main features found in the GA model as represented in Figs. 6 (maps)
391 and 8 (cross-sections). Further details on the velocity pattern imaged in the Atlantic portion of the
392 GA model can be found in Monna et al. (2015). The tomographic images show:

393 1) A high velocity body with arcuate geometry under the Betics-Alboran Sea area (Al-HVA). This
394 fast structure depicts an L-shaped slab steeply dipping from the uppermost mantle to the transition
395 zone where it becomes less curved.

396 2) A high-velocity body under the Horseshoe Abyssal Plain in the Atlantic region (HAP-HVA).

397 3) A diffuse low velocity anomaly (EAt-LVA) present in the Eastern Atlantic region south of the
398 Gloria fault, down to the mantle transition zone.

399 4) A prominent low velocity anomaly below the Gulf of Cadiz (GC-LVA) which separates the two
400 high-velocity bodies found under the Alboran (Al-HVA) and Atlantic regions (HAP-HVA).

401 Al-HVA extends from the surface to the base of our model (Figs. 6 and 8), and its maximum width
402 is ~300 km in the EW direction below the Granada region (AA'). The AA' profile, which crosses
403 the southern tip of the Iberian peninsula, shows the transition from the Atlantic to the Alboran
404 domain, and the width of the slab (100–200 km). Section BB' crosses the Alboran Sea and shows
405 the north-south extension of Al-HVA (approximately 300 km). Subcrustal seismicity is distributed
406 along an arc-shaped belt with the deeper events contained in the uppermost part of the Al-HVA.
407 These intermediate-depth earthquakes have a distribution which is not typical of subduction zones,
408 in contrast with the clear Benioff zone of the Calabrian Arc (Fig. 9). Nevertheless, they provide
409 information on the subducted oceanic slab beneath the Alboran basin, as their occurrence is usually
410 linked to dehydration reactions in subducting oceanic lithosphere (e. g. Hacker et al., 2003).

411 GC-LVA extends from the top of the model down to ~250 km depth in (AA'). Below the
412 NEAREST OBS array, roughly under the Horseshoe Abyssal Plain, the model shows HAP-HVA
413 down to a depth of ~240km (Fig. 6). From profile AA' we obtain an east-west extension for HAP-
414 HVA of ~250 km. This feature has been interpreted as a developed subduction process in the
415 Gorringe Bank region (Monna et al., 2015).

416

417 **3.2 Calabrian Arc (CA) model**

418 The teleseismic events were collected from the Italian National Network (managed by INGV) and
419 from temporary experiments performed both at sea (TYDE (Dahm et al., 2002) and NEMO-SN1
420 (Favali et al., 2013) and on-land (SAPTEX (Cimini et al., 2006) and SeSCAL (Frepoli et al., 2011))

421 during the last decade. The integrated network used in this study includes 209 stations (Fig. 4;
422 right). The dataset spans the years 2000-2008 and consists of 276 events for a total of 8635
423 residuals. Crustal corrections of traveltimes residuals were performed on the basis of two models
424 (Monna et al., 2013b), one for the continental part (Sicily and Apennines) and one for the oceanic
425 part (southern Tyrrhenian and Ionian Seas). Differently from the GA data set, the CA data set
426 comes all from very accurate handpicked arrival times with an estimated average error of 0.16s
427 which is almost 1/3 of the GA time pick error. The high quality of the CA data led to a solution
428 model which is associated to a significant reduction of the residual variance.

429 The CA-Tyrrhenian Basin model lateral extension (Fig. 3; right) spans 8.0° in latitude (from 36.0°N
430 to 44.0°N), and 12.0° in longitude (from 9.0°E to 21.0°E). The 3-D velocity grid comprises 3344
431 nodes spaced apart, 60 km in all the three directions, as for the GA model. For the CA model we
432 obtained a variance improvement of over 51%, from 0.41 to 0.20 s^2 .

433 The main features found in the CA model, represented in Figs. 7 (maps) and 9 (cross-sections), are:

- 434 1) A high velocity body with slab-like shape under the Tyrrhenian Sea area (STy-HVA).
- 435 2) A high-velocity body under the Apennines (Ap-HVA).
- 436 3) A high velocity anomaly visible below the Adriatic Sea (Adr-HVA) adjacent to the Ap-HVA
437 visible below 300 km depth.
- 438 4) A diffuse low velocity anomaly (STy-LVA) adjacent to Sty-HVA and Ap-HVA, found down to
439 ~ 350 km depth. In the depth interval ~ 100 -300 km, STy-LVA and the prominent low velocity zone
440 imaged in the Ionian side (Io-LVA) join in a continuous belt surrounding the main fast structures.
- 441 5) A low velocity anomaly (Ap-LVA) at lithospheric depths below the central and southern
442 Apennines, down to 120 km depth. Ap-LVA interrupts the lateral continuity of Ap-HVA,
443 suggesting that the Apenninic slab has been subjected to tearing and slab window formation
444 processes. Its geometry is clearly defined by the NW-SE profile shown in Fig. 10 (cross-section
445 CC').

446 The deep seismicity delineates a well defined Wadati-Benioff plane, which is included in the
447 volumes with the highest velocity perturbations, and is mostly concentrated in the 100-350 km
448 depth range (Figs. 7 and 9). The high velocity slab shows a remarkable horseshoe shape in the 100-
449 300 km interval. STy-HVA extends from crustal depths down to the bottom of the model (the lower
450 part of the transition zone), and its lateral extension is about 350 km (Fig. 9, BB'). Ap-HVA appears
451 from uppermost mantle depths down to ~ 120 km depth, as two distinct anomalies, one under the
452 central (CAp-HVA) and the other below the southern Apennines (SAp-HVA). Ap-HVA seems to
453 merge with Sty-HVA from 180 km depth down to the bottom of the model (Fig. 7).

454 The pattern of low P-wave velocity perturbations visible around Sty-HVA (Fig. 7), is recognizable
455 also in the PM0.5 model by Piromallo and Morelli (2003) at 150 and 200 km depth.

456

457 **4. Discussion**

458 The aim of this discussion is not to tackle the reconstruction of the long-term evolution of the
459 Western Mediterranean region, which has been described in several papers, but rather to focus on
460 the final stages of arc formation in the Western Mediterranean and, in particular, on the interaction
461 of the subduction system with the portions of continental margin that are approaching the
462 subduction zone. Some key features of the Gibraltar and Calabrian subduction systems are
463 compared and contrasted on the basis of the two presented tomographic models and other
464 geophysical and geological data. We first describe and compare the lithosphere-asthenosphere
465 structure of the two arcs, then their seismicity and active tectonics, and finally we focus on the slabs
466 evolution.

467

468 *Lithosphere-asthenosphere structure*

469 There are two main high velocity anomalies (HVA) evident in the horizontal layers (Figs. 6 and 7),
470 that underlie the Alboran (Al-HVA) and the Tyrrhenian (STy-HVA) basins. Both HVAs reach the
471 mantle transition zone down to at least 600 km depth, the bottom of our models. While the STy-
472 HVA presents a more evident arcuate shape, the Al-HVA is thicker, and the stronger part of the
473 anomaly is blob-like, especially in the top 300 km. Moreover, the STy-HVA mostly underlies the
474 Tyrrhenian basin, whereas the Al-HVA is mostly located below the Betics and the Granada area,
475 where the scarce deep seismicity is found.

476 In both areas there are strong LVAs that surround the slab. In the Calabrian Arc the LVA underlies
477 the Tyrrhenian basin (STy-LVA) and the oceanic crust of the Ionian Sea (Fig. 9) . The lithosphere-
478 asthenosphere structure under the Ionian side is only partially resolved due to the lack of long term
479 broadband OBS deployments in the Western Ionian Sea. Continuity of the slab is inferred only from
480 indirect evidence (e.g., slab geometry and seismicity). On the contrary, the lithosphere-
481 asthenosphere structure below the Gulf of Cadiz (GC-LVA, Fig. 8) is well resolved and represents
482 the key feature separating the two high velocity anomalies underlying the Atlantic and the Alboran,
483 respectively (Monna et al., 2013a). We are confident that GC-LVA is not an effect of low velocity
484 uppermost crustal layers smeared down the uppermost mantle, given the strong crustal correction we
485 applied that includes a thick low-velocity sedimentary layer (see Table 1 in Monna et al., 2013a).

486

487 *Seismicity and active tectonics*

488 Comparison of vertical profiles in Figs. 8 and 9 also clearly shows a very different spatial
489 distribution of sub-crustal seismicity, with a typical Wadati-Benioff zone for the CA and a belt of
490 intermediate-depth seismicity (<120km) for the GA. While for the CA seismicity is included in the

491 volume with the largest positive velocity anomalies, for the GA seismicity is concentrated on top of
492 the HVA. Profiles BB' give a measure of the width of the two slabs, which is about 300 km for Al-
493 HVA and 350 km for STy-HVA.

494 The different patterns of sub-crustal seismicity in the Gibraltar and Calabrian Arcs, suggests that a
495 different tectonic regime is active in the two arcs (Fig. 3). It is noteworthy that only limited
496 seismicity occurs offshore in the CA accretionary prism, but remarkable seismicity with large
497 earthquakes, mostly historical but also instrumental, characterizes the onshore, uplifted region of
498 the arc, continuing into the southern Apennines. Focal mechanisms of crustal earthquakes indicate
499 orogen-perpendicular extension (Vannucci et al., 2004; Frepoli et al., 2011). In the GA almost no
500 seismicity occurs in the outer accretionary prism; instead, seismicity (found also down to ~60 km)
501 is present in the Gorringe Bank-Horseshoe Abyssal Plain (e.g., Geissler et al., 2010), where it is
502 associated to a high velocity subducting lithosphere (Monna et al., 2015). No relevant seismicity is
503 present at the apex of the GA, whereas some seismicity is related to the right-lateral strike-slip
504 regime found in the eastern Betics, and a remarkable crustal seismicity is present in the Alboran
505 basin (Serpelloni et al., 2007; Stich et al., 2006; 2010), along the Trans-Alboran shear zone
506 (Alvarez-Marron, 1999). The distribution of crustal seismicity appears to reflect the occurrence of a
507 diffuse plate boundary deformation that shifts from the Gloria Fault-Gorringe-SW Iberia system to
508 the Maghrebides of north Africa; this southward shift occurs just across the Alboran basin (Fig. 3)
509 (Serpelloni et al., 2007).

510

511 *Evolution of the two subduction systems*

512 The evolution of the Mediterranean subduction is strongly controlled by the paleogeography of the
513 African margin (lower plate), and in particular by the location and extent of its oceanic domains. A
514 tectonic reconstruction at Tortonian time (Fig. 11) shows the different stages in the formation of the
515 Gibraltar and Calabrian arcs. This time is crucial since the Tyrrhenian basin was in its initial stage,
516 and the Calabrian Arc formed subsequently, driven by the subduction and rollback of the
517 Neotethyan ocean located between Africa and Adria. On the contrary, the Gibraltar Arc was almost
518 completely defined. We propose an interpretation that is summarized in Fig. 12.

519

520 During the evolution of the retreating Mediterranean subduction, the soft collision of the outward-
521 migrating orogen with the African margin first occurred in the Magrebides (e.g., Lonergan and
522 White, 1997; Rosenbaum and Lister, 2004). The soft collision was followed by a slab breakoff,
523 marked by a change from orogenic to anorogenic magmatism (Maury et al., 2000; Abbassene et al.,
524 2016), that disrupted the originally continuous subducted slab, and propagated laterally both
525 eastward and westward (Fig. 12), to originate the Calabrian and Gibraltar Arcs, respectively

526 (Wortel and Spakman, 2004). Slab tearing focussed trench retreat, favouring the formation of
527 tightly arcuate subduction zones (e.g., Schellart et al., 2007). The narrow CA subducted slab (Fig.
528 9; BB') is discontinuous on either side, underneath Sicily and southern Apennines. The lack of high
529 velocity bodies underneath western Sicily is likely a result of progressive lithospheric tearing.
530 Tearing propagated eastward along the north African continental margin, removing the slab, during
531 the Tyrrhenian opening from 10 to 2 Ma (Carminati et al., 1999; Faccenna et al., 2004; Goes et al.,
532 2004; Argnani, 2009). An interruption of the slab or slab window underneath the Southern
533 Apennines (Fig. 12) is visible in the tomography models as a low velocity anomaly at lithospheric
534 depths (Fig. 10). The presence of a slab window is consistent with abundant volcanic products
535 younger than 2 Ma in the Campania Magmatic Province, which supports the tapping of deep mantle
536 reservoirs (Serri, 1990).

537 The low mantle velocity underneath Calabria (e.g., Mele, 1998) suggests a decoupling of the slab
538 from the overlying lithosphere, that can be partly responsible for the recent uplift of Calabria
539 (Gvirtzman and Nur, 1999; Argnani, 2000). A role of toroidal mantle flow dynamically sustaining
540 the Calabrian topography has also been inferred (Faccenna et al., 2011), although the contribution
541 of dynamic topography is likely a minor one (Molnar et al., 2015). The existence of lithospheric
542 tears located on either side of the Calabrian Arc is supported also by local earthquake and seismic
543 velocity distribution. Some authors have inferred the occurrence of north-west-trending tears, that
544 are supposed to favor the south-eastward drift of Calabria (e.g., Neri et al., 2012). The seismicity
545 gaps and reduced seismic velocities presented by Neri et al. (2012), however, seem to outline
546 discontinuities that propagated parallel to the trench, which are difficult to reconcile to north-west-
547 trending lithospheric tears that would allow displacement perpendicular to the trench. In this last
548 case, in fact, the tomographic model should suggest slab segments that are laterally shifted in the
549 north-west-direction with respect to each other, a feature that is not observed (Fig. 7). In fact, the
550 only discontinuity perpendicular to the trench is an incipient, ca. north-south-trending, lithospheric
551 tear (STEP fault) (Govers and Wortel, 2005) which is located offshore eastern Sicily (Figs. 2b and
552 11) (Argnani, 2009).

553 As described in the following, we infer that the portion of continental lithosphere defined by our
554 tomography (Fig. 6) may have played a role in preventing a further evolution of the Gibraltar Arc.
555 In the Gibraltar system the narrow (ca. 300 km wide) high velocity body is not a typical subducting
556 slab, given its seismicity and its blob-like shape underneath the Betics (Fig. 6). Recent studies show
557 that underneath most of the Betics the subducted slab is partly torn off its adjacent continental
558 margin, whereas underneath the Rif it is still attached to the crust (e.g., Levander et al., 2014). In
559 particular, observations from seismic tomography (Bezada et al., 2013; Palomeras et al., 2014) and
560 receiver function analysis (Mancilla et al., 2015; Thurner et al., 2014) are consistent with the

561 presence of continental crust that was removed from the continental margins and is now part of the
562 slab.

563 Both slabs below the Alboran and Tyrrhenian basins are thought to belong to narrow oceanic
564 basins. The original oceanic domain belonged to the Alpine Tethys and Neotethys for the Calabrian
565 subduction (e.g., Stampfli and Borel, 2002; Argnani, 2005), and to the Alpine Tethys and Central
566 Atlantic for the Gibraltar subduction (e.g., Gutscher et al., 2012). However, the physical connection
567 between Alpine Tethys and the Central Atlantic proposed by several authors (see Section 2.1) can
568 be questioned. In fact the occurrence of an arcuate structure underneath the Gibraltar Arc, with a
569 seismic velocity pertaining to continental lithosphere, suggests the presence of a possible
570 continental domain located just west of Gibraltar in the GA model (Figs. 6 and 8; Monna et al.
571 (2013a, 2015)). Recent tomography models (Bonnin et al., 2014; Villaseñor et al., 2015) show a
572 low velocity anomaly at lithospheric depths just west of the Gibraltar Strait, which agrees very well
573 with our GC-LVA.

574 The existence of possibly Jurassic oceanic crust in the Gulf of Cadiz has been documented by
575 refraction data (Sallares et al., 2011), but the refraction profile is located further to the west of the
576 low-velocity anomaly that we attribute to continental lithosphere (Fig. 2a), and recent refraction
577 data across the Gibraltar Strait show a continental crustal structure (Gil et al., 2014). The boundary
578 between continental and oceanic mantle domain is placed just east of Gibraltar Arc (Morais et al,
579 2015) through receiver function analysis, and the continuity of the thickened crust along the
580 Gibraltar Arc (Mancilla et al., 2015) seems to support the occurrence of a substrate of continental
581 nature. Although Mancilla et al (2015) propose an oceanic connection between the Atlantic and the
582 subducted slab, their receiver functions data are also compatible with our hypothesis, as their data
583 do not constrain the nature of the crust in the western offshore of Gibraltar.

584 The presence of a portion of continental lithosphere that has limited the Alpine Tethys to the west,
585 and that is now choking the subduction underneath the Alboran basin, fits well with other recent
586 high resolution tomography models (Bonnin et al., 2014; Palomeras et al., 2014; Villaseñor, 2015).
587 These tomography images can be explained by a process of ongoing delamination, with a sinking
588 oceanic slab pulling and thinning the lithosphere of the Betics and Rif.

589 In our interpretation, continental lithosphere is entering subduction in the Gibraltar Arc from the
590 west, and due to its positive buoyancy it contrasts the slab pull effect, favoring slab break-off,
591 delamination, and limiting asthenosphere wedging west of the Gibraltar Arc, and thus limiting
592 uplift and extension. Active extensional tectonics and recent uplift, in fact, have not been observed
593 at the apex of the Gibraltar Arc; recent uplift occurs mostly in the Sierra Nevada (Perez-Pena et al.,
594 2010; Braga et al., 2003). On the contrary, in the CA, subduction of oceanic lithosphere is well
595 documented, with the slab connected to the oceanic Ionian lithosphere (Fig. 11) (Argnani, 2005;

596 Speranza et al., 2012). The slab pull, which is still active, favored the wedging of asthenospheric
597 mantle and ensuing uplift (Gvirtzman and Nur, 1999). The uplift, in turn, promotes gravitational
598 collapse towards the topographically low Ionian Sea and possibly triggers the extension which is
599 ongoing in Calabria (Argnani, 2000; D'Agostino et al., 2011).

600

601 **5. Summary and Conclusions**

602 The Western Mediterranean subduction system was active mostly during the Neogene, creating the
603 arcuate mountain belts and deep basins that characterize the Mediterranean orogen. Slab sinking
604 and trench retreat contributed to the opening of the Balearic and Tyrrhenian basins. Although the
605 main driving force is likely given by trench retreat of oceanic subduction within a low plate-
606 convergence setting, additional complexities came into play throughout the evolution of the
607 Western Mediterranean, the major factor being the interaction between the European subduction in
608 the Alps and the African subduction in the Apennines (e.g., Argnani, 2012). In this paper we focus
609 on the origin of the two tight loops of the Gibraltar and Calabrian Arcs using two teleseismic
610 tomography models. These two arcuate features have been often described together and considered
611 as typical of the Western Mediterranean evolution (Horvath and Berckhemer, 1982; Rosenbaum
612 and Lister, 2004; Faccenna et al., 2004). The fact that trench retreat has overtaken convergence
613 throughout the Neogene evolution of the Mediterranean implies that the nature of the lower plate
614 lithosphere may strongly affect the geodynamic balance of the system. In fact, the arcuate orogenic
615 belts were mostly formed in the final stages of the Western Mediterranean evolution and, apart from
616 trench rollback, they were affected in an important way by the geometry of the continental margins.
617 In the Gibraltar Arc both slab rollback and gravitational potential of a thickened orogen have been
618 driving forces for the emplacement of the Alboran units in the early Miocene.

619 **The continuity of oceanic subduction represents the major difference between the Calabrian and**
620 **Gibraltar arcs. In the Gibraltar Arc the continental margin domain is entering subduction.** The GA
621 tomography model suggests that the Gibraltar Arc was docking into a portion of thinned continental
622 crust, located just west of Gibraltar (Fig. 12). This buoyant lithosphere was likely responsible for
623 the end of trench retreat, and its related extension in the Alboran basin. As the subduction of the
624 oceanic lithosphere was progressively completed, the continental margin lithosphere of Africa and
625 Iberia entered into the subduction zone and was pulled down by the sinking oceanic slab, leading to
626 ongoing continental delamination underneath the western Rif and the Betics and slab breakoff
627 (Bezada et al., 2013; Levander et al., 2014; Thurner et al., 2014; Mancilla et al., 2013, 2015).
628 Active deformation in the region is reflected in the location of the roughly east-west-trending
629 Africa-Iberia plate boundary. This boundary shifts from the southwest Iberian margin to north
630 Africa just across the Alboran Sea, mostly ignoring the arcuate structures of the Gibraltar Arc, and

631 confirming that subduction is not the main operating mechanism at the moment (Zitellini et al.,
632 2009).

633 In the case of the Calabrian Arc, the slab is connected to the Ionian basin that is likely floored by
634 oceanic lithosphere (Argnani, 2005; Speranza et al., 2012). The opening of the southern Tyrrhenian
635 basin caused a soft collision of the outward migrating fold-and-thrust belt into the continental
636 margins of Adria (southern Apennines) and Africa (Sicilian Maghrebides). This soft collision was
637 followed by a trench-parallel slab break-off in both the southern Apennines and Sicilian
638 Maghrebides (Fig. 12). This process produced the slab window visible, in our CA tomographic
639 model (Figs. 7 and 10). The window underneath Sicily is much wider because the slab was
640 progressively torn off at the African margin during the Tyrrhenian backarc opening (Argnani,
641 2009), whereas the slab window under the Southern Apennines formed in the last 2 Ma and extends
642 for about 300 km along the chain (Fig. 12). A choked subduction, at much reduced rates, of a
643 narrow oceanic slab continued underneath Calabria. The pull exerted by the sinking oceanic
644 lithosphere, narrowed after slab breakoff on either side of the arc, promoted the initiation of lateral
645 tears (or STEP fault) (Govers and Wortel, 2005), particularly on the western Ionian side and along
646 the north-south branch of the Aeolian Islands (Argnani and Bonazzi, 2005; Argnani et al., 2007;
647 Argnani, 2009). The sinking Ionian slab decoupled from the overlying Calabrian orogen and
648 released the upper plate from compressional stresses, favouring the wedging of asthenosphere, as
649 indicated by reduced upper mantle Pn velocities (Mele et al., 1998) and confirmed by seismic
650 attenuation measurements (Chiarabba et al., 2008; Monna and Dahm, 2009); this last process, in
651 turn, promoted uplift and extension in the Calabrian Arc.

652

653

654

655 **Acknowledgements**

The OBS teleseismic data was collected during the NEAREST EC-project (coordinator N. Zitellini) and the TYDE project (participants: INGV, ISMAR-CNR, IfM-GEOMAR and University of Hamburg University). We thank the NEAREST and TYDE Working Group for making the seismic data available. Waveforms for the CA model can be downloaded from the European Integrated Data Archive (EIDA; <http://eida.rm.ingv.it>). Arrival times at land station for the GA model were extracted from the International Seismic Center (ISC; <http://www.isc.ac.uk>). Teleseismic event location is provided by the National Earthquake Information Center (NEIC; <http://earthquake.usgs.gov/research>). Data from SAPTEX and SeSCAL experiment are available upon request from giovannibattista.cimini@ingv.it. The figures were produced with GMT (Wessel and Smith, 1991).

656

657 **References**

- 658 Abbassene, F., Chazot, G., Bellon, H., Bruguier, O., Ouabadi, A., Maury, R.C., Déverchère, J.,
659 Bosch, D., Monié, P., 2016. A 17Ma onset for the post-collisional K-rich calc-alkaline
660 magmatism in the Maghrebides: Evidence from Bougaroun (northeastern Algeria) and
661 geodynamic implications. *Tectonophysics*, 674, 114–134.
- 662 Alvarez-Marrón, J., 1999. Pliocene to Holocene structure of the Eastern Alboran Sea (Western
663 Mediterranean). *Proceedings of the Ocean Drilling Program, Scientific Results*, 161, 345-
664 355. doi:10.2973/odp.proc.sr.161.224.1999
- 665 Amato, A., Alessandrini, B., Cimini, G.B., 1993. Teleseismic wave tomography of Italy, in: Iyer,
666 H.M., Hirahaha, K. (Eds.), *Seismic Tomography: Theory and Practice*. Chapman and Hall,
667 London, pp. 361–397.
- 668 Argnani, A., 2012. Plate motion and the evolution of Alpine Corsica and Northern Apennines.
669 *Tectonophysics, Orogenic processes and structural heritage in Alpine-type mountain belts*
670 579, 207–219. doi:10.1016/j.tecto.2012.06.010
- 671 Argnani, A., 2009. Evolution of the southern Tyrrhenian slab tear and active tectonics along the
672 western edge of the Tyrrhenian subducted slab, in: Hinsbergen, D.J.J.V., Edwards, M.A.,
673 Govers, R. (Eds.), *Collision and Collapse at the Africa–Arabia–Eurasia Subduction Zone*.
674 The Geological Society, London, Special Publications, pp. 193 – 212.
- 675 Argnani, A., 2006. Some issues regarding the central Mediterranean neotectonics. *Boll. Geof. Teor.*
676 *Appl.* 47, 13 – 37.
- 677 Argnani, A., 2005. Possible record of a Triassic ocean in the southern Apennines. *Boll. Soc. Geol.*
678 *It.* 124, 109 – 121.
- 679 Argnani, A., 2000. The southern Apennines-Tyrrhenian system within the kinematic frame of the
680 central Mediterranean. *Mem. Soc. Geol. It* 55, 115 – 122.
- 681 Argnani, A., Savelli, C., 1999. Cenozoic volcano-tectonics in the southern Tyrrhenian Sea: Space–
682 time distribution and geodynamic significance. *J. Geodyn.* 27, 409 – 432.
- 683 Argnani A. and Bonazzi C., 2005. Tectonics of Eastern Sicily Offshore. *Tectonics* 24, TC4009,
684 doi:10.1029/2004TC001656
- 685 Argnani, A., Serpelloni, E., Bonazzi, C., 2007. Pattern of deformation around the central Aeolian
686 Islands: evidence from multichannel seismics and GPS data. *Terra Nova* 19, 317–323.
687 doi:10.1111/j.1365-3121.2007.00753.x
- 688 Baccheschi, P., Margheriti, L., Steckler, M.S., 2008. SKS splitting in Southern Italy: Anisotropy
689 variations in a fragmented subduction zone. *Tectonophysics* 462, 49–67.
690 doi:10.1016/j.tecto.2007.10.014
- 691 Barberi, F., Innocenti, F., Ferrara, G., Keller, J., Villari, L., 1974. Evolution of Eolian arc volcanism

- 692 (Southern Tyrrhenian Sea). *Earth and Planetary Science Letters* 21, 269–276.
693 doi:10.1016/0012-821X(74)90161-7
- 694 Bezada, M.J., Humphreys, E.D., Toomey, D.R., Harnafi, M., Dávila, J.M., Gallart, J., 2013.
695 Evidence for slab rollback in westernmost Mediterranean from improved upper mantle
696 imaging. *Earth and Planetary Science Letters* 368, 51–60. doi:10.1016/j.epsl.2013.02.024
- 697 Bigi, G., Cosentino, D., Parotto, M., Sartori, R., Scandone, P., 1990 Structural Model of Italy
698 1:500.000. CNR, Progetto Finalizzato Geodinamica.
- 699 Biju-Duval, B., Morel, Y., Baudrimont, A., Bizon, G., Bizon, J.J., 1982. Données nouvelles sur les
700 marges du Bassin Ionien profond (Méditerranée Orientale). Résultats des campagnes
701 Escarmed. *Oil & Gas Science and Technology - Rev. IFP* 37, 713–732.
702 doi:10.2516/ogst:1982036
- 703 Bijwaard, H., Spakman, W., 2000. Non-linear global P-wave tomography by iterated linearized
704 inversion. *Geophysical Journal International* 141, 71–82. doi:10.1046/j.1365-
705 246X.2000.00053.x
- 706 Blanco, M.J., Spakman, W., 1993. The P-wave velocity structure of the mantle below the Iberian
707 Peninsula: evidence for subducted lithosphere below southern Spain. *Tectonophysics* 221,
708 13–34. doi:10.1016/0040-1951(93)90025-F
- 709 Blankenship, C.L., 1992. Structure and palaeogeography of the External Betic Cordillera, southern
710 Spain. *Marine and Petroleum Geology* 9, 256–264. doi:10.1016/0264-8172(92)90074-O
- 711 Bonardi, G., Cavazza, W., Perrone, V., Rossi, S., 2001. Calabria-Peloritani terrane and northern
712 Ionian Sea, in: Vai, G.B., Martini, I.P. (Eds.), *Anatomy of an Orogen: The Apennines and*
713 *Adjacent Mediterranean Basins*. Springer Netherlands, pp. 287–306.
- 714 **Bonnin, M., Nolet, G., Villaseñor, A., Gallart, J., Thomas, C., 2014. Multiple-frequency**
715 **tomography of the upper mantle beneath the African/Iberian collision zone, *Geophys. J. Int.*,**
716 **198(3), 1458-1473, doi:10.1093/gji/ggu214.**
- 717 Booth-Rea, G., Ranero, C.R., Martínez-Martínez, J.M., Grevemeyer, I., 2007. Crustal types and
718 Tertiary tectonic evolution of the Alborán sea, western Mediterranean. *Geochem. Geophys.*
719 *Geosyst.* 8, Q10005. doi:10.1029/2007GC001639
- 720 Bordoni, P., Valensise, G., 1998. Deformation of the 125 ka marine terrace in Italy: Tectonic
721 implications, in: Stewart, I.S., Finzi, C.V. (Eds.), *Coastal Tectonics, Special Publications*.
722 The Geological Society, London, pp. 71 – 110.
- 723 **Braga, J.C., Martín, J.M., Quesada, C., 2003. Patterns and average rates of late Neogene– recent**
724 **uplift of the Betic Cordillera, SE Spain. *Geomorphology* 50, 3–26, doi:10.1016/S0169-**
725 **555X(02)00205-2**
- 726 Buforn, E., Bezzeghoud, M., Udías, A., Pro, C., 2004. Seismic Sources on the Iberia-African Plate

727 Boundary and their Tectonic Implications. *Pure appl. geophys.* 161, 623–646.
728 doi:10.1007/s00024-003-2466-1

729 Buforn, E., Pro, C., Cesca, S., Udias, A. S., del Fresno, C., 2011. The 2010 Granada, Spain, deep
730 earthquake, *Bull. Seism. Soc. Am.*, 101(5):2418-2430. doi: 10.1785/0120110022.

731 Burchfiel, B.C., Royden, L.H., 1991. Antler orogeny: A Mediterranean-type orogeny. *Geology*, 19,
732 66–69.

733 Butler, J.P., Beaumont, C., Jamieson, R.A., 2014. The Alps 2: Controls on crustal subduction and
734 (ultra)high-pressure rock exhumation in Alpine-type orogens, *J. Geophys. Res. Solid Earth*,
735 119, 5987–6022, doi:10.1002/ 2013JB010799.

736 Calvert, A., Sandvol, E., Seber, D., Barazangi, M., Vidal, F., Alguacil, G., Jabour, N., 2000.
737 Propagation of regional seismic phases (Lg and Sn) and Pn velocity structure along the
738 Africa–Iberia plate boundary zone: tectonic implications. *Geophysical Journal International*
739 142, 384–408. doi:10.1046/j.1365-246x.2000.00160.x

740 Carminati, E., Giunchi, C., Argnani, A., Sabadini, R., Fernandez, M., 1999. Plio-Quaternary vertical
741 motion of the Northern Apennines: Insights from dynamic modeling. *Tectonics* 18, 703–
742 718. doi:10.1029/1999TC900015

743 Carminati, E., Lustrino, M., Doglioni, C., 2012. Geodynamic evolution of the central and western
744 Mediterranean: Tectonics vs. igneous petrology constraints. *Tectonophysics, Orogenic*
745 *processes and structural heritage in Alpine-type mountain belts* 579, 173–192.
746 doi:10.1016/j.tecto.2012.01.026

747 Carminati, E., Wortel, M.J.R., Spakman, W., Sabadini, R., 1998. The role of slab detachment
748 processes in the opening of the western–central Mediterranean basins: some geological and
749 geophysical evidence. *Earth and Planetary Science Letters* 160, 651–665.
750 doi:10.1016/S0012-821X(98)00118-6

751 Carrara, G., NEAREST Team, 2008. NEAREST 2008 CRUISE PRELIMINARY REPORT R/V
752 URANIA, 1st Aug 2008- 04th Sept 2008, Technical Report. ISMAR CNR.




753 Chamot-Rooke, N., Jestin, F., 1997. Constraints on Moho Depth and Crustal Thickness in the
754 Liguro-Provençal Basin from a 3d Gravity Inversion: Geodynamic Implications. *REVUE*
755 *DE L' INSTITUT FRANCAIS DU PETROLE* 52, 557–583. doi:10.2516/ogst:1997060

756 Channell, J.E.T., Oldow, J.S., Catalano, R., D'Argenio, B., 1990. Paleomagnetically determined
757 rotations in the western Sicilian fold and thrust belt. *Tectonics* 9, 641–660.
758 doi:10.1029/TC009i004p00641

759 Chertova, M.V., Spakman, W., Geenen, T., van den Berg, A.P., van Hinsbergen, D.J.J., 2014.
760 Underpinning tectArgnani A. and Bonazzi C. (2005) - Tectonics of Eastern Sicily Offshore. *Tectonics*, 24,
761 TC4009, doi:10.1029/2004TC001656.onic reconstructions of the western Mediterranean region

- 762 with dynamic slab evolution from 3-D numerical modeling. *J. Geophys. Res. Solid Earth*
763 119, 2014JB011150. doi:10.1002/2014JB011150
- 764 Chiarabba, C., De Gori, P., Speranza, F., 2008. The southern Tyrrhenian subduction zone: Deep
765 geometry, magmatism and Plio-Pleistocene evolution. *Earth and Planetary Science Letters*
766 268, 408–423. doi:10.1016/j.epsl.2008.01.036
- 767 Cifelli, F., Mattei, M., Porreca, M., 2008. New paleomagnetic data from Oligocene–upper Miocene
768 sediments in the Rif chain (northern Morocco): Insights on the Neogene tectonic evolution
769 of the Gibraltar arc. *J. Geophys. Res.* 113, B02104. doi:10.1029/2007JB005271
- 770 Cifelli, F., Mattei, M., Rossetti, F., 2007. Tectonic evolution of arcuate mountain belts on top of a
771 retreating subduction slab: The example of the Calabrian Arc. *J. Geophys. Res.* 112,
772 B09101. doi:10.1029/2006JB004848
- 773 Cimini, G.B., 1999. P-wave deep velocity structure of the Southern Tyrrhenian Subduction Zone
774 from nonlinear teleseismic travelttime tomography. *Geophys. Res. Lett.* 26, 3709–3712.
775 doi:10.1029/1999GL010907
- 776 Cimini, G.B., De Gori, P., Frepoli, A., 2006. Passive seismology in southern Italy: the SAPTEX
777 array *Ann. Geophys.*, 49 (2/3), 825–840.
- 778 Cimini, G.B., Marchetti, A., 2006. Deep structure of peninsular Italy from seismic tomography and
779 subcrustal seismicity. *Ann. Geophys. Supplement - to - Vol - 49*, 331 – 345.
- 780 Cloos, M., 1993. Lithospheric buoyancy and collisional orogenesis: subduction of oceanic plateaus,
781 continental margins, island arcs, spreading ridges, and seamounts. *Bulletin of the Geological*
782 *Society of America* 105, 715–737.
- 783 D’Agostino, N., D’Anastasio, E., Gervasi, A., Guerra, I., Nedimović, M.R., Seeber, L., Steckler,
784 M., 2011. Forearc extension and slow rollback of the Calabrian Arc from GPS
785 measurements. *Geophys. Res. Lett.* 38, L17304. doi:10.1029/2011GL048270
- 786 Dahm, T., Thorwart, M., Flueh, E.R., Braun, T., Herber, R., Favali, P., Beranzoli, L., D’Anna, G.,
787 Frugoni, F., Smriglio, G., 2002. Ocean bottom seismometers deployed in Tyrrhenian Sea.
788 *Eos Trans. AGU* 83, 309–315. doi:10.1029/2002EO000221
- 789 De Astis, G., Ventura, G., Vilaro, G., 2003. Geodynamic significance of the Aeolian volcanism
790 (Southern Tyrrhenian Sea, Italy) in light of structural, seismological, and geochemical data.
791 *Tectonics* 22, 1040. doi:10.1029/2003TC001506
- 792 Dewey, J.F., 1988. Extensional collapse of orogens. *Tectonics* 7, 1123–1139.
793 doi:10.1029/TC007i006p01123
- 794 Dewey, J.F., Helman, M.L., Knott, S.D., Turco, E., Hutton, D.H.W., 1989. Kinematics of the
795 western Mediterranean. Geological Society, London, Special Publications 45, 265–283.
796 doi:10.1144/GSL.SP.1989.045.01.15

- 797 Dewey, J.F., Pitman, W.C., Ryan, W.B.F., Bonnin, J., 1973. Plate Tectonics and the Evolution of
798 the Alpine System. *Geological Society of America Bulletin* 84, 3137–3180.
799 doi:10.1130/0016-7606(1973)84<3137:PTATEO>2.0.CO;2
- 800 Duarte, J.C., Rosas, F.M., Terrinha, P., Schellart, W.P., Boutelier, D., Gutscher, M.-A., Ribeiro, A.,
801 2013. Are subduction zones invading the Atlantic? Evidence from the southwest Iberia
802 margin. *Geology* G34100.1. doi:10.1130/G34100.1
- 803 Duggen, S., Hoernle, K., Bogaard, P.V.D., Garbe-Schönberg, D., 2005. Post-Collisional Transition
804 from Subduction- to Intraplate-type Magmatism in the Westernmost Mediterranean:
805 Evidence for Continental-Edge Delamination of Subcontinental Lithosphere. *J. Petrology*
806 46, 1155–1201. doi:10.1093/petrology/egi013
- 807 Faccenna, C., Mattei, M., Funiciello, R., Jolivet, L., 1997. Styles of back-arc extension in the
808 Central Mediterranean. *Terra Nova* 9, 126–130. doi:10.1046/j.1365-3121.1997.d01-12.x
- 809 Faccenna, C., Molin, P., Orecchio, B., Olivetti, V., Bellier, O., Funiciello, F., Minelli, L., Piromallo,
810 C., Billi, A., 2011. Topography of the Calabria subduction zone (southern Italy): Clues for
811 the origin of Mt. Etna. *Tectonics* 30, TC1003. doi:10.1029/2010TC002694
- 812 Faccenna, C., Piromallo, C., Crespo-Blanc, A., Jolivet, L., Rossetti, F., 2004. Lateral slab
813 deformation and the origin of the western Mediterranean arcs. *Tectonics* 23, TC1012.
814 doi:10.1029/2002TC001488
- 815 Favali, P., Chierici, F., Marinaro, G., Giovanetti, G., Azzarone, A., Beranzoli, L., De Santis, A.,
816 Embriaco, D., Monna, S., Bue, N. Lo, Sgroi, T., Cianchini, G., Badiali, L., Qamili, E., De
817 Caro, M.G., Falcone, G., Montuori, C., Frugoni, F., Riccobene, G., Sedita, M., Barbagallo,
818 G., Cacopardo, G., Cali, C., Cocimano, R., Coniglione, R., Costa, M., D'Amico, A., Del
819 Tevere, F., Distefano, C., Ferrera, F., Giordano, V., Imbesi, M., Lattuada, D., Migneco, E.,
820 Musumeci, M., Orlando, A., Papaleo, R., Piattelli, P., Raia, G., Rovelli, A., Sapienza, P.,
821 Speziale, F., Trovato, A., Viola, S., Ameli, F., Bonori, M., Capone, A., Masullo, R.,
822 Simeone, F., Pignagnoli, L., Zitellini, N., Bruni, F., Gasparoni, F., Pavan, G., 2013. NEMO-
823 SN1 Abyssal Cabled Observatory in the Western Ionian Sea. *IEEE Journal of Oceanic*
824 *Engineering* 38, 358–374. doi:10.1109/JOE.2012.2224536
- 825 Fillerup, M.A., Knapp, J.H., Knapp, C.C., Raileanu, V. 2010. Mantle earthquakes in the absence of
826 subduction? Continental delamination in the Romanian Carpathians. *Lithosphere* 2. 333–
827 340, doi: 10.1130/L102.1
- 828 Frepoli, A., Maggi, C., Cimini, G.B., Marchetti, A., Chiappini, M., 2011. Seismotectonic of
829 Southern Apennines from recent passive seismic experiments. *Journal of Geodynamics,*
830 *Active Tectonics of the Circum-Adriatic Region* 51, 110–124.
831 doi:10.1016/j.jog.2010.02.007

- 832 Frepoli, A., Selvaggi, G., Chiarabba, C., Amato, A., 1996. State of stress in the Southern
833 Tyrrhenian subduction zone from fault-plane solutions. *Geophys. J. Int.* 125, 879–891.
834 doi:10.1111/j.1365-246X.1996.tb06031.x
- 835 Gattacceca, J., Speranza, F., 2002. Paleomagnetism of Jurassic to Miocene sediments from the
836 Apenninic carbonate platform (southern Apennines, Italy): evidence for a 60°
837 counterclockwise Miocene rotation. *Earth and Planetary Science Letters* 201, 19–34.
838 doi:10.1016/S0012-821.
- 839 Geissler, W.H., Matias, L., Stich, D., Carrilho, F., Jokat, W., Monna, S., IbenBrahim, A., Mancilla,
840 F., Gutscher, M.-A., Sallarès, V., Zitellini, N., 2010. Focal mechanisms for sub-crustal
841 earthquakes in the Gulf of Cadiz from a dense OBS deployment. *Geophys. Res. Lett.* 37,
842 L18309. doi:10.1029/2010GL044289
- 843 Giacomuzzi, G., Chiarabba, C., De Gori, P., 2011. Linking the Alps and Apennines subduction
844 systems: New constraints revealed by high-resolution teleseismic tomography. *Earth and*
845 *Planetary Science Letters* 301, 531–543. doi:10.1016/j.epsl.2010.11.033
- 846 Giacomuzzi, G., Civalleri, M., De Gori, P., Chiarabba, C., 2012. A 3D Vs model of the upper
847 mantle beneath Italy: Insight on the geodynamics of central Mediterranean. *Earth and*
848 *Planetary Science Letters* 335–336, 105–120. doi:10.1016/j.epsl.2012.05.004
- 849 Gil, A., Gallart, J., Diaz, J., Carbonell, R., Torne, M., Levander, A., Harnafi, M., 2014. Crustal
850 structure beneath the Rif Cordillera, North Morocco, from the RIFSIS wide-angle reflection
851 seismic experiment. *Geochem. Geophys. Geosyst.* 15, 4712–4733.
852 doi:10.1002/2014GC005485
- 853 Goes, S., Giardini, D., Jenny, S., Hollenstein, C., Kahle, H.-G., Geiger, A., 2004. A recent tectonic
854 reorganization in the south-central Mediterranean. *Earth and Planetary Science Letters* 226,
855 335–345. doi:10.1016/j.epsl.2004.07.038
- 856 
- 857 
- 858 
- 859 Grad, M., Tiira, T., ESC Working Group, 2009. The Moho depth map of the European Plate.
860 *Geophysical Journal International* 176, 279–292. doi:10.1111/j.1365-246X.2008.03919.x
- 861 Gutscher, M.-A., Dominguez, S., Westbrook, G.K., Le Roy, P., Rosas, F., Duarte, J.C., Terrinha, P.,
862 Miranda, J.M., Graindorge, D., Gailler, A., Sallares, V., Bartolome, R., 2012. The Gibraltar
863 subduction: A decade of new geophysical data. *Tectonophysics* 574–575, 72–91.
864 doi:10.1016/j.tecto.2012.08.038
- 865 Gutscher, M.-A., Malod, J., Rehault, J.-P., Contrucci, I., Klingelhoefer, F., Mendes-Victor, L.,
866 Spakman, W., 2002. Evidence for active subduction beneath Gibraltar. *Geology* 30, 1071–

867 1074. doi:10.1130/0091-7613.

868 Gvirtzman, Z., Nur, A., 1999. The formation of Mount Etna as the consequence of slab rollback.
869 Nature 401, 782–785. doi:10.1038/44555

870 Hacker, B.R., Peacock, S.M., Abers, G.A., Holloway, S.D., 2003. Subduction factory 2. Are
871 intermediate-depth earthquakes in subducting slabs linked to metamorphic dehydration
872 reactions? J. Geophys. Res. 108, 2030. doi:10.1029/2001JB001129

873 Hacker, B.R., Andersen, T.B., Johnston, S., Kylander-Clark, A.R.C., Peterman, E.M., Walsh, E.O.,
874 Young, D., 2010. High-temperature deformation during continental-margin subduction &
875 exhumation: The ultrahigh-pressure Western Gneiss Region of Norway. Tectonophysics
876 480: 149-171.

877 Horvath, F., Berckhemer, H., 1982. Mediterranean backarc basins, in: Berckhemer, H., Hsu, K.
878 (Eds.), Alpine-Mediterranean Geodynamics, AGU Geodynamic Series. pp. 141 – 173.

879 Jolivet, L., Faccenna, C., 2000. Mediterranean extension and the Africa-Eurasia collision. Tectonics
880 19, 1095–1106. doi:10.1029/2000TC900018

881 Jenny, S., Goes, S., Giardini, D., Kahle, H.-G., 2006. Seismic potential of Southern Italy,
882 Tectonophysics., 415, 81–101. doi:10.1016/j.tecto.2005.12.003

883

884 Kastens, K., Mascle, J., Auroux, C., Bonatti, E., Broglia, C., Channell, J., Curzi, P., Emeis, K.-C.,
885 Glaçon, G., Hasegawa, S., Hieke, W., Mascle, G., McCOY, F., Mckenzie, J., Mendelson, J.,
886 Müller, C., Réhault, J.-P., Robertson, A., Sartori, R., Sprovieri, R., Torii, M., 1988. ODP
887 Leg 107 in the Tyrrhenian Sea: Insights into passive margin and back-arc basin evolution.
888 Geological Society of America Bulletin 100, 1140–1156. doi:10.1130/0016-7606

889 Kennett, B.L.N., Engdahl, E.R., Buland, R., 1995. Constraints on seismic velocities in the Earth
890 from traveltimes. Geophysical Journal International 122, 108–124. doi:10.1111/j.1365-
891 246X.1995.tb03540.x

892 Koulakov, I., Kaban, M.K., Tesauro, M., Cloetingh, S., 2009. P- and S-velocity anomalies in the
893 upper mantle beneath Europe from tomographic inversion of ISC data. Geophysical Journal
894 International 179, 345–366. doi:10.1111/j.1365-246X.2009.04279.x

895 Krijgsman, W., Garcés M., 2004. Paleomagnetic constraints on the geodynamic evolution of the
896 Gibraltar Arc. Terra Nova 281–287.

897 Le Pichon, X., 1982. Land-locked oceanic basins and continental collision: The Eastern
898 Mediterranean as a case example. In K.J. HSU (ed Mountain Building Processes,,
899 Academic Press, London, 201-211.

900 Le Pichon, X., Bergerat, F., Roulet, M.-J., 1988. Plate kinematics and tectonics leading to the
901 Alpine belt formation; A new analysis, in: Geological Society of America Special Papers.

902 Geological Society of America, pp. 111–132.

903 Levander, A., Bezada, M.J., Niu, F., Humphreys, E.D., Palomeras, I., Thurner, S.M., Masy, J.,
904 Schmitz, M., Gallart, J., Carbonell, R., Miller, M.S., 2014. Subduction-driven recycling of
905 continental margin lithosphere. *Nature* 515, 253–256. doi:10.1038/nature13878

906 Lindquist, K.G., Engle, K., Stahlke, D., Price, E., 2004. Global topography and bathymetry grid
907 improves research efforts. *Eos Trans. AGU* 85, 186–186. doi:10.1029/2004EO190003

908 Lonergan, L., White, N., 1997. Origin of the Betic-Rif mountain belt. *Tectonics* 16, 504–522.
909 doi:10.1029/96TC03937

910 Malinverno, A., Ryan, W.B.F., 1986. Extension in the Tyrrhenian Sea and shortening in the
911 Apennines as result of arc migration driven by sinking of the lithosphere. *Tectonics* 5, 227–
912 245. doi:10.1029/TC005i002p00227

913 Mancilla, F. de L., Stich, D., Berrocoso, M., Martín, R., Morales, J., Fernandez-Ros, A., Páez, R.,
914 Pérez-Peña, A., 2013. Delamination in the Betic Range: Deep structure, seismicity, and GPS
915 motion. *Geology* 41, 307–310. doi:10.1130/G33733.1

916 Mancilla, F. de L., Booth-Rea, G., Stich, D., Pérez-Peña, J.V., Morales, J., Azañón, J.M., Martin,
917 R., Giaconia, F., 2015. Slab rupture and delamination under the Betics and Rif constrained
918 from receiver functions. Original Research Article *Tectonophysics*, In Press.

919 Mascle, J., Kastens, K., Auroux, C., 1988. A land-locked back-arc basin: preliminary results from
920 ODP Leg 107 in the Tyrrhenian Sea. *Tectonophysics* 146, 149–162. doi:10.1016/0040-
921 1951(88)90088-1

922 Mauffret, A., Frizon de Lamotte, D., Lallemand, S., Gorini, C., Maillard, A., 2004. E–W opening of
923 the Algerian Basin (Western Mediterranean). *Terra Nova*, 16, 257–264.

924 Maury, R. C., R., Fourcade, S., Coulon, C., Azzouzi, M. El, Bellon, H., Coutelle, A., Ouabadi, A.,
925 Semroud, B., Megartsi, M., Cotten, J., Belanteur, O., Louni-Hacini, A., Piqué, A.,
926 Capdevila, R., Hernandez, J., Réhault, J.-P., 2000. Post-collisional Neogene magmatism of
927 the Mediterranean Maghreb margin: a consequence of slab breakoff. *Comptes Rendus de*
928 *l'Académie des Sciences - Series IIA - Earth and Planetary Science* 331, 159–173.
929 doi:10.1016/S1251-8050(00)01406-3

930 Medaouri, M., Déverchère, J., Graindorge, D., Bracene, R., Badji, R., Ouabadi, A., Yelles-
931 Chaouche, K., Bendiab, F., 2014. The transition from Alboran to Algerian basins (Western
932 Mediterranean Sea): Chronostratigraphy, deep crustal structure and tectonic evolution at the
933 rear of a narrow slab rollback system. *Journal of Geodynamics*, SI: Geodynamic evolution
934 of the Alboran domain 77, 186–205. doi:10.1016/j.jog.2014.01.003

935 Mele, G., Rovelli, A., Seber, D., Hearn, T.M., Barazangi, M., 1998. Compressional velocity
936 structure and anisotropy in the uppermost mantle beneath Italy and surrounding regions. *J.*

937 Geophys. Res. 103, 12529–12543. doi:10.1029/98JB00596

938 Molnar, P., England, P.C., Jones, C.H., 2015. Mantle dynamics, isostasy, and the support of high
939 terrain. *J. Geophys. Res. Solid Earth* 120, 2014JB011724. doi:10.1002/2014JB011724

940 Monna, S., Argnani, A., Cimini, G.B., Frugoni, F., Montuori, C., 2015. Constraints on the
941 geodynamic evolution of the Africa–Iberia plate margin across the Gibraltar Strait from
942 seismic tomography. *Geoscience Frontiers, Special Issue: Plate and plume tectonics:
943 Numerical simulation and seismic tomography* 6, 39–48. doi:10.1016/j.gsf.2014.02.003

944 Monna, S., Cimini, G.B., Montuori, C., Matias, L., Geissler, W.H., Favali, P., 2013a. New insights
945 from seismic tomography on the complex geodynamic evolution of two adjacent domains:
946 Gulf of Cadiz and Alboran Sea. *J. Geophys. Res. Solid Earth* 118, 1587–1601.
947 doi:10.1029/2012JB009607

948 Monna, S., Dahm, T., 2009. Three-dimensional P wave attenuation and velocity upper mantle
949 tomography of the southern Apennines–Calabrian Arc subduction zone. *J. Geophys. Res.*
950 114, B06304. doi:10.1029/2008JB005677

951 Monna, S., Frugoni, F., Montuori, C., Beranzoli, L., Favali, P., 2005. High quality seismological
952 recordings from the SN-1 deep seafloor observatory in the Mt. Etna region. *Geophys. Res.*
953 *Lett.* 32, L07303. doi:10.1029/2004GL021975

954 Monna, S., Sgroi, T., Dahm, T., 2013b. New insights on volcanic and tectonic structures of the
955 southern Tyrrhenian (Italy) from marine and land seismic data. *Geochem. Geophys.*
956 *Geosyst.* 14, 3703–3719. doi:10.1002/ggge.20227

957 Montuori, C., Cimini, G.B., Favali, P., 2007. Teleseismic tomography of the southern Tyrrhenian
958 subduction zone: New results from seafloor and land recordings. *J. Geophys. Res.* 112,
959 B03311. doi:10.1029/2005JB004114

960 Morais, I., Vinnik, L., Silveira, G., Kiselev, S., Matias, L., 2015. Mantle beneath the Gibraltar Arc
961 from receiver functions. *Geophys. J. Int.* 200, 1155–1171. doi:10.1093/gji/ggu456

962 Neri, G., Marotta, A.M., Orecchio, B., Presti, D., Totaro, C., Barzaghi, R., Borghi, A., 2012. How
963 lithospheric subduction changes along the Calabrian Arc in southern Italy: geophysical
964 evidences. *Int J Earth Sci (Geol Rundsch)* 101, 1949–1969. doi:10.1007/s00531-012-0762-7

965 Otsuki, K., 1989. Empirical relationships among the convergence rate of plates, rollback rate of
966 trench axis and island-arc tectonics: “laws of convergence rate of plates.” *Tectonophysics*
967 159, 73–94. doi:10.1016/0040-1951(89)90171-6

968 Palomeras, I., Thurner, S., Levander, A., Liu, K., Villasenor, A., Carbonell, R., Harnafi, M., 2014.
969 Finite-frequency Rayleigh wave tomography of the western Mediterranean: Mapping its
970 lithospheric structure. *Geochem. Geophys. Geosyst.* 15, 140–160.
971 doi:10.1002/2013GC004861

- 972 Patacca, E., Sartori, R., Scandone, P., 1993. Tyrrhenian Basin and Apennines. Kinematic Evolution
973 and Related Dynamic Constraints, in: Boschi, E., Mantovani, E., Morelli, A. (Eds.), Recent
974 Evolution and Seismicity of the Mediterranean Region, NATO ASI Series. Springer
975 Netherlands, pp. 161–171.
- 976 Pérez-Peña, J.V., Azor, A., Azañón, J.M., Keller, E.A., 2010. Active tectonics in the Sierra Nevada
977 (Betic Cordillera, SE Spain): insights from geomorphic indexes and drainage pattern
978 analysis. *Geomorphology* 119, 74–87.
- 979 Piromallo, C., Morelli, A., 2003. P wave tomography of the mantle under the Alpine-Mediterranean
980 area. *J. Geophys. Res.* 108, 2065. doi:10.1029/2002JB001757
- 981 Platt, J., Allerton, S., Kirker, A., Platzman, E., 1995. Origin of the western Subbetic arc (South
982 Spain): palaeomagnetic and structural evidence. *Journal of Structural Geology* 17, 765–775.
983 doi:10.1016/0191-8141(94)00110-L
- 984 Platt, J.P., Behr, W.M., Johanesen, K., Williams, J.R., 2013. The Betic-Rif Arc and Its Orogenic
985 Hinterland: A Review. *Annual Review of Earth and Planetary Sciences* 41, 313–357.
986 doi:10.1146/annurev-earth-050212-123951
- 987 Platt, J.P., Vissers, R.L.M., 1989. Extensional collapse of thickened continental lithosphere: A
988 working hypothesis for the Alboran Sea and Gibraltar arc. *Geology* 17, 540.
989 doi:10.1130/0091-7613
- 990 Platzman, E.S., Platt, J.P., Olivier, P., 1993. Palaeomagnetic rotations and fault kinematics in the
991 Rif arc of Morocco. *J. Geol. Soc. Lond.* 150:707–18
- 992 Pondrelli, S., Piromallo, C., Serpelloni, E., 2004. Convergence vs. retreat in Southern Tyrrhenian
993 Sea: Insights from kinematics. *Geophys. Res. Lett.* 31, L06611. doi:10.1029/2003GL019223
- 994 Prada, M., Sallares, V., Ranero, C.R., Vendrell, M.G., Grevemeyer, I., Zitellini, N., de Franco, R.,
995 2014. Seismic structure of the Central Tyrrhenian basin: Geophysical constraints on the
996 nature of the main crustal domains. *J. Geophys. Res. Solid Earth* 119, 2013JB010527.
997 doi:10.1002/2013JB010527
- 998 Rawlinson, N., Reading, A.M., Kennett, B.L.N., 2006. Lithospheric structure of Tasmania from a
999 novel form of teleseismic tomography. *J. Geophys. Res.* 111, B02301.
1000 doi:10.1029/2005JB003803
- 1001 Rehault, J.-P., Boillot, G., Mauffret, A., 1984. The Western Mediterranean Basin geological
1002 evolution. *Marine Geology* 55, 447 – 477. doi:http://dx.doi.org/10.1016/0025-
1003 3227(84)90081-1
- 1004 Rosenbaum, G., Gasparon, M., Lucente, F.P., Peccerillo, A., Miller, M.S., 2008. Kinematics of slab
1005 tear faults during subduction segmentation and implications for Italian magmatism.
1006 *Tectonics* 27, TC2008. doi:10.1029/2007TC002143

- 1007 Rosenbaum, G., Lister, G.S., 2004. Formation of arcuate orogenic belts in the western
1008 Mediterranean region. *Geological Society of America Special Papers* 383, 41–56.
1009 doi:10.1130/0-8137-2383-3
- 1010 Rosenbaum, G., Lister, G.S., Duboz, C., 2002. Relative motions of Africa, Iberia and Europe during
1011 Alpine orogeny. *Tectonophysics* 359, 117–129. doi:10.1016/S0040-1951
- 1012 Royden, L.H., 1993. Evolution of retreating subduction boundaries formed during continental
1013 collision. *Tectonics* 12, 629–638. doi:10.1029/92TC02641
- 1014 Sallarès, V., Gailler, A., Gutscher, M.-A., Graindorge, D., Bartolomé, R., Gràcia, E., Díaz, J.,
1015 Dañobeitia, J., Zitellini, N., 2011. Seismic evidence for the presence of Jurassic oceanic
1016 crust in the central Gulf of Cadiz (SW Iberian margin). *Earth and Planetary Science Letters*
1017 311, 1–2, 1, 112–123, doi:10.1016/j.epsl.2011.09.003
- 1018 Schettino, A., Turco, E., 2006. Plate kinematics of the Western Mediterranean region during the
1019 Oligocene and Early Miocene. *Geophysical Journal International* 166, 1398–1423.
1020 doi:10.1111/j.1365-246X.2006.02997.x
- 1021 Seber, D., Barazangi, M., Ibenbrahim, A., Demnati, A., 1996. Geophysical evidence for lithospheric
1022 delamination beneath the Alboran Sea and Rif–Betic mountains. *Nature* 379, 785–790.
1023 doi:10.1038/379785a0
- 1024 Séranne, M., 1999. The Gulf of Lion continental margin (NW Mediterranean) revisited by IBS: an
1025 overview. *Geological Society, London, Special Publications* 156, 15–36.
1026 doi:10.1144/GSL.SP.1999.156.01.03
- 1027 Serpelloni, E., Vannucci, G., Pondrelli, S., Argnani, A., Casula, G., Anzidei, M., Baldi, P.,
1028 Gasperini, P., 2007. Kinematics of the Western Africa-Eurasia plate boundary from focal
1029 mechanisms and GPS data. *Geophysical Journal International* 169, 1180–1200.
1030 doi:10.1111/j.1365-246X.2007.03367.x
- 1031 Serri, G., 1990. Neogene-Quaternary magmatism of the Tyrrhenian region: Characterization of the
1032 magma sources and its geodynamic implications. *Mem. Soc. Geol. It.* 41, 219 – 242.
- 1033 Serri, G., Innocenti, F., Manetti, P., 1993. Geochemical and petrological evidence of the subduction
1034 of delaminated Adriatic continental lithosphere in the genesis of the Neogene-Quaternary
1035 magmatism of central Italy. *Tectonophysics* 223, 117 – 147.
1036 doi:http://dx.doi.org/10.1016/0040-1951(93)90161-C
- 1037 Sethian, J.A., Popovici, A.M., 1999. 3-D travelttime computation using the fast marching method.
1038 *Geophysics* 64, 516–523. doi:10.1190/1.1444558
- 1039 Spakman, W., Wortel, R., 2004. A Tomographic View on Western Mediterranean Geodynamics, in:
1040 Cavazza, P.D.W., Roure, D.F., Spakman, P.W., Stampfli, P.G.M., Ziegler, P.P.A. (Eds.),
1041 The TRANSMED Atlas. The Mediterranean Region from Crust to Mantle. Springer Berlin

- 1042 Heidelberg, pp. 31–52.
- 1043 Speranza, F., Maniscalco, R., Mattei, M., Di Stefano, A., Butler, R.W.H., Funicello, R., 1999.
1044 Timing and magnitude of rotations in the frontal thrust systems of southwestern Sicily.
1045 *Tectonics* 18, 1178–1197. doi:10.1029/1999TC900029
- 1046 Speranza, F., Minelli, L., Pignatelli, A., Chiappini, M., 2012. The Ionian Sea: The oldest in situ
1047 ocean fragment of the world? *J. Geophys. Res.* 117, B12101. doi:10.1029/2012JB009475
- 1048 Srivastava, S.P., Roest, W.R., Kovacs, L.C., Oakey, G., Lévesque, S., Verhoef, J., Macnab, R.,
1049 1990. Alpine Evolution of Iberia and its Continental Margins Motion of Iberia since the Late
1050 Jurassic: Results from detailed aeromagnetic measurements in the Newfoundland Basin.
1051 *Tectonophysics* 184, 229 – 260. doi:http://dx.doi.org/10.1016/0040-1951
- 1052 Stampfli, G.M., Borel, G.D., 2002. A plate tectonic model for the Paleozoic and Mesozoic
1053 constrained by dynamic plate boundaries and restored synthetic oceanic isochrons. *Earth and*
1054 *Planetary Science Letters* 196, 17–33. doi:10.1016/S0012-821X(01)00588-X
- 1055 Stich, D., R. Martin, and J. Morales (2010), Moment tensor inversion for Iberia–Maghreb
1056 earthquakes 2005–2008, *Tectonophysics.*, 483, 390-398
- 1057 Stich, D., Serpelloni, E., de Lis Mancilla, F., Morales, J., 2006. Kinematics of the Iberia–Maghreb
1058 plate contact from seismic moment tensors and GPS observations. *Tectonophysics* 426,
1059 295–317. doi:10.1016/j.tecto.2006.08.004
- 1060 Thurner, S. Palomeras, I., Levander, A., Carbonell, R., Lee, C. T., 2014. Ongoing lithospheric
1061 removal in the Western Mediterranean: Ps receiver function results from the PICASSO
1062 project. *Geochem. Geophys. Geosyst.* 15, 1113–1127.
- 1063 Tortorici, L., Monaco, C., Tansi, C., Cocina, O., 1995. Recent and active tectonics in the Calabrian
1064 arc (Southern Italy). *Tectonophysics, Kinematics of distributed deformation in plate*
1065 *boundary zones with emphasis on the Mediterranean, Anatolia and Eastern Asia* 243, 37–55.
1066 doi:10.1016/0040-1951(94)00190-K
- 1067 van Hinsbergen, D.J.J., Vissers, R.L.M., Spakman, W., 2014. Origin and consequences of western
1068 Mediterranean subduction, rollback, and slab segmentation. *Tectonics* 33, 2013TC003349.
1069 doi:10.1002/2013TC003349
- 1070 Vannucci, G., Pondrelli, S., Argnani, A., Morelli, A., Gasperini, P., Boschi, E., 2004. An atlas of
1071 Mediterranean seismicity. *Ann. Geophys.* 47. doi:10.4401/ag-3276
- 1072 Vergés, J., Fernández, M., 2012. Tethys–Atlantic interaction along the Iberia–Africa plate
1073 boundary: The Betic–Rif orogenic system. *Tectonophysics, Orogenic processes and*
1074 *structural heritage in Alpine-type mountain belts.* *Tectonophysics* 579, 144–172.
1075 doi:10.1016/j.tecto.2012.08.032.
- 1076 Villaseñor, A., Chevrot, S., Harnafi, M., Gallart, J., Pazos, A., Serrano, I., Córdoba, D., Pulgar, J.

1077 A., Ibarra, P., 2015. Subduction and volcanism in the Iberia-North Africa collision zone
1078 from tomographic images of the upper mantle. *Tectonophysics* 663, 238-249,
1079 doi:10.1016/j.tecto.2015.08.042.

1080 **Visser, R.L.M., Meijer, P. Th, 2012. Iberian plate kinematics and Alpine collision in the Pyrenees.**
1081 **Earth Science Reviews 114, 61e83, doi: 10.1016/j.earscirev.2012.05.001**

1082 Watts, A.B., Platt, J.P., Buhl, P., 1993. Tectonic evolution of the Alboran Sea basin. *Basin Research*
1083 5, 153–177.

1084 Westaway, R., 1993. Quaternary uplift of southern Italy. *J. Geophys. Res.* 98, 21741–21772.
1085 doi:10.1029/93JB01566.

1086 **Wessel, P., and W. H. Smith (1991), Free software helps map and display**
1087 **data, *Eos Trans. AGU*, 72(41), 441.**

1088 Wildi, W., 1983. La Chaîne tello-rifaine (Algérie, Maroc, Tunisie): structure, stratigraphie et
1089 évolution du trias au miocène *Rev. Geol. Dyn. Geogr. Phys.*, 24, 201-297.

1090 Wortel, M.J.R., Spakman, W., 2000. Subduction and Slab Detachment in the Mediterranean-
1091 Carpathian Region. *Science* 290, 1910–1917. doi:10.1126/science.290.5498.1910

1092 Wortel, M.J.R., Spakman, W., 1992. Structure and dynamics of subducted lithosphere in the
1093 Mediterranean region. *Proc. Kon. Ned. Acad. Wetensch* 95, 325 – 347.

1094 Zeck, H.P., 1996. Betic-Rif orogeny: subduction of Mesozoic Tethys lithosphere under eastward
1095 drifting Iberia, slab detachment shortly before 22 Ma, and subsequent uplift and extensional
1096 tectonics. *Tectonophysics* 254, 1–16. doi:10.1016/0040-1951(95)00206-5

1097 Zitellini, N., Gràcia, E., Matias, L., Terrinha, P., Abreu, M.A., DeAlteriis, G., Henriët, J.P.,
1098 Dañobeitia, J.J., Masson, D.G., Mulder, T., Ramella, R., Somoza, L., Diez, S., 2009. The
1099 quest for the Africa–Eurasia plate boundary west of the Strait of Gibraltar. *Earth and*
1100 *Planetary Science Letters* 280, 13–50. doi:10.1016/j.epsl.2008.12.005

1101
1102
1103
1104
1105
1106
1107
1108
1109
1110

1111

1112

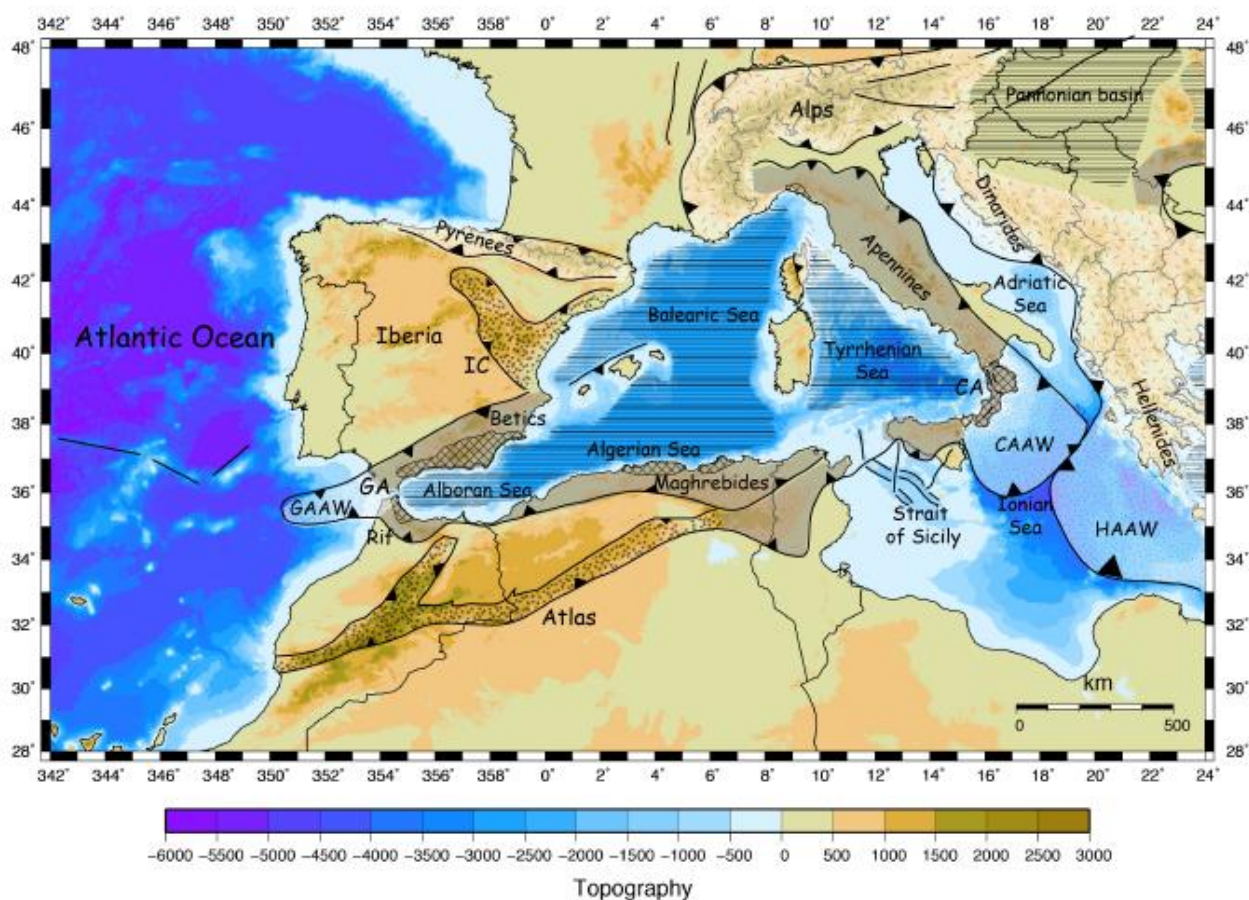
1113

1114

1115

1116

1117 **Figure 1**



1118 **Fig. 1.** Simplified geological map of the CWM region. The system of fold-and-thrust belts,
1119 indicated in gray, formed from Late Oligocene to Pliocene, during the opening of the backarc basins
1120 (horizontal rules; also including the volcanic arcs). The accretionary wedges related to oceanic
1121 subduction are indicated with fine dots (GAAW: Gibraltar Arc Accretionary Wedge; CAAW:
1122 Calabrian Arc Accretionary Wedge; HAAW: Hellenic Arc Accretionary Wedge). The units
1123 belonging to the internal domain are shown with cross hatching. The collisional belts are indicated
1124 with random dashes, whereas the Atlas and Iberian Chain (IC) intracontinental belts are indicated
1125 with coarse dots. BF: Bradanic foredeep basin; GCF: Gela-Catania foredeep basin.

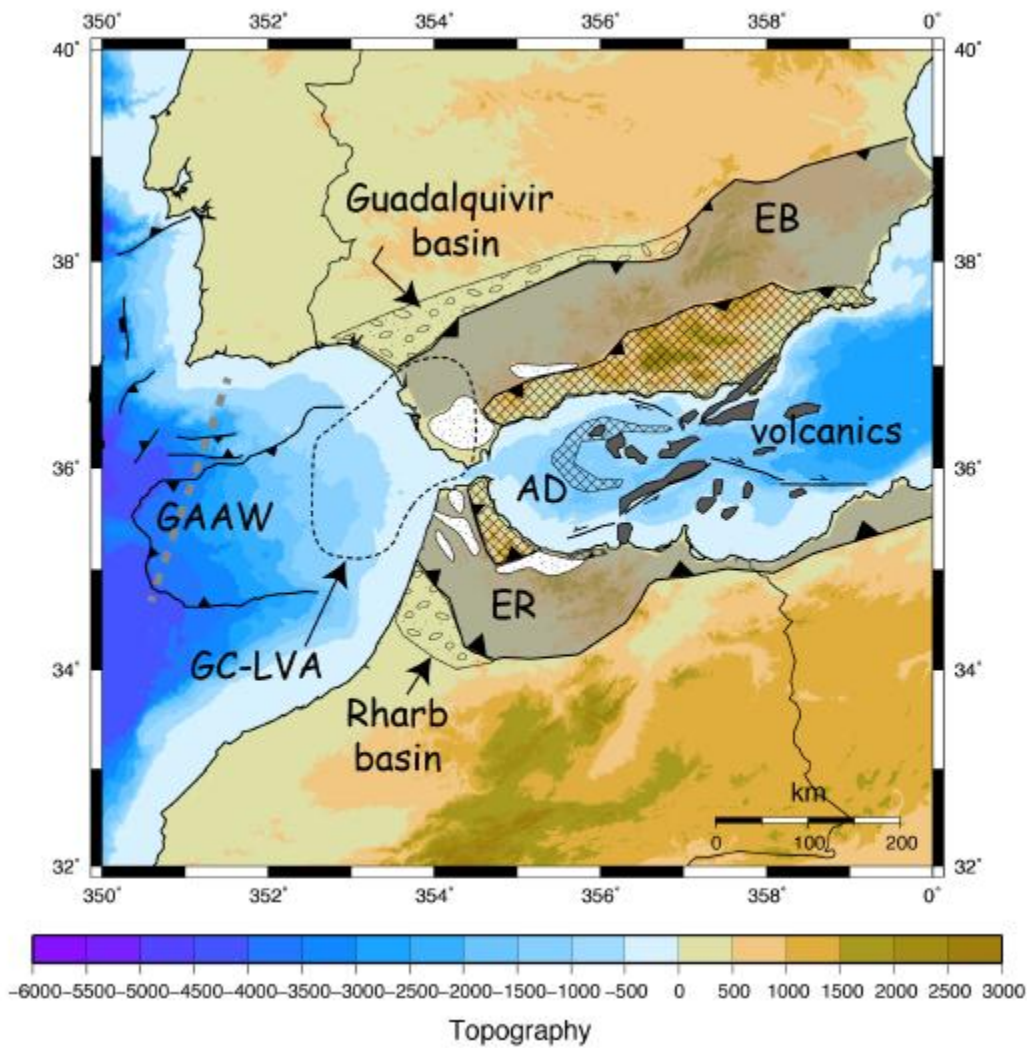


Fig. 2. Simplified geological maps of the two study regions. **a)** Gibraltar-Alboran region

1142 (after

1143 Alvarez-Marron, 1999; Platt et al., 2013; Gutscher et al., 2012; Duarte et al., 2013). The Alboran
 1144 Domain (AD), that includes the Internal Betics and Internal Rif, is indicated by cross hatched
 1145 pattern. The External Betics (EB in gray pattern) includes the Subbetic and Prebetic, and the
 1146 External Rif (ER in gray pattern) includes the Intrarif and Mesorif. The white field with dotted
 1147 pattern represents the Flysch belt, and the volcanics are indicated in dark gray. GAAW: Gibraltar
 1148 Arc Accretionary Wedge; GC-LVA: approximate location of the low-velocity anomaly (from 100
 1149 to 200 km depth). Trace of seismic refraction profile (Sallares et al., 2011) indicated by thick gray
 1150 dashed line. (After Monna et al., 2015).

1151

1152 **Figure 2b**

1153 Calab

1154 rian

1155 Arc-

1156 South

1157 ern

1158 Tyrrh

1159 enian

1160 regio

1161 n

1162 (after

1163 Bigi

1164 et al.,

1165 1990;

1166 Argn

1167 ani,

1168 2005). The outcrops of Apulian and Hyblean (HF) foreland are indicated with large brick pattern,

1169 whereas the carbonate units encased within basal units of the Southern Apennines-Maghrebides

1170 are indicated as white fields with brick pattern. The conglomerate pattern indicates the Bradanic

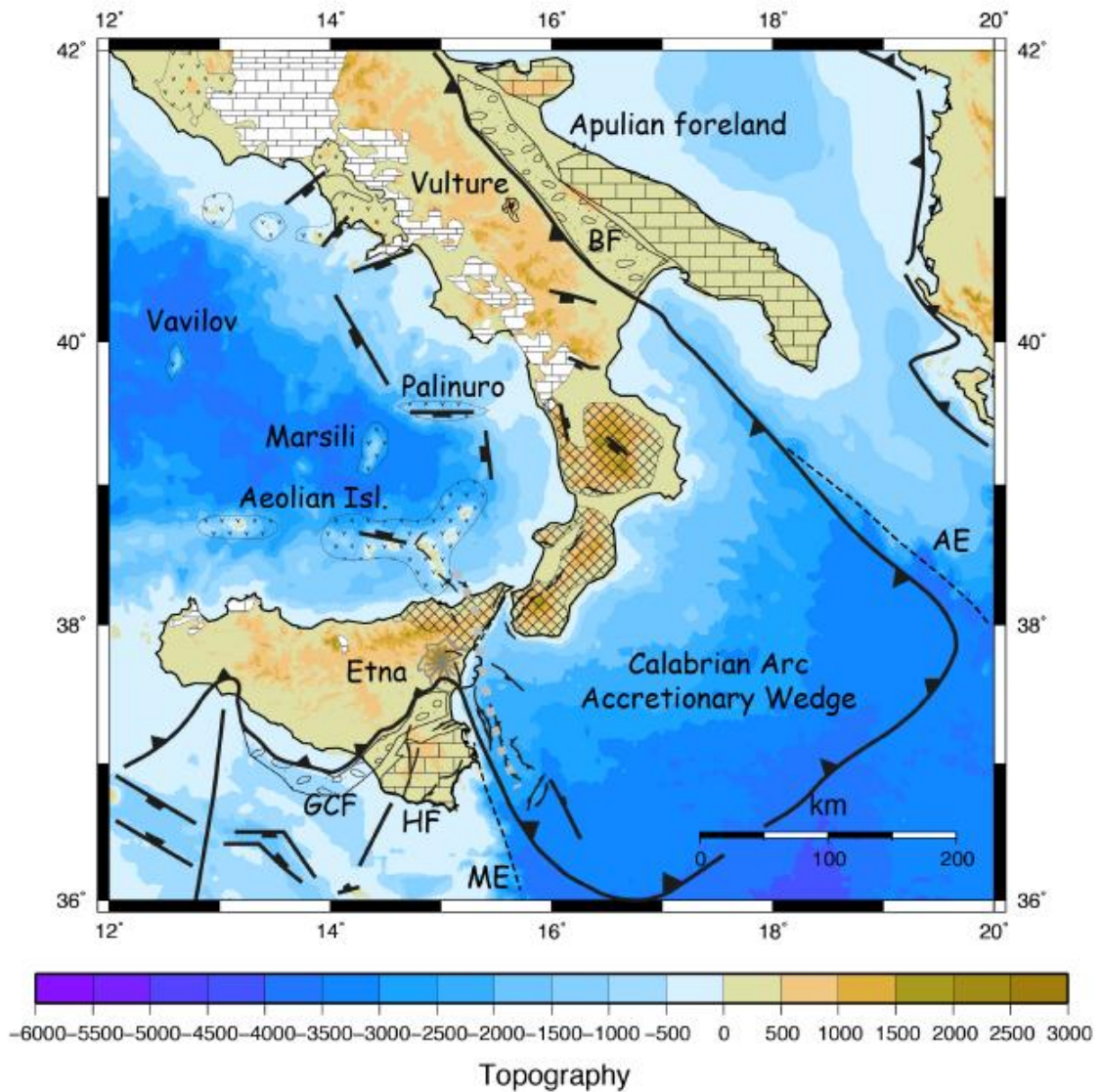
1171 (BF) and Gela-Catania (GCF) foreland basins. The mostly crystalline units of the Calabrian Arc are

1172 shown with cross hatching. The V pattern indicates Pliocene-Quaternary volcanics, including the

1173 Campania Magmatic Province. The Malta and Apulia Escarpments (ME and AE, respectively) are

1174 also indicated with a dashed line. The thick, gray dashed line offshore eastern Sicily marks the

1175 approximate location of the incipient lithospheric tear (after Argnani, 2009).



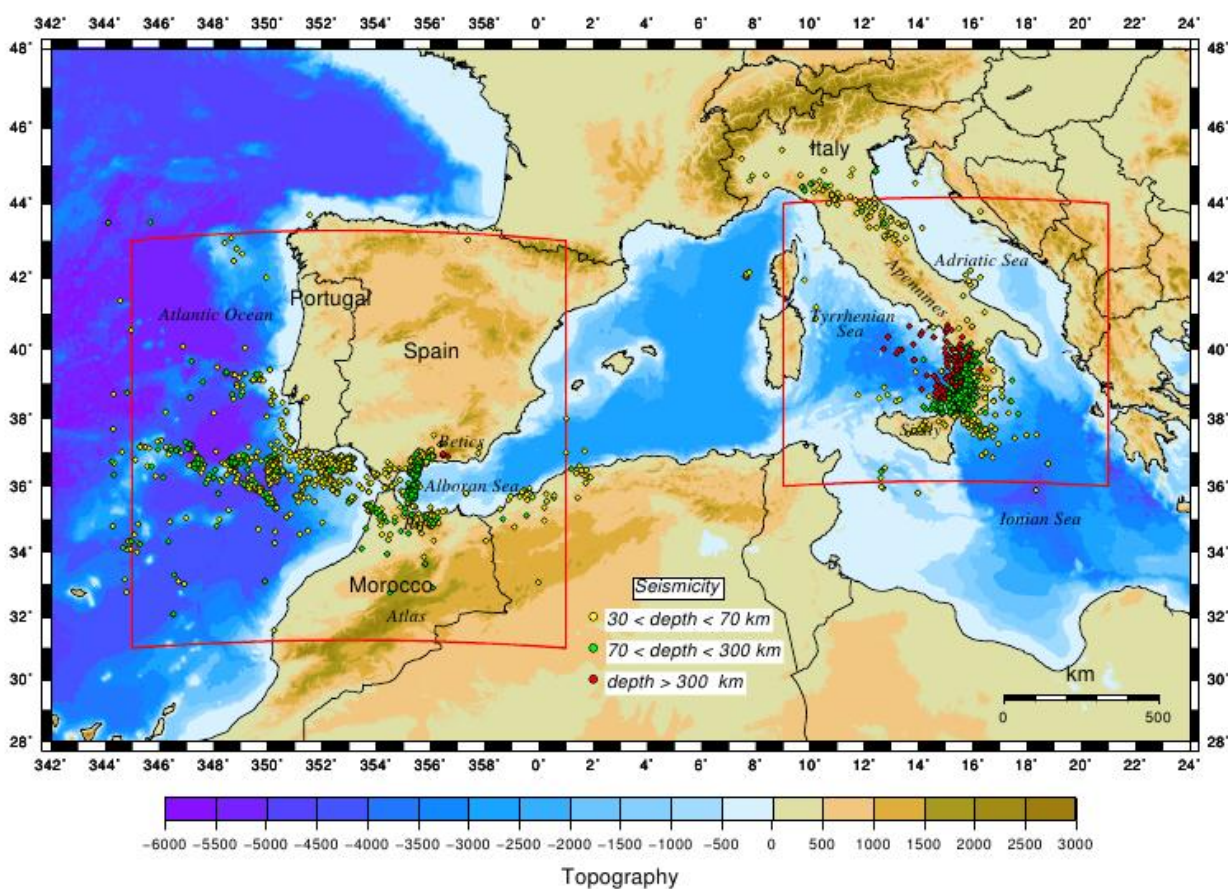
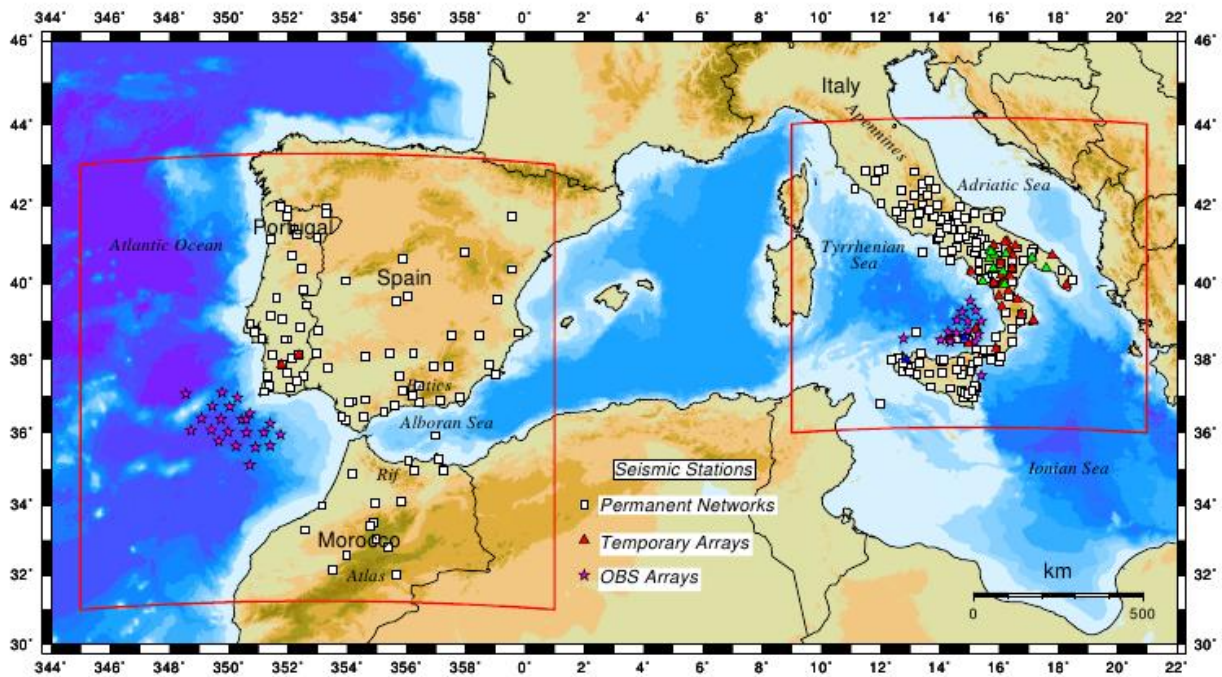


Fig
 . 3.
 Ma
 p of
 the
 C
 W
 M
 regi
 on
 wit
 h

1190 the two study areas. Colored circles show the sub-crustal seismicity ($M \geq 3$) which occurred in the
 1191 years 1990-2013. Hypocentral parameters from IGN catalogue and INGV bulletins.
 1192 Topography/bathymetric profiles are from the Global-Integrated-Topo/Bathymetry Grid (GINA)
 1193 (Lindquist et al., 2004).



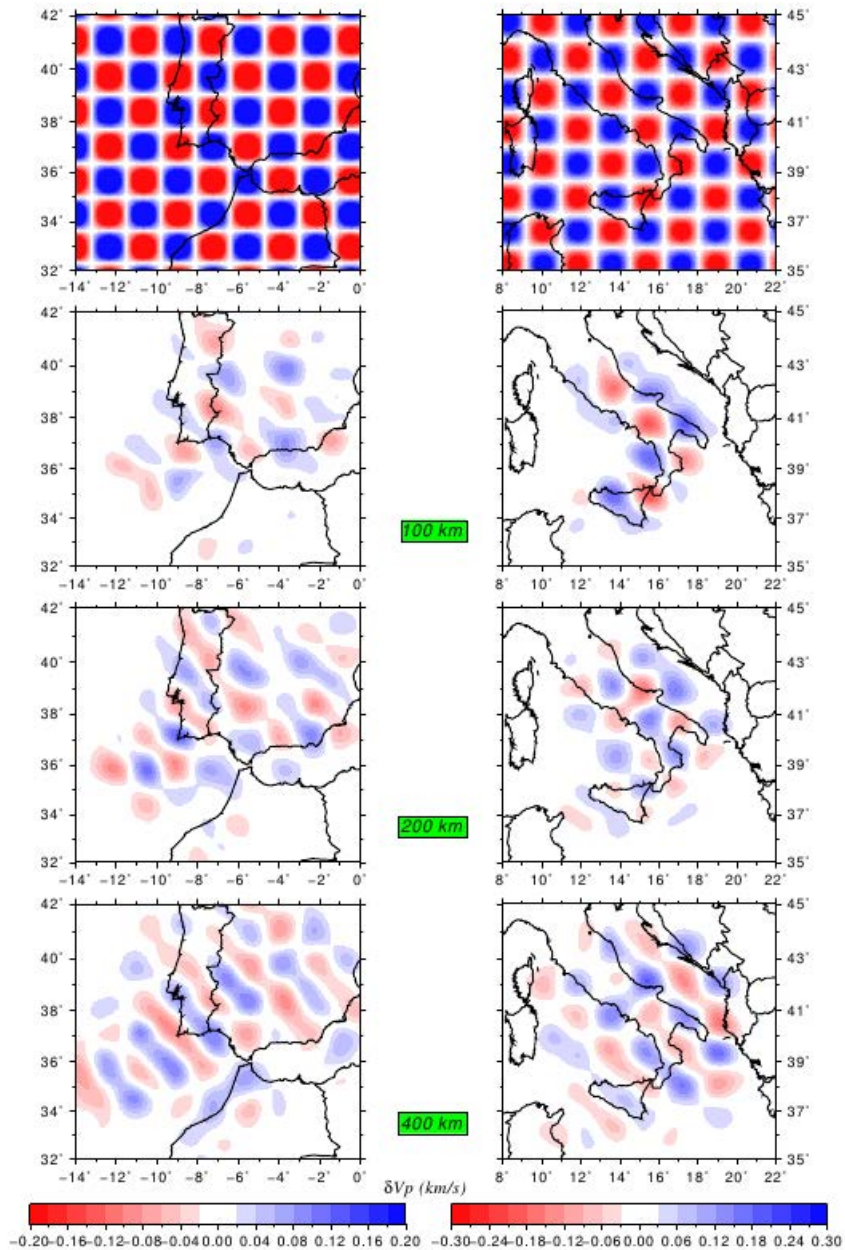
1194 **Figure 4**

1195

1196 **Fig. 4.** Map of the seismic stations used in the two tomographic inversions. The OBS
 1197 Gulf of Cadiz was deployed during the NEAREST project (<http://nearest.bo.ismar.cnr.it>). The OBS
 1198 in the Southern Tyrrhenian were deployed during the TYDE (Dahm et al., 2002) and SN1 (Monna
 1199 et al., 2005) experiments. The temporary land arrays were deployed in Southern Italy during the
 1200 SAPTEX (red triangles) (Cimini et al., 2006) and SeSCAL (green triangles) (Frepoli et al., 2011)
 1201 experiments.

1202

Figure 5



1223

1224 **Fig. 5.** Results of the checkerboard resolution test for three depth slices of the two tomographic
1225 models. Left panels are for the GA model, right panels for the CA model. Panels at the top are the
1226 input checkerboard velocity models. These patterns consist of alternating 100x100 km cells of fast
1227 and slow anomalies varying in latitude, longitude, and depth. The recovered patterns show wide
1228 areas of good resolution for both the models. The synthetic data sets, based on the source-receiver
1229 geometries of the GA and CA teleseismic inversions, include gaussian noise with standard
1230 deviations of 0.15s and 0.50s, respectively for picked and bulletin data.

1231

Figure 6

1232

1233

1234

1235

1236

1237

1238

1239

1240

1241

1242

1243

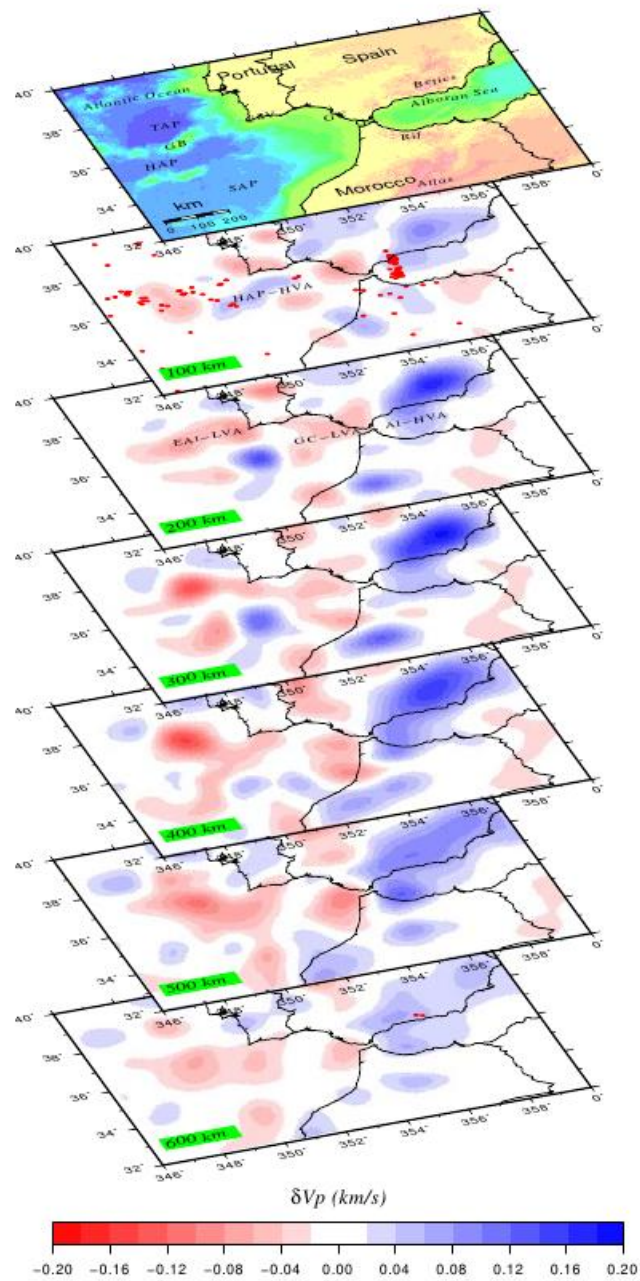
1244

1245

1246

1247

1248



1249 **Fig. 6.** Perspective view showing a series of horizontal slices extracted from the GA velocity model

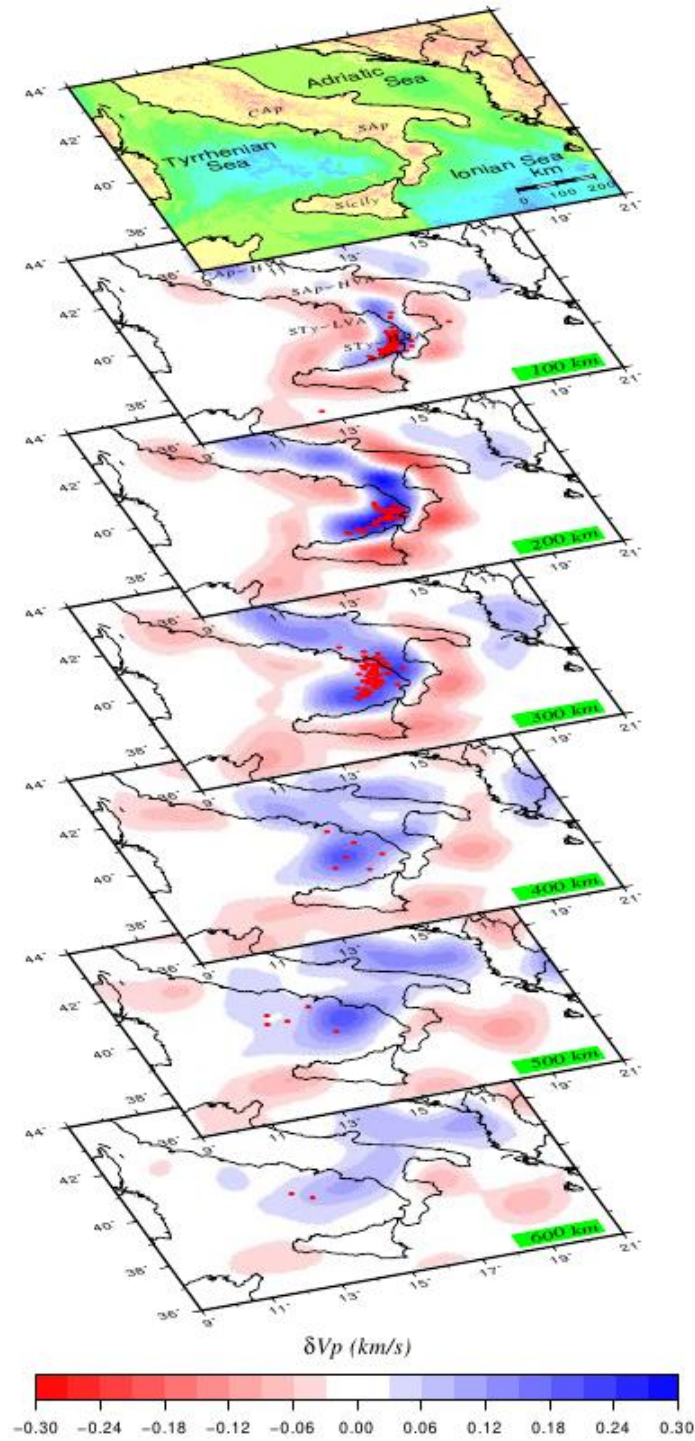
1250 at depth intervals of 100 km. Blue colored areas indicate high velocity anomalies, present in the

1251 Betic-Alboran region (Al-HVA) and in the Atlantic SW Portugal (HAP-HVA). Red colored areas

1252 are zones of low velocity anomalies in the Eastern Atlantic (EAt-LVA) and the Gulf of Cadiz (GC-

1253 LVA). (After Monna et al., 2015).

Figure 7

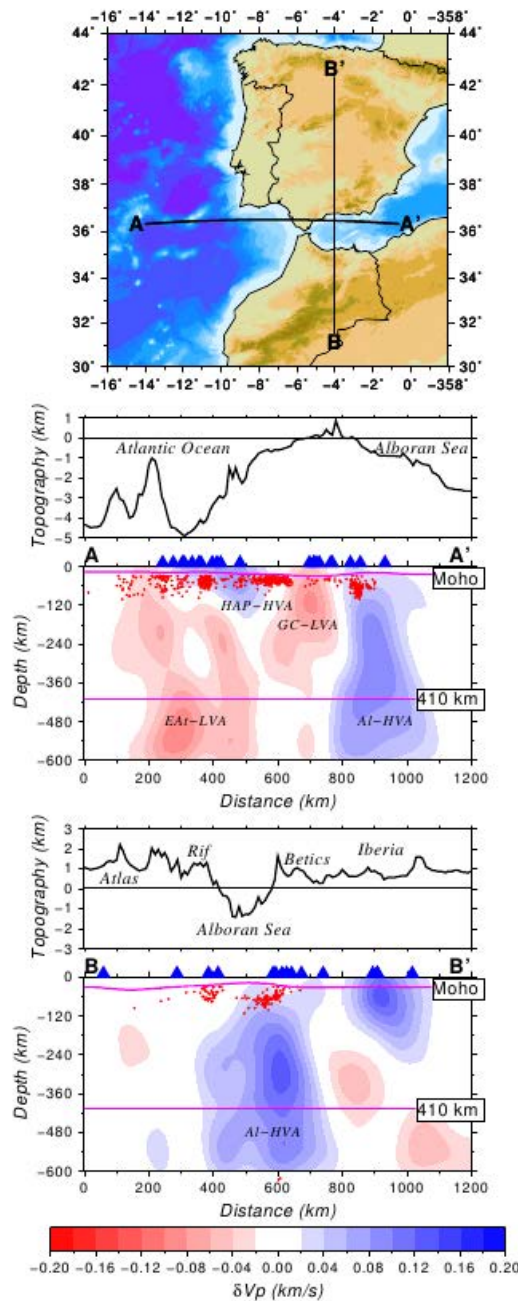


12/4

1275 **Fig. 7.** Perspective view showing a series of horizontal slices extracted from the CA velocity model
1276 at depth intervals of 100 km. As in Fig. 6, blue colored areas indicate high velocity anomalies,
1277 present in the Southern Tyrrhenian region (STyHVA) and in the Southern Apennines (SAP-HVA).
1278 Red colored areas are zones of low velocity anomalies in the Tyrrhenian Sea (STy-LVA) and the
1279 Ionian Sea (Io-LVA).

1280
1281
1282
1283
1284
1285
1286
1287
1288
1289
1290
1291
1292
1293
1294
1295
1296
1297

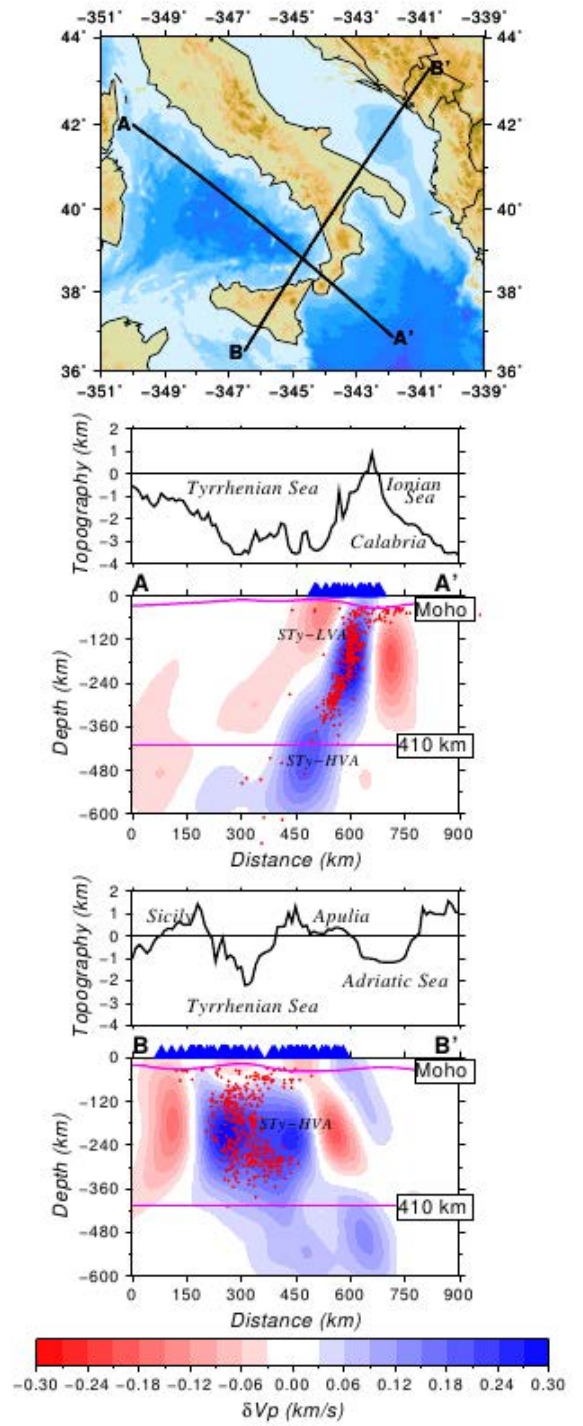
Figure 8



1298 **Fig. 8.** Vertical slices displaying the velocity anomalies of the GA model along a west to east
1299 profile crossing the Gibraltar Arc (AA'), and along a south to north profile crossing the Atlantic the
1300 Alboran Sea (BB'). SAP = Seine Abyssal Plain; HAP = Horseshoe Abyssal Plain; TAP = Tagus
1301 Abyssal Plain. High velocity anomalies: Al-HVA=Betic-Alboran; HAP-HVA=Horseshoe Abyssal
1302 Plane. Low velocity anomalies: GC-LVA=Gulf of Cadiz; EAt-LVA=Eastern Atlantic. Blue
1303 triangles indicate the seismic stations and red dots the subcrustal seismicity, located within a 100
1304 km wide zone centered on the profile. In profile BB', hypocenters deeper than 600 km represent the
1305 deep events below the Granada region. Moho topography is from the European Moho depth map

1306 (Grad et al., 2009). (After Monna et al., 2013a).

Figure 9

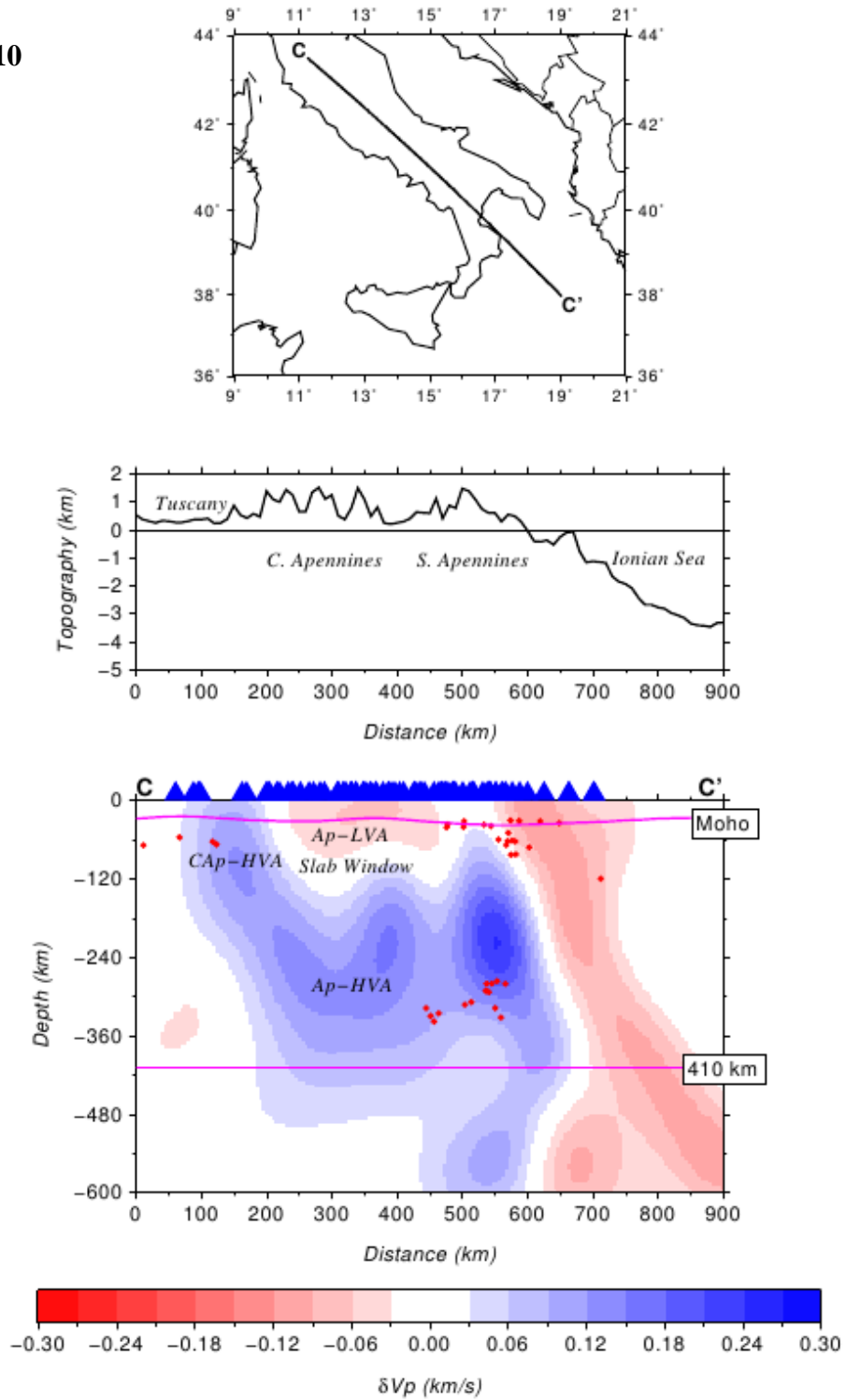


1327 **Fig. 9.** Vertical slices displaying the velocity anomalies of the CA model along a northwest to
 1328 southeast profile crossing the Calabrian Arc (AA'), and along a southwest-northeast profile crossing
 1329 the southern Tyrrhenian basin (BB'). CAP = Central Apennines; SAP = Southern Apennines. **High**
 1330 **velocity anomalies: STy-HVA=Southern Tyrrhenian. Low velocity anomaly: STy-LVA=Southern**
 1331 **Tyrrhenian.** Blue triangles and red dots indicate the seismic stations and the subcrustal seismicity
 1332 located within a 100 km wide zone centered on the profile. Moho topography is from the European

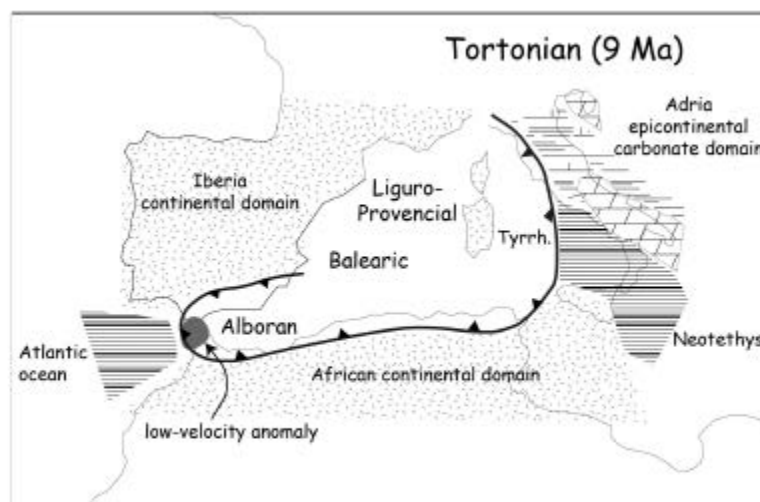
1333 Moho depth map (Grad et al., 2009).

1334
1335
1336
1337
1338
1339
1340
1341
1342
1343
1344
1345
1346
1347
1348
1349
1350
1351
1352
1353
1354

Figure 10

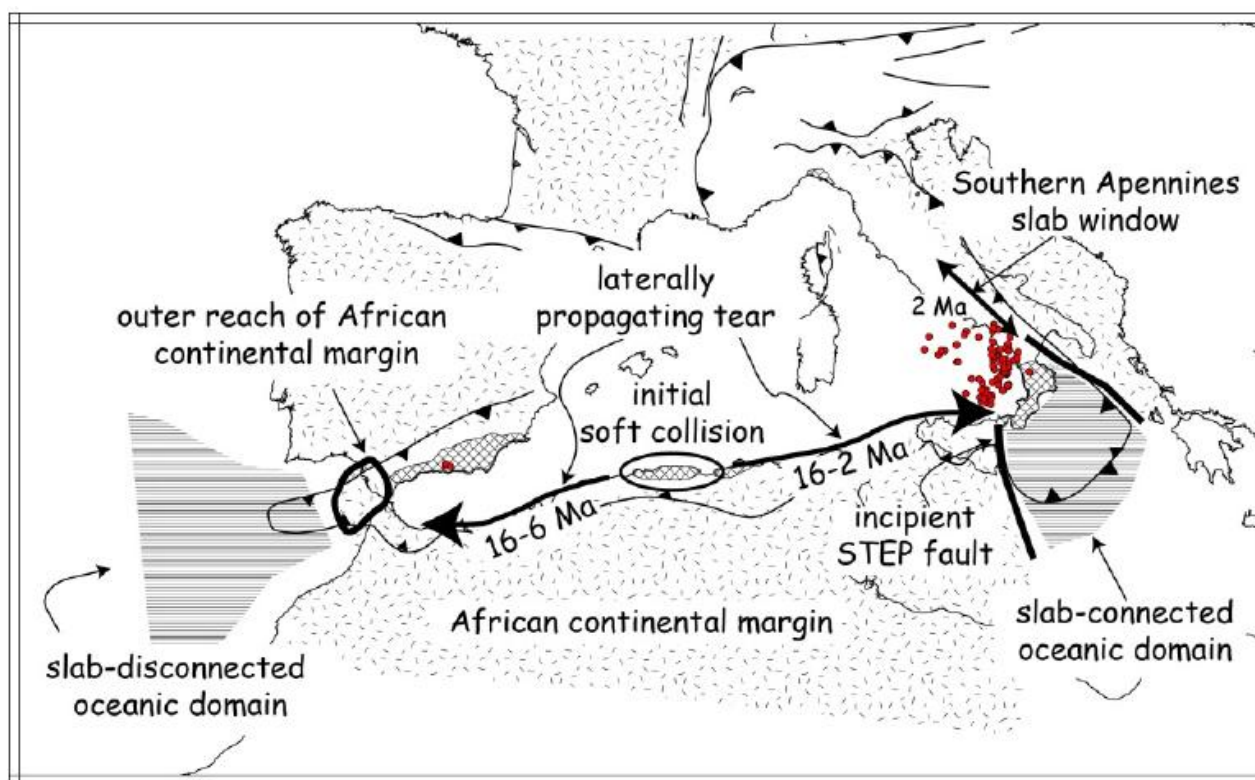


1355 **Fig. 10.** Vertical slice displaying the velocity anomalies of the CA model along a northwest to
1356 southeast profile crossing the Southern Apennines (CC'). The trace and topographic profile are
1357 shown in the top and middle panels, respectively. A well defined slab window underneath the
1358 Southern Apennines is visible (lower panel). High velocity anomalies: Cap-HVA=Central
1359 Apennines; Ap-HVA=Apennines. Low velocity anomaly: Ap-LVA=Apennines-slab window.



1370

1371 **Fig. 11.** Simplified tectonic reconstruction of the Mediterranean in Tortonian time. The African and
1372 Italian coasts are positioned with respect to stable Europe. Note that the Gibraltar arc was almost
1373 completely formed, whereas the Calabrian arc was still to be defined. During the Pliocene-
1374 Pleistocene the subduction and rollback of the narrow Neotethyan branch shaped the final arcuate
1375 of the Calabrian arc. The segment of African continental margin imaged just offshore Gibraltar
1376 (LVA, low-velocity anomaly) likely prevented any further development of the Gibraltar arc,
1377 favouring slab breakoff.



1379

1380

1381 **Fig. 12.** Interpretation of the evolution of the CWM subduction system highlighting the main
 1382 features which controlled arc formation. Slab tearing propagated laterally along the north African
 1383 continental margin, following the initial soft collision in Algeria (ca. 16 Ma). Arc formation
 1384 proceeded on either side, driven by slab sinking and trench retreat, but slab retreat was impeded in
 1385 its westward motion by the segment of thinned continental margin imaged by the GA tomography
 1386 underneath Gibraltar (GC-LVA). The eastward progression of arc formation, on the other hand,
 1387 continued until very recently, with the opening of the Tyrrhenian basin, driven by the sinking Ionian
 1388 slab. In its final stage the sinking also promoted the formation of a slab window underneath the
 1389 Southern Apennines, which is responsible for the magmatism of the Campania Magmatic Province
 1390 (Serri, 1990). Dots represent deep (depth > 300 km) $M \geq 3$ seismicity.

1391

1 Title

2 **The role of continental margins in the final stages of arc formation: Constraints from**
3 **teleseismic tomography of the Gibraltar and Calabrian Arc (Western Mediterranean)**

4

5 **Authors**

6 Andrea Argnani ^a

7 a Istituto di Scienze Marine – Consiglio Nazionale delle Ricerche

8 Via Gobetti, 101

9 Bologna, 40129, Italy

10 andrea.argnani@bo.ismar.cnr.it

11 Telephone +39 051 6398886

12

13 Giovanni Battista Cimini ^b

14 b Istituto Nazionale di Geofisica e Vulcanologia

15 Via di Vigna Murata, 605

16 Rome, 00143, Italy

17 giovannibattista.cimini@ingv.it

18 Telephone: +39-06-51860-407

19

20 Francesco Frugoni ^b

21 b Istituto Nazionale di Geofisica e Vulcanologia

22 Via di Vigna Murata, 605

23 Rome, 00143, Italy

24 francesco.frugoni@ingv.it

25 Telephone: +39-06-51860-547

26

27 Stephen Monna ^b

28 b Istituto Nazionale di Geofisica e Vulcanologia

29 Via di Vigna Murata, 605

30 Rome, 00143, Italy

31 stephen.monna@ingv.it

32 Telephone: +39-06-51860-404

33

34 Caterina Montuori ^b

35 b Istituto Nazionale di Geofisica e Vulcanologia

36 Via di Vigna Murata, 605
37 Rome, 00143, Italy
38 caterina.montuori@ingv.it
39 Telephone: +39-06-51860-496

40

41

42 Corresponding author

43 Giovanni Battista Cimini

44 giovannibattista.cimini@ingv.it

45

46

47 **Abstract**

48 The deep seismicity and lateral distribution of seismic velocity in the Central Western
49 Mediterranean, point to the existence under the Alboran and Tyrrhenian Seas of two lithospheric
50 slabs reaching the mantle transition zone. Gibraltar and Calabrian narrow arcs correspond to the
51 slabs. Similarities in the tectonic and mantle structure of the two areas have been explained by a
52 common subduction and roll-back mechanism, in which the two arcs are symmetrical end members.
53 We present a new 3-D tomographic model at mantle scale for the Calabrian Arc and compare it
54 with a recently published model for the Gibraltar Arc by Monna et al. (2013a). The two models,
55 calculated with inversion of teleseismic phase arrivals, have a scale and parametrization that allow
56 for a direct comparison. The inclusion in both inversions of ocean bottom seismometer broadband
57 data improves the resolution of the areas underlying the seafloor networks. This additional
58 information is used to resolve the deep structure and constrain the reconstruction of the Central
59 Western Mediterranean geodynamic evolution. The Gibraltar tomography model suggests that the
60 slab is separated from the Atlantic oceanic domain by a portion of African continental margin,
61 whereas the Calabrian model displays a continuous oceanic slab that is connected, via a narrow
62 passage (~350 km), to the Ionian basin oceanic domain. Starting from the comparison of the two
63 models we propose the following interpretation: within the Mediterranean geodynamic regime
64 (dominated by slab rollback) the geometry of the African continental margin, located on the lower
65 plate, represents a critical control on the evolution of subduction. As buoyant continental
66 lithosphere entered the subduction zones, slab pull caused tears in the subducted lithosphere. This
67 tectonic response in the final stages of arc evolution, strongly controlled by the paleogeography of
68 the subducted plates, explains the observed differences between the Gibraltar and Calabrian Arcs.

69

70 **Key words:** teleseismic tomography, upper mantle, Gibraltar Arc, Calabrian Arc, subduction zone

72 **1. Introduction**

73 One of the outstanding and controversial features of the Mediterranean region is the presence of
74 large-scale extensional basins within a convergent domain located between the African and
75 European plates. Early studies recognized that the Central Western Mediterranean (CWM)
76 extensional basins (Fig. 1) developed in a backarc setting (Dewey et al., 1973, 1989; Horvath and
77 Berckhemer, 1982; Rehault et al., 1984), and also hypothesized that outward migration of
78 subduction, due to slab sinking and retreat, was the most likely explanation for the observables
79 (Malinverno and Ryan, 1986). Several papers stemmed from these early concepts, with progressive
80 refinement of the timing and kinematics of backarc extensional and outward migration of the fold-
81 and-thrust belt (e.g., Royden, 1993; Lonergan and White, 1997; Seranne, 1999; Argnani and
82 Savelli, 1999).

83 A remarkable lateral variability in the character of the fold-and-thrust belts, timing of extension of
84 backarc basins, and so on, is present in the Mediterranean orogen. Two main factors contributed to
85 this result: i) non linear continental margins of the converging plates; and ii) gravitational instability
86 of the subducted lithosphere.

87 The land-locked condition of the Mediterranean plate boundary, due to the presence of the Adriatic
88 promontory, enhanced the effects of slab rollback (Le Pichon, 1982; Mascle et al., 1988). In fact,
89 the collision of the Adriatic promontory with Eurasia around the Paleocene caused a slowdown in
90 the Africa–Eurasia plate convergence, particularly for the N-ward component (Le Pichon et al.,
91 1988; Dewey et al., 1989). This, in turn, promoted the activation of processes operating within the
92 orogen, such as lithospheric root detachment, lithosphere delamination, lateral escape towards areas
93 of depressed topography and rollback of dense oceanic slab, which are responsible for the origin of
94 the Mediterranean extensional basins (i.e. Le Pichon, 1982; Dewey, 1988; Le Pichon et al., 1988;
95 Otsuki, 1989; Argnani, 2000; Jolivet and Faccenna, 2000).

96 An additional important aspect is the interaction between lithospheric slabs and asthenosphere
97 which could possibly result into slab breakoff or detachment and delamination of continental
98 lithosphere. Lateral migration of slab breakoff has been proposed as a key factor for lithosphere
99 dynamics in this region in the last 20-30 Ma, especially in the final stage of subduction (Wortel and
100 Spakman, 1992, 2000; Carminati et al., 1998; Faccenna et al., 2004; Rosenbaum et al., 2008;
101 Argnani, 2009). Within this setting, mantle flow possibly played a role in the deformation of the
102 Gibraltar and Calabrian slabs (Gvirtzman and Nur, 1999; Faccenna et al., 2004; Baccheschi et al.,
103 2008). Delamination of continental lithosphere is a process that likely operated within the
104 Mediterranean orogens, following the subductional consumption of oceanic lithosphere (e.
105 g., Serri et al., 1993; Fillerup et al., 2010; Argnani, 2012; Levander et al., 2014). Although it is

106 known that continental rocks can experience subduction to depth over 100 km, before returning to
107 shallow depth and becoming exhumed to the surface (e.g., Hacker et al., 2010; Butler et al., 2014),
108 continental subduction is likely to be limited, both in extent and rate of subduction, as suggested by
109 the overall stability of continents (Cloos, 1993). The tectonic evolution of the Mediterranean type
110 orogen suggests that when a continental margin enters a retreating subduction zone (soft collision),
111 the processes of subduction and slab retreat get to the end (e.g., Burchfiel and Royden 1991; Wortel
112 and Spakman, 2000; Argnani, 2009).

113 The present structure and origin of the Gibraltar Arc-Alboran Basin system (GA) (Fig. 1) does not
114 fit well in this unifying picture based on slab subduction and rollback, and alternative evolution
115 scenarios have been proposed. Several authors do suggest that subduction of oceanic lithosphere
116 (active or extinct) caused extension within the Alboran Basin in the Miocene by slab rollback
117 (Royden, 1993; Lonergan and White 1997; Bijward and Spakman, 2000; Gutscher et al., 2002) or
118 by slab detachment (Zeck, 1996). Alternatively, another group of authors presents an evolution for
119 the Alboran basin initiating with lithospheric thickening during the Paleogene caused by the
120 collision of Europe and Africa. The thickened continental lithosphere was later (ca. 25 Ma)
121 detached by convective removal (Platt and Vissers, 1989) or by delamination (Calvert et al., 2000),
122 leading to recycling of continental material (Levander et al., 2014). The collapse of this lithosphere
123 caused extension of the Alboran and Algerian basins and uplift around the margin, edge
124 delamination under the Betics and Rif margins and mixed continental-oceanic subduction (Booth-
125 Rea et al., 2007; Duggen et al., 2005; Medaouri et al., 2014).

126 On the other hand, there is a general consensus that the Calabrian Arc-Tyrrhenian Basin system
127 (CA) (Fig. 1) does fit well in the unifying picture: subduction with slab rollback has been the main
128 factor in the opening of the Tyrrhenian Sea (Malinverno and Ryan, 1986), a well defined Wadati-
129 Benioff zone is contained in a high seismic velocity body (Cimini and Marchetti, 2006, and
130 references therein), and subduction-related magmatism is active under the CA (Barberi et al., 1974;
131 De Astis et al., 2003).

132 Several tomography studies have concentrated on the Mediterranean mantle at different scales.
133 They range from the global (e.g., Bijwaard and Spakman, 2000), to the European (e.g., Koulakov et
134 al., 2009), to the Mediterranean scale (e.g., Piromallo and Morelli, 2003), down to a more regional
135 scale (e.g., Cimini and Marchetti, 2006; Montuori et al., 2007; Bezada et al., 2013).

136 In this paper we focus on two tomographic P-wave velocity models of the upper mantle beneath the
137 GA and CA regions, which give , with respect to previous models, a more resolved 3-D picture of
138 the two subduction zones and surrounding asthenospheric mantle. Both tomographies take
139 advantage of improved teleseismic-phase arrivals datasets obtained by integrating recordings from
140 permanent national networks with recordings from recent dense deployments of temporary land and

141 marine (Ocean Bottom Seismometers - OBS) broad band arrays (Dahm et al., 2002; Monna et al.,
142 2005; NEAREST project, <http://nearest.bo.ismar.cnr.it>). The teleseismic inversions were performed
143 using a modern iterative technique (Rawlinson et al., 2006), by employing the same grid
144 parametrization and depth extension (600 km) of the target volume, which allows for a direct
145 comparison of the images. The GA tomography has been recently published (Monna et al., 2013a,
146 2015), while for the CA we present a new tomography model. Regarding the deep structure of GA
147 the model shows features that were previously undetected or poorly resolved, in particular the
148 lithosphere-upper mantle structure of the Gibraltar Strait-Atlantic sector, whereas for the CA the
149 slab geometry and the surrounding asthenosphere are more accurately defined with respect to a
150 previous models based on OBS data (Montuori et al., 2007). The inversion results are the starting
151 point for a discussion and comparison of the two subduction systems within the geodynamic and
152 tectonic framework of the Western Mediterranean region.

153

154 **2 Geodynamic and tectonic evolution of the Central Western Mediterranean**

155 Africa moved several 100's km towards Europe from the Cenomanian to the Chattian, and 200-300
156 km of convergence occurred in the Eocene-Oligocene time interval. Average N-S convergence
157 between Africa and Europe slowed down since the Chattian, following the Alpine collision, and, as
158 a result, rollback of subducted lithosphere initiated the opening of the backarc basins and the
159 concomitant outward migration of the fold-and-thrust belts, that characterize the Western
160 Mediterranean (Fig. 2) (Le Pichon, 1982; Dewey, 1988; Le Pichon et al., 1988; Argnani, 2000;
161 Jolivet and Faccenna, 2000). The concomitant presence of calc-alkaline volcanism along the
162 European margin (Sardinia, offshore western Corsica, Provence) is an evidence that subduction of
163 oceanic lithosphere occurred during the formation of these backarc basins (Argnani and Savelli,
164 1999).

165 The Balearic backarc basin was the first to open (Fig. 1) from late Oligocene to early-middle
166 Miocene (Rehault et al., 1984; Chamot-Rooke et al., 1997; Faccenna et al., 1997) and extend to the
167 western end of the Mediterranean, up to the Alboran basin (Watts et al., 1993; Booth-Rea et al.,
168 2007). In the Algerian sector, the opening of the basin continued until late Miocene, possibly with
169 oceanic crust emplacement in late Miocene (Mauffret et al., 2004; Booth-Rea et al., 2007; Medaouri
170 et al., 2014). The Tyrrhenian backarc basin opened from Late Miocene to Pleistocene above the
171 NW-dipping subduction of the Ionian lithosphere (Malinverno and Ryan, 1986; Kastens et al.,
172 1988; Argnani and Savelli, 1999). Evidence from regional geophysics, arguments from plate
173 kinematics and palaeo-reconstructions, suggest that the oceanic lithosphere, that subducted during
174 the Tyrrhenian opening, belonged to a Triassic seaway (Argnani, 2005; Speranza et al., 2012).

175 The most striking feature in this process of backarc basin opening is the formation of the two tightly

176 arcuate features: the Gibraltar and Calabrian arcs (Fig. 1) (Horvath and Berckhemer, 1982;
177 Faccenna et al., 2004; Rosenbaum and Lister 2004). The foreland of the Calabrian Arc fold-and-
178 thrust belt faces the African plate (s.l.), although the nature of the lithosphere varies from oceanic in
179 the apex of the arc to continental on either side. The foreland of the Gibraltar Arc fold-and-thrust
180 belt, instead, covers both the African and Iberian plates; this plate boundary location contributes to
181 additional tectonic complexity.

182 The large-scale models, that explain the Gibraltar and Calabrian arc subduction as coming from a
183 single slab SE-ward retreat of the western Mediterranean (Faccenna et al., 2004; Carminati et al.,
184 2012), may be too oversimplified to account for the geological complexity of the Alboran region.
185 Other evolutionary models start with a shorter subduction zone, that is initially limited to the
186 Balearic region (e.g., Lonergan and White, 1997; Rosenbaum et al., 2002; van Hinsbergen et al.,
187 2014); this class of models seem to explain more satisfactorily the geological evolution of the
188 Alboran region (Platt et al., 2013; Chertova et al., 2014).

189

190 **2.1 Gibraltar Arc-Alboran Basin**

191 The Atlantic sea-floor magnetic anomalies (Srivastava et al., 1990) indicate that the Iberia plate
192 experienced a complex kinematics within the Africa-Eurasia convergence. Iberia was part of Africa
193 from Late Cretaceous to Early Oligocene, whereas from Late Oligocene to present it became part of
194 Europe, following the Pyrenean collision. As an alternative, recent reviews of the magnetic
195 anomalies (Vissers and Meijer, 2012) allow for some 50-70 km convergence between Africa and
196 Iberia for the Late Cretaceous-Middle Eocene time span. The west-ward arc propagation of the
197 Betic-Rif fold-and-thrust belt is larger than the 200-250 km N-S convergence between Africa and
198 Iberia, as suggested by the length of the east-dipping subducted slab imaged by high-resolution
199 seismic tomography (e.g., Bezada et al., 2013; Palomeras et al., 2014). This propagation has been
200 modelled with a substantial westward slab rollback (e.g., Royden, 1993; Lonergan and White, 1997;
201 Gutscher et al., 2002; Rosenbaum et al., 2002). The internal Betics and Rif units (Fig. 2a) have a
202 continental substrate of Palaeozoic age with a Mesozoic-Cenozoic sedimentary cover, and have
203 been affected by Palaeogene HP/LT metamorphism (Platt et al., 2013). These internal units have
204 been also recovered in the Alboran Sea, defining the so-called Alboran Domain. The external Betics
205 and Rif units are characterized by successions derived from the Iberian and African passive
206 continental margins that were emplaced during the opening of the Alboran basin (e.g., Blankenship,
207 1992; Wildi, 1983). The sediments of the Flysch basin were thrust by the Alboran Domain units
208 that were moving west-southwest-ward during the Oligocene-Early Miocene (Fig. 2a; Wildi, 1983).
209 The basement of the Flysch basin domain was likely oceanic and could correspond to the oceanic
210 slab imaged by tomography under the Alboran basin. Most of the vertical-axis rotation and arc

211 formation in the Rif and western Betics was accomplished by the early Pliocene, as indicated by
212 paleomagnetic data (e.g., Platt et al., 1995; Platzman et al., 1993; Krijgsman and Garces, 2004;
213 Cifelli et al., 2008; Fig. 2a).

214 The Alboran Sea basin, which was formed in the Neogene as a result of extensional tectonics, is
215 currently floored by thinned continental crust, 13-20 km thick (Watts et al., 1993), and by
216 magmatically accreted arc-type crust in its eastern sector (Booth-Rea et al., 2007).

217 Recent tectonic models try to account for the details of the geological evolution of the Alboran
218 region. Platt et al. (2013), following their previous work, propose a NW-ward Paleogene subduction
219 that originated the Alboran Domain, followed (during the Early Miocene) by orogenic collapse and
220 a new subduction on the Iberian side of the Alboran Domain. As an alternative explanation, Vergés
221 and Fernandez (2012) propose a continuous southward subduction of the Iberian plate, with slab
222 rollback and slab break-off, that would account for both the Paleogene and Miocene subduction
223 events. This reconstruction which describes the evolution of the Betics, requires the occurrence of a
224 major transform boundary that separates the Betics (northward polarity) from the eastern
225 Maghrebides (southward polarity) subduction segments, and implies some difference in the tectonic
226 evolution of the Maghrebian belt of north Africa, for which there is not much evidence in the field.
227 Finally, a recent reconstruction (Van Hinsbergen et al., 2014) assumes that the Alboran terranes
228 mostly formed along an oblique subduction zone located south of the Balearic islands, partly
229 building on the reconstruction of Rosenbaum and Lister (2004). Here, the early Miocene heating
230 and exhumation affecting the peridotite mantle and overlaying Alboran terranes occurred within a
231 forearc setting, with the Alboran terranes subsequently dispersed across the western Mediterranean
232 during backarc opening.

233 A number of tomographic studies have been performed in the last decade to image the deep seismic
234 velocity structure of the GA. These studies agree on the presence of a high-velocity body under the
235 Alboran Sea, down to mantle depths (Blanco and Spakman, 1993; Bijwaard and Spakman, 2000;
236 Calvert et al., 2000). Very recent high-resolution tomography studies (Bezada et al., 2013;
237 Palomeras et al., 2014; Thurner et al., 2014; Bonnín et al., 2014; Villaseñor et al., 2015) confirm the
238 presence of a slab-shaped high velocity body, seen from the surface down to the bottom of the
239 transition zone. The GA slab has a small curvature radius, similarly to the CA, but it does not show
240 a Wadati-Benioff plane. In fact, sub-crustal seismicity (Figs. 3 and 8) is mostly located near the
241 Strait of Gibraltar within 120 km depth and distributed in a very narrow north-south oriented
242 vertical band (Seber et al., 1996), with a mixture of focal mechanisms showing both compression
243 and extension (Buforn et al., 2004). Deep earthquakes (depth > 300km) are rare and occur at the
244 bottom of the transition zone (~630 km depth) under southern Spain in the Granada area, and show
245 dip-slip motion with a vertical north-south plane and a nearly horizontal plane with the pressure

246 axis dipping 45° to the east (Buforn et al., 2004, 2011).

247 The large amount of geophysical and geological data for this area confirms a complex geodynamic
248 evolution, and in fact the high velocity anomaly below the Alboran has been interpreted as a
249 continuous subducting slab (Gutscher et al., 2002; Piromallo and Morelli, 2003), as a broken-off
250 slab (Blanco and Spakman, 1993), and as lithosphere which has undergone delamination (Calvert et
251 al., 2000), or convective removal of the root (Platt and Vissers, 1989).

252 One of the open problems for the GA has been the interaction between the Atlantic and Alboran
253 domains, west and east of the Gibraltar Strait. Although global scale tomography studies cover both
254 regions, they do not have the capability to resolve the finer details. On the other hand, in spite of the
255 increase in available data, the great majority of the higher resolution (regional scale) tomography
256 models do not image the mantle below the Atlantic region west of the Gibraltar Strait due to a lack
257 of station coverage at sea. A recent regional scale tomography model (WMGC-OBS) based on OBS
258 data which includes both domains, has been proposed by Monna et al. (2013a). A relevant aspect of
259 model WMGC-OBS is that there is a separation of the two lithospheres of the two domains, thus
260 excluding the existence of a single continuous slab coming from the Atlantic side and subducting
261 eastward below the Alboran.

262

263 **2.2 Calabrian Arc-Tyrrhenian Basin**

264 The Calabrian Arc connects the Sicilian Maghrebides and Southern Apennines and is characterized
265 by a stack of basement units, coming from different levels of a Hercinian continental crust (Fig. 2b)
266 (Bonardi et al., 2001). A thick forearc sedimentary succession crops out in the Ionian side of
267 Calabria, supporting the accretion of the Calabrian Arc terranes within a subduction system
268 (Bonardi et al., 2001). The wide accretionary complex of the External Calabrian Arc extends into
269 the Ionian Sea and is confined to the NE and SW by the Apulian and Malta Escarpments,
270 respectively (e.g., Biju Duval et al., 1982; Argnani and Bonazzi, 2005; Argnani, 2006).

271 The evolution of the Calabrian Arc is strictly related to the opening of the Tyrrhenian backarc basin
272 (Malinverno and Ryan, 1986; Patacca et al., 1993) and is marked by a progressive narrowing of the
273 subducted slab. Palaeomagnetic data support the saloon-door opening of the Tyrrhenian basin
274 (Cifelli et al., 2007), as the structural units of the Southern Apennines experienced a counter-
275 clockwise rotation of 60° during Middle-Late Miocene (Gattacceca and Speranza, 2002), whereas
276 the structural units of the Sicilian Maghrebides show a large clockwise rotation of ca. 70° between
277 Langhian and Late Tortonian (Channell et al., 1990; Speranza et al., 1999).

278 The Tyrrhenian Basin is located on the wake of the Apennines and Sicilian Maghrebides. The
279 amount of extension is greater in the southern basin which, in fact, is characterized by a thin crust
280 (less than 10 km) and high heat flow (Kastens et al., 1988), with possibly wide stretches of

281 exhumed mantle (Prada et al., 2014). A girdle of volcanic islands, the Aeolian Islands, located north
282 of Sicily represents the volcanic arc of the Tyrrhenian subduction, with calc-alkaline activity that
283 spans from 1 Ma to the Present (Fig. 2b) (Barberi et al., 1974; De Astis et al., 2003). The rocks of
284 the Campania Magmatic Province (Fig. 2b), that includes the Campi Flegrei high potassium
285 calcalkaline (2.0 - 1.6 Ma), the Campi Flegrei, Ischia and Procida shoshonites (100 ka - Present),
286 and the Vesuvio leucitite and leucitite basanite (1 Ma - Present), also show affinity with island arc
287 magmatism. Magmatic rocks from Campania and the Aeolian volcanic arc have comparable
288 geochemical features, suggesting a similar Oceanic Island Basalt mantle source, enriched by
289 components derived from subducted oceanic lithosphere (Serri, 1990).

290 The onshore Calabrian Arc has been affected by major uplift in the last 0.8 Ma, with rates up to 2.0
291 mm/yr (Westaway, 1993; Bordoni and Valensise, 1998), and presents extensional grabens filled by
292 Late Pliocene-Quaternary sediments, trending both parallel and perpendicular to the arc (Tortorici
293 et al., 1995). This active tectonic regime is supported by extensional focal mechanisms (e.g.,
294 Vannucci et al., 2004). To the west of the central Aeolian Islands, earthquake focal mechanisms
295 indicate that active compressional deformation occurs offshore northern Sicily (Pondrelli et al.,
296 2004; Argnani et al., 2007; Serpelloni et al., 2007), although the seismogenic structures have not
297 been properly identified. This compressional boundary has been considered as part of a kinematic
298 rearrangement that occurred about 2 Myr ago (Jenny et al., 2006).

299 For the CA there is a wide consensus that subduction of oceanic lithosphere below the southern
300 Tyrrhenian is taking place. In the tomographic images the subduction is represented as a narrow
301 arc-shaped high velocity body which flattens in the transition zone at the 660 km discontinuity
302 between upper and lower mantle (Cimini, 1999; Piromallo and Morelli, 2003; Spakman and Wortel,
303 2004; Montuori et al., 2007). The existence of subduction and overlying mantle wedge for the CA
304 is confirmed by other geophysical and geochemical observations, such as, for example, the presence
305 of a volcanic arc (Barberi et al., 1974; De Astis et al., 2003). Furthermore, the spatial distribution of
306 the deep events (Figs. 3 and 9) (Frepoli et al., 1996) shows a Wadati-Benioff zone dipping $\sim 70^\circ$
307 NW beneath the southern Tyrrhenian, down to about 600 km depth (Cimini and Marchetti, 2006,
308 and references therein). The focal mechanism P-axes show steep down-dip compression at
309 intermediate depths (between 160 and 370 km). The deepest events (below 370 km) have P-axes
310 with shallower dip (Frepoli et al., 1996).

311 The tomographic models have been interpreted as representing the final result of a subduction with
312 rollback process which has caused the opening of the Tyrrhenian Sea in the last ~ 13 Ma (Wortel
313 and Spakman, 2000; Piromallo and Morelli, 2003).

314 The tomographic images show that there is not a continuous slab under the Italian peninsula, as it is
315 interrupted by a low-average velocity volume below the central-southern Apennines at lithospheric

316 depths. Other distinct high velocity bodies are found below the Northern Apennines and the Alps
317 (Spakman and Wortel, 2004; Piromallo and Morelli, 2003; Giacomuzzi et al., 2012). This
318 distribution in space of the high velocity bodies, prompted several authors to hypothesize the
319 existence of an original single slab which had undergone one or more slab tears and/or detachment
320 (e.g., Wortel and Spakman, 1992; 2000; Amato et al., 1993; Spakman and Wortel, 2004).

321 In recent years, thanks to the improvement of the Italian National Seismic Network, regional
322 tomography studies could resolve finer details of the CA lithosphere-asthenosphere structure (e.g.,
323 Chiarabba et al., 2008). Furthermore, inversion of the 3-D attenuation structure (Chiarabba et al.,
324 2008; Monna and Dahm, 2009) has added independent constraints, which are especially helpful in
325 distinguishing the role of chemical composition and temperature as causes for seismic velocity
326 anomalies.

327

328 **3. Teleseismic tomography models of GA and CA based on OBS data**

329 In this section we describe 3-D P-wave velocity models computed for the upper mantle of GA and
330 CA. The CA images are derived from the new tomographic model presented in this work The GA
331 images are derived from model WMGC-OBS presented in two recent papers (Monna et al., 2013a,
332 2015). To calculate both models we used accurate time picks of teleseismic waveforms recorded by
333 the integrated arrays shown in Fig. 4 at epicentral distances between 25° and 95° (P phases) from
334 worldwide $M_w \geq 5.5$ earthquakes. The time picks were corrected for station elevation/bathymetry,
335 Earth's ellipticity, local crustal structure (see sections 3.1 and 3.2), and then reduced to relative
336 arrival time residuals using the ak135 global velocity model (Kennett et al., 1995). We applied the
337 iterative nonlinear tomography method developed by Rawlinson et al. (2006) to map these residuals
338 into 3-D P wave velocity anomalies. We note that inversion of relative traveltimes residuals
339 produces only 3-D velocity perturbations with respect to an average (usually 1-D) Earth model
340 modified for the appropriate crustal structure. In the inversion scheme, the calculation of teleseismic
341 wavefronts and the traveltimes from the base of the model volume to the array of receivers on the
342 surface is performed with the fast marching method (FMM) (Sethian and Popovici, 1999). For both
343 study regions, the bottom of the 3-D model was set at 600 km depth and the grid spacing used for
344 the parametrization of mantle structure was 60 km. Outside the model volume the Earth is assumed
345 to be spherically symmetric, which allows the use of a 1-D global reference model to rapidly
346 compute the traveltimes from the distant sources to all grid nodes at the bottom. For a detailed
347 description of the technique and the inversion equation we refer the reader to Rawlinson et al.
348 (2006). In both cases, the nonlinear inversion was performed by testing different values of the
349 maximum iteration number, to check the overall stability and performance in modeling the residual
350 data. The tomographic images displayed in the following subsections describe the velocity field

351 computed at the third iteration, as only minor improvements in the data fit (<1%) and small
352 structural changes in the velocity patterns were observed, for both cases, with successive inversion
353 steps. Since the parametrization for the two models is the same, their direct comparison is possible.
354 In general, the images for the CA show stronger anomalies, which explains the different scale of the
355 color palettes in Figs. 6-10, +/- 0.2 km/s for the GA and +/- 0.3 km/s for the CA, in spite of the
356 stronger regularization applied in the CA inversion. The difference in the amplitude of the
357 anomalies could be explained by differences in accuracy of the two datasets and in the RMS
358 reduction, but also by a greater heterogeneity of the CA upper mantle with respect to GA. With
359 respect to previous tomographic studies at the same scale (e.g., Montuori et al., 2007; Giacomuzzi
360 et al., 2011) the CA inversion we present has greater resolution and coverage of the oceanic areas.
361 A comparison between the resolution of the GA and CA models is performed using the
362 “checkerboard tests” displayed in Fig. 5. In this test the input velocity model is formed by
363 alternating regions of fast and slow anomalies (with added gaussian noise to account for errors in
364 the data; Monna et al., 2013a). The recovered pattern provides information on the well resolved
365 areas of the models. We note that the CA model could be parametrized with a smaller grid (~80
366 km), but we have chosen the same parametrization as for GA (100 km) to better compare them. In
367 any case, in both cases the parts that we interpret are in volumes of the models that are reliably
368 reconstructed in the synthetic tests. We have clarified this aspect in the text.

369

370 **3.1 Gibraltar Arc (GA) model**

371 The information on the GA model that we present in the following is an updated summary of the
372 results presented in Monna et al. (2013a, 2015). The teleseismic data set for the GA model is
373 composed by 152 events recorded in the period 2007-2009 by the permanent networks of Spain,
374 Portugal, and Morocco, and by the NEAREST OBS array (Carrara et al., 2008) deployed in the
375 Gulf of Cadiz from August 2007 to August 2008 (in total 111 seismic stations; Fig. 4; left). This
376 data set provided 6238 residuals for the tomography. The OBS array (25 seafloor broad band
377 stations) recorded waveforms from 67 events. Other waveforms were collected from two land
378 stations operating in SW Portugal installed during the experiment, and from the European
379 Integrated Data Archive (EIDA; <http://eida.rm.ingv.it>). To improve ray coverage, arrival times
380 extracted from the ISC bulletin (<http://www.isc.ac.uk>) were also added. The average time pick error
381 was estimated in 0.43s. A crustal correction was applied based on four models which take into
382 account up-to-date information available from published studies. These four models represent the
383 Atlantic Ocean Domain, the Iberian Peninsula, Betics and Rif, and Atlas (see Table 1 in Monna et
384 al., 2013a).

385 The GA-Alboran Basin model lateral extension (Fig. 3; left) spans 12.0° in latitude (from 31.0°N to

386 43.0°N), and 16.0° in longitude (from 15.0°W to 1.0°E). The 3-D velocity grid comprises 5544
387 nodes at 60 km spacing in all three dimensions (depth, latitude, longitude). The tomographic
388 inversion was carried out with damping and smoothing parameters of 5.0 and 2.5, respectively. The
389 three-step inversion reduced the data variance by 26% from 0.53 to 0.39 s² (Monna et al., 2013a).

390 We now briefly describe the main features found in the GA model as represented in Figs. 6 (maps)
391 and 8 (cross-sections). Further details on the velocity pattern imaged in the Atlantic portion of the
392 GA model can be found in Monna et al. (2015). The tomographic images show:

393 1) A high velocity body with arcuate geometry under the Betics-Alboran Sea area (Al-HVA). This
394 fast structure depicts an L-shaped slab steeply dipping from the uppermost mantle to the transition
395 zone where it becomes less curved.

396 2) A high-velocity body under the Horseshoe Abyssal Plain in the Atlantic region (HAP-HVA).

397 3) A diffuse low velocity anomaly (EAt-LVA) present in the Eastern Atlantic region south of the
398 Gloria fault, down to the mantle transition zone.

399 4) A prominent low velocity anomaly below the Gulf of Cadiz (GC-LVA) which separates the two
400 high-velocity bodies found under the Alboran (Al-HVA) and Atlantic regions (HAP-HVA).

401 Al-HVA extends from the surface to the base of our model (Figs. 6 and 8), and its maximum width
402 is ~300 km in the EW direction below the Granada region (AA'). The AA' profile, which crosses
403 the southern tip of the Iberian peninsula, shows the transition from the Atlantic to the Alboran
404 domain, and the width of the slab (100–200 km). Section BB' crosses the Alboran Sea and shows
405 the north-south extension of Al-HVA (approximately 300 km). Subcrustal seismicity is distributed
406 along an arc-shaped belt with the deeper events contained in the uppermost part of the Al-HVA.
407 These intermediate-depth earthquakes have a distribution which is not typical of subduction zones,
408 in contrast with the clear Benioff zone of the Calabrian Arc (Fig. 9). Nevertheless, they provide
409 information on the subducted oceanic slab beneath the Alboran basin, as their occurrence is usually
410 linked to dehydration reactions in subducting oceanic lithosphere (e. g. Hacker et al., 2003).

411 GC-LVA extends from the top of the model down to ~250 km depth in (AA'). Below the
412 NEAREST OBS array, roughly under the Horseshoe Abyssal Plain, the model shows HAP-HVA
413 down to a depth of ~240km (Fig. 6). From profile AA' we obtain an east-west extension for HAP-
414 HVA of ~250 km. This feature has been interpreted as a developed subduction process in the
415 Gorringe Bank region (Monna et al., 2015).

416

417 **3.2 Calabrian Arc (CA) model**

418 The teleseismic events were collected from the Italian National Network (managed by INGV) and
419 from temporary experiments performed both at sea (TYDE (Dahm et al., 2002) and NEMO-SN1
420 (Favali et al., 2013) and on-land (SAPTEX (Cimini et al., 2006) and SeSCAL (Frepoli et al., 2011))

421 during the last decade. The integrated network used in this study includes 209 stations (Fig. 4;
422 right). The dataset spans the years 2000-2008 and consists of 276 events for a total of 8635
423 residuals. Crustal corrections of traveltimes residuals were performed on the basis of two models
424 (Monna et al., 2013b), one for the continental part (Sicily and Apennines) and one for the oceanic
425 part (southern Tyrrhenian and Ionian Seas). Differently from the GA data set, the CA data set
426 comes all from very accurate handpicked arrival times with an estimated average error of 0.16s
427 which is almost 1/3 of the GA time pick error. The high quality of the CA data led to a solution
428 model which is associated to a significant reduction of the residual variance.

429 The CA-Tyrrhenian Basin model lateral extension (Fig. 3; right) spans 8.0° in latitude (from 36.0°N
430 to 44.0°N), and 12.0° in longitude (from 9.0°E to 21.0°E). The 3-D velocity grid comprises 3344
431 nodes spaced apart, 60 km in all the three directions, as for the GA model. For the CA model we
432 obtained a variance improvement of over 51%, from 0.41 to 0.20 s².

433 The main features found in the CA model, represented in Figs. 7 (maps) and 9 (cross-sections), are:

- 434 1) A high velocity body with slab-like shape under the Tyrrhenian Sea area (STy-HVA).
- 435 2) A high-velocity body under the Apennines (Ap-HVA).
- 436 3) A high velocity anomaly visible below the Adriatic Sea (Adr-HVA) adjacent to the Ap-HVA
437 visible below 300 km depth.
- 438 4) A diffuse low velocity anomaly (STy-LVA) adjacent to Sty-HVA and Ap-HVA, found down to
439 ~350 km depth. In the depth interval ~100-300 km, STy-LVA and the prominent low velocity zone
440 imaged in the Ionian side (Io-LVA) join in a continuous belt surrounding the main fast structures.
- 441 5) A low velocity anomaly (Ap-LVA) at lithospheric depths below the central and southern
442 Apennines, down to 120 km depth. Ap-LVA interrupts the lateral continuity of Ap-HVA,
443 suggesting that the Apenninic slab has been subjected to tearing and slab window formation
444 processes. Its geometry is clearly defined by the NW-SE profile shown in Fig. 10 (cross-section
445 CC').

446 The deep seismicity delineates a well defined Wadati-Benioff plane, which is included in the
447 volumes with the highest velocity perturbations, and is mostly concentrated in the 100-350 km
448 depth range (Figs. 7 and 9). The high velocity slab shows a remarkable horseshoe shape in the 100-
449 300 km interval. STy-HVA extends from crustal depths down to the bottom of the model (the lower
450 part of the transition zone), and its lateral extension is about 350 km (Fig. 9, BB'). Ap-HVA appears
451 from uppermost mantle depths down to ~120 km depth, as two distinct anomalies, one under the
452 central (CAp-HVA) and the other below the southern Apennines (SAp-HVA). Ap-HVA seems to
453 merge with Sty-HVA from 180 km depth down to the bottom of the model (Fig. 7).

454 The pattern of low P-wave velocity perturbations visible around Sty-HVA (Fig. 7), is recognizable
455 also in the PM0.5 model by Piromallo and Morelli (2003) at 150 and 200 km depth.

456

457 **4. Discussion**

458 The aim of this discussion is not to tackle the reconstruction of the long-term evolution of the
459 Western Mediterranean region, which has been described in several papers, but rather to focus on
460 the final stages of arc formation in the Western Mediterranean and, in particular, on the interaction
461 of the subduction system with the portions of continental margin that are approaching the
462 subduction zone. Some key features of the Gibraltar and Calabrian subduction systems are
463 compared and contrasted on the basis of the two presented tomographic models and other
464 geophysical and geological data. We first describe and compare the lithosphere-asthenosphere
465 structure of the two arcs, then their seismicity and active tectonics, and finally we focus on the slabs
466 evolution.

467

468 *Lithosphere-asthenosphere structure*

469 There are two main high velocity anomalies (HVA) evident in the horizontal layers (Figs. 6 and 7),
470 that underlie the Alboran (Al-HVA) and the Tyrrhenian (STy-HVA) basins. Both HVAs reach the
471 mantle transition zone down to at least 600 km depth, the bottom of our models. While the STy-
472 HVA presents a more evident arcuate shape, the Al-HVA is thicker, and the stronger part of the
473 anomaly is blob-like, especially in the top 300 km. Moreover, the STy-HVA mostly underlies the
474 Tyrrhenian basin, whereas the Al-HVA is mostly located below the Betics and the Granada area,
475 where the scarce deep seismicity is found.

476 In both areas there are strong LVAs that surround the slab.

477 In the Calabrian Arc the LVA underlies the Tyrrhenian basin (STy-LVA) and the oceanic crust of
478 the Ionian Sea (Fig. 9) . The lithosphere-asthenosphere structure under the Ionian side is only
479 partially resolved due to the lack of long term broadband OBS deployments in the Western Ionian
480 Sea. Continuity of the slab is inferred only from indirect evidence (e.g., slab geometry and
481 seismicity). On the contrary, the lithosphere-asthenosphere structure below the Gulf of Cadiz (GC-
482 LVA, Fig. 8) is well resolved and represents the key feature separating the two high velocity
483 anomalies underlying the Atlantic and the Alboran, respectively (Monna et al., 2013a). We are
484 confident that GC-LVA is not an effect of low velocity uppermost crustal layers smeared down the
485 uppermost mantle, given the strong crustal correction we applied that includes a thick low-velocity
486 sedimentary layer (see Table 1 in Monna et al., 2013a).

487

488

489 *Seismicity and active tectonics*

490 Comparison of vertical profiles in Figs. 8 and 9 also clearly shows a very different spatial

491 distribution of sub-crustal seismicity, with a typical Wadati-Benioff zone for the CA and a belt of
492 intermediate-depth seismicity (<120km) for the GA. While for the CA seismicity is included in the
493 volume with the largest positive velocity anomalies, for the GA seismicity is concentrated on top of
494 the HVA. Profiles BB' give a measure of the width of the two slabs, which is about 300 km for Al-
495 HVA and 350 km for STy-HVA.

496 The different patterns of sub-crustal seismicity in the Gibraltar and Calabrian Arcs, suggests that a
497 different tectonic regime is active in the two arcs (Fig. 3). It is noteworthy that only limited
498 seismicity occurs offshore in the CA accretionary prism, but remarkable seismicity with large
499 earthquakes, mostly hystorical but also instrumental, characterizes the onshore, uplifted region of
500 the arc, continuing into the southern Apennines. Focal mechanisms of crustal earthquakes indicate
501 orogen-perpendicular extension (Vannucci et al., 2004; Frepoli et al., 2011). In the GA almost no
502 seismicity occurs in the outer accretionary prism; instead, seismicity (found also down to ~60 km)
503 is present in the Gorringe Bank-Horseshoe Abyssal Plain (e.g., Geissler et al., 2010), where it is
504 associated to a high velocity subducting lithosphere (Monna et al., 2015). No relevant seismicity is
505 present at the apex of the GA, whereas some seismicity is related to the right-lateral strike-slip
506 regime found in the eastern Betics, and a remarkable crustal seismicity is present in the Alboran
507 basin (Serpelloni et al., 2007; Stich et al., 2006; 2010), along the Trans-Alboran shear zone
508 (Alvarez-Marron, 1999). The distribution of crustal seismicity appears to reflect the occurrence of a
509 diffuse plate boundary deformation that shifts from the Gloria Fault-Gorringe-SW Iberia system to
510 the Maghrebides of north Africa; this southward shift occurs just across the Alboran basin (Fig. 3)
511 (Serpelloni et al., 2007).

512

513 *Evolution of the two subduction systems*

514 The evolution of the Mediterranean subduction is strongly controlled by the paleogeography of the
515 African margin (lower plate), and in particular by the location and extent of its oceanic domains. A
516 tectonic reconstruction at Tortonian time (Fig. 11) shows the different stages in the formation of the
517 Gibraltar and Calabrian arcs. This time is crucial since the Tyrrhenian basin was in its initial stage,
518 and the Calabrian Arc formed subsequently, driven by the subduction and rollback of the
519 Neotethyan ocean located between Africa and Adria. On the contrary, the Gibraltar Arc was almost
520 completely defined.

521 We propose an interpretation that is summarized in Fig. 12.

522

523 During the evolution of the retreating Mediterranean subduction, the soft collision of the outward-
524 migrating orogen with the African margin first occurred in the Magrebides (e.g., Lonergan and
525 White, 1997; Rosenbaum and Lister, 2004). The soft collision was followed by a slab breakoff,

526 marked by a change from orogenic to anorogenic magmatism (Maury et al., 2000; Abbassene et al.,
527 2016), that disrupted the originally continuous subducted slab, and propagated laterally both
528 eastward and westward (Fig. 12), to originate the Calabrian and Gibraltar Arcs, respectively
529 (Wortel and Spakman, 2004). Slab tearing focussed trench retreat, favouring the formation of
530 tightly arcuate subduction zones (e.g., Schellart et al., 2007). The narrow CA subducted slab (Fig.
531 9; BB') is discontinuous on either side, underneath Sicily and southern Apennines. The lack of high
532 velocity bodies underneath western Sicily is likely a result of progressive lithospheric tearing.
533 Tearing propagated eastward along the north African continental margin, removing the slab, during
534 the Tyrrhenian opening from 10 to 2 Ma (Carminati et al., 1999; Faccenna et al., 2004; Goes et al.,
535 2004; Argnani, 2009). An interruption of the slab or slab window underneath the Southern
536 Apennines (Fig. 12) is visible in the tomography models as a low velocity anomaly at lithospheric
537 depths (Fig. 10). The presence of a slab window is consistent with abundant volcanic products
538 younger than 2 Ma in the Campania Magmatic Province, which supports the tapping of deep mantle
539 reservoirs (Serri, 1990).

540 The low mantle velocity underneath Calabria (e.g., Mele, 1998) suggests a decoupling of the slab
541 from the overlying lithosphere, that can be partly responsible for the recent uplift of Calabria
542 (Gvirtzman and Nur, 1999; Argnani, 2000). A role of toroidal mantle flow dynamically sustaining
543 the Calabrian topography has also been inferred (Faccenna et al., 2011), although the contribution
544 of dynamic topography is likely a minor one (Molnar et al., 2015). The existence of lithospheric
545 tears located on either side of the Calabrian Arc is supported also by

546
547 local earthquake and seismic velocity distribution. Some authors have inferred the occurrence of
548 north-west-trending tears, that are supposed to favor the south-eastward drift of Calabria (e.g., Neri
549 et al., 2012). The seismicity gaps and reduced seismic velocities presented by Neri et al. (2012),
550 however, seem to outline discontinuities that propagated parallel to the trench, which are difficult to
551 reconcile to north-west-trending lithospheric tears that would allow displacement perpendicular to
552 the trench. In this last case, in fact, the tomographic model should suggest slab segments that are
553 laterally shifted in the north-west-direction with respect to each other, a feature that is not observed
554 (Fig. 7). In fact, the only discontinuity perpendicular to the trench is an incipient, ca. north-south-
555 trending, lithospheric tear (STEP fault) (Govers and Wortel, 2005) which is located offshore eastern
556 Sicily (Figs. 2b and 11) (Argnani, 2009).

557 As described in the following, we infer that the portion of continental lithosphere defined by our
558 tomography (Fig. 6) may have played a role in preventing a further evolution of the Gibraltar Arc.
559 In the Gibraltar system the narrow (ca. 300 km wide) high velocity body is not a typical subducting
560 slab, given its seismicity and its blob-like shape underneath the Betics (Fig. 6). Recent studies show

561 that underneath most of the Betics the subducted slab is partly torn off its adjacent continental
562 margin, whereas underneath the Rif it is still attached to the crust (e.g., Levander et al., 2014). In
563 particular, observations from seismic tomography (Bezada et al., 2013; Palomeras et al., 2014) and
564 receiver function analysis (Mancilla et al., 2015; Thurner et al., 2014) are consistent with the
565 presence of continental crust that was removed from the continental margins and is now part of the
566 slab.

567 Both slabs below the Alboran and Tyrrhenian basins are thought to belong to narrow oceanic
568 basins. The original oceanic domain belonged to the Alpine Tethys and Neotethys for the Calabrian
569 subduction (e.g., Stampfli and Borel, 2002; Argnani, 2005), and to the Alpine Tethys and Central
570 Atlantic for the Gibraltar subduction (e.g., Gutscher et al., 2012). However, the physical connection
571 between Alpine Tethys and the Central Atlantic proposed by several authors (see Section 2.1) can
572 be questioned. In fact the occurrence of an arcuate structure underneath the Gibraltar Arc, with a
573 seismic velocity pertaining to continental lithosphere, suggests the presence of a possible
574 continental domain located just west of Gibraltar in the GA model (Figs. 6 and 8; Monna et al.
575 (2013a, 2015)). Recent tomography models (Bonnin et al., 2014; Villaseñor et al., 2015) show a
576 low velocity anomaly at lithospheric depths just west of the Gibraltar Strait, which agrees very well
577 with our GC-LVA.

578 The existence of possibly Jurassic oceanic crust in the Gulf of Cadiz has been documented by
579 refraction data (Sallares et al., 2011), but the refraction profile is located further to the west of the
580 low-velocity anomaly that we attribute to continental lithosphere (Fig. 2a), and recent refraction
581 data across the Gibraltar Strait show a continental crustal structure (Gil et al., 2014). The boundary
582 between continental and oceanic mantle domain is placed just east of Gibraltar Arc (Morais et al.,
583 2015) through receiver function analysis, and the continuity of the thickened crust along the
584 Gibraltar Arc (Mancilla et al., 2015) seems to support the occurrence of a substrate of continental
585 nature. Although Mancilla et al (2015) propose an oceanic connection between the Atlantic and the
586 subducted slab, their receiver functions data are also compatible with our hypothesis, as their data
587 do not constrain the nature of the crust in the western offshore of Gibraltar.

588 The presence of a portion of continental lithosphere that has limited the Alpine Tethys to the west,
589 and that is now choking the subduction underneath the Alboran basin, fits well with other recent
590 high resolution tomography models (Bonnin et al., 2014; Palomeras et al., 2014; Villaseñor, 2015).
591 These tomography images can be explained by a process of ongoing delamination, with a sinking
592 oceanic slab pulling and thinning the lithosphere of the Betics and Rif.

593 In our interpretation, continental lithosphere is entering subduction in the Gibraltar Arc from the
594 west, and due to its positive buoyancy it contrasts the slab pull effect, favoring slab break-off,
595 delamination, and limiting asthenosphere wedging west of the Gibraltar Arc, and thus limiting

596 uplift and extension. Active extensional tectonics and recent uplift, in fact, have not been observed
597 at the apex of the Gibraltar Arc; recent uplift occurs mostly in the Sierra Nevada (Perez-Pena et al.,
598 2010; Braga et al., 2003). On the contrary, in the CA, subduction of oceanic lithosphere is well
599 documented, with the slab connected to the oceanic Ionian lithosphere (Fig. 11) (Argnani, 2005;
600 Speranza et al., 2012). The slab pull, which is still active, favored the wedging of asthenospheric
601 mantle and ensuing uplift (Gvirtzman and Nur, 1999). The uplift, in turn, promotes gravitational
602 collapse towards the topographically low Ionian Sea and possibly triggers the extension which is
603 ongoing in Calabria (Argnani, 2000; D'Agostino et al., 2011).

604

605 **5. Summary and Conclusions**

606 The Western Mediterranean subduction system was active mostly during the Neogene, creating the
607 arcuate mountain belts and deep basins that characterize the Mediterranean orogen. Slab sinking
608 and trench retreat contributed to the opening of the Balearic and Tyrrhenian basins. Although the
609 main driving force is likely given by trench retreat of oceanic subduction within a low plate-
610 convergence setting, additional complexities came into play throughout the evolution of the
611 Western Mediterranean, the major factor being the interaction between the European subduction in
612 the Alps and the African subduction in the Apennines (e.g., Argnani, 2012). In this paper we focus
613 on the origin of the two tight loops of the Gibraltar and Calabrian Arcs using two teleseismic
614 tomography models. These two arcuate features have been often described together and considered
615 as typical of the Western Mediterranean evolution (Horvath and Berckhemer, 1982; Rosenbaum
616 and Lister, 2004; Faccenna et al., 2004). The fact that trench retreat has overtaken convergence
617 throughout the Neogene evolution of the Mediterranean implies that the nature of the lower plate
618 lithosphere may strongly affect the geodynamic balance of the system. In fact, the arcuate orogenic
619 belts were mostly formed in the final stages of the Western Mediterranean evolution and, apart from
620 trench rollback, they were affected in an important way by the geometry of the continental margins.
621 In the Gibraltar Arc both slab rollback and gravitational potential of a thickened orogen have been
622 driving forces for the emplacement of the Alboran units in the early Miocene.

623 The continuity of oceanic subduction represents the major difference between the Calabrian and
624 Gibraltar arcs. In the Gibraltar Arc the continental margin domain is entering subduction. The GA
625 tomography model suggests that the Gibraltar Arc was docking into a portion of thinned continental
626 crust, located just west of Gibraltar (Fig. 12). This buoyant lithosphere was likely responsible for
627 the end of trench retreat, and its related extension in the Alboran basin. As the subduction of the
628 oceanic lithosphere was progressively completed, the continental margin lithosphere of Africa and
629 Iberia entered into the subduction zone and was pulled down by the sinking oceanic slab, leading to
630 ongoing continental delamination underneath the western Rif and the Betics and slab breakoff

631 (Bezada et al., 2013; Levander et al., 2014; Thurner et al., 2014; Mancilla et al., 2013, 2015).
632 Active deformation in the region is reflected in the location of the roughly east-west-trending
633 Africa-Iberia plate boundary. This boundary shifts from the southwest Iberian margin to north
634 Africa just across the Alboran Sea, mostly ignoring the arcuate structures of the Gibraltar Arc, and
635 confirming that subduction is not the main operating mechanism at the moment (Zitellini et al.,
636 2009).

637 In the case of the Calabrian Arc, the slab is connected to the Ionian basin that is likely floored by
638 oceanic lithosphere (Argnani, 2005; Speranza et al., 2012). The opening of the southern Tyrrhenian
639 basin caused a soft collision of the outward migrating fold-and-thrust belt into the continental
640 margins of Adria (southern Apennines) and Africa (Sicilian Maghrebides). This soft collision was
641 followed by a trench-parallel slab break-off in both the southern Apennines and Sicilian
642 Maghrebides (Fig. 12). This process produced the slab window visible, in our CA tomographic
643 model (Figs. 7 and 10). The window underneath Sicily is much wider because the slab was
644 progressively torn off at the African margin during the Tyrrhenian backarc opening (Argnani,
645 2009), whereas the slab window under the Southern Apennines formed in the last 2 Ma and extends
646 for about 300 km along the chain (Fig. 12). A choked subduction, at much reduced rates, of a
647 narrow oceanic slab continued underneath Calabria. The pull exerted by the sinking oceanic
648 lithosphere, narrowed after slab breakoff on either side of the arc, promoted the initiation of lateral
649 tears (or STEP fault) (Govers and Wortel, 2005), particularly on the western Ionian side and along
650 the north-south branch of the Aeolian Islands (Argnani and Bonazzi, 2005; Argnani et al., 2007;
651 Argnani, 2009). The sinking Ionian slab decoupled from the overlying Calabrian orogen and
652 released the upper plate from compressional stresses, favouring the wedging of asthenosphere, as
653 indicated by reduced upper mantle Pn velocities (Mele et al., 1998) and confirmed by seismic
654 attenuation measurements (Chiarabba et al., 2008; Monna and Dahm, 2009); this last process, in
655 turn, promoted uplift and extension in the Calabrian Arc.

656

657

658 **Acknowledgements**

The OBS teleseismic data was collected during the NEAREST EC-project (coordinator N. Zitellini) and the TYDE project (participants: INGV, ISMAR-CNR, IfM-GEOMAR and University of Hamburg University). We thank the NEAREST and TYDE Working Group for making the seismic data available. Waveforms for the CA model can be downloaded from the European Integrated Data Archive (EIDA; <http://eida.rm.ingv.it>). Arrival times at land station for the GA model were extracted from the International Seismic Center (ISC; <http://www.isc.ac.uk>). Teleseismic event location is provided by the National Earthquake Information Center (NEIC; <http://earthquake.usgs.gov/research>).

Data from SAPTEX and SeSCAL experiment are available upon request from giovannibattista.cimini@ingv.it. The figures were produced with GMT (Wessel and Smith, 1991).

659 **References**

- 660 Abbassene, F., Chazot, G., Bellon, H., Bruguier, O., Ouabadi, A., Maury, R.C., Déverchère, J.,
661 Bosch, D., Monié, P., 2016. A 17Ma onset for the post-collisional K-rich calc-alkaline
662 magmatism in the Maghrebides: Evidence from Bougaroun (northeastern Algeria) and
663 geodynamic implications. *Tectonophysics*, 674, 114–134.
- 664 Alvarez-Marrón, J., 1999. Pliocene to Holocene structure of the Eastern Alboran Sea (Western
665 Mediterranean). *Proceedings of the Ocean Drilling Program, Scientific Results*, 161, 345-
666 355. doi:10.2973/odp.proc.sr.161.224.1999
- 667 Amato, A., Alessandrini, B., Cimini, G.B., 1993. Teleseismic wave tomography of Italy, in: Iyer,
668 H.M., Hirahata, K. (Eds.), *Seismic Tomography: Theory and Practice*. Chapman and Hall,
669 London, pp. 361–397.
- 670 Argnani, A., 2012. Plate motion and the evolution of Alpine Corsica and Northern Apennines.
671 *Tectonophysics, Orogenic processes and structural heritage in Alpine-type mountain belts*
672 579, 207–219. doi:10.1016/j.tecto.2012.06.010
- 673 Argnani, A., 2009. Evolution of the southern Tyrrhenian slab tear and active tectonics along the
674 western edge of the Tyrrhenian subducted slab, in: Hinsbergen, D.J.J.V., Edwards, M.A.,
675 Govers, R. (Eds.), *Collision and Collapse at the Africa–Arabia–Eurasia Subduction Zone*.
676 The Geological Society, London, Special Publications, pp. 193 – 212.
- 677 Argnani, A., 2006. Some issues regarding the central Mediterranean neotectonics. *Boll. Geof. Teor.*
678 *Appl.* 47, 13 – 37.
- 679 Argnani, A., 2005. Possible record of a Triassic ocean in the southern Apennines. *Boll. Soc. Geol.*
680 *It.* 124, 109 – 121.
- 681 Argnani, A., 2000. The southern Apennines-Tyrrhenian system within the kinematic frame of the
682 central Mediterranean. *Mem. Soc. Geol. It* 55, 115 – 122.
- 683 Argnani, A., Savelli, C., 1999. Cenozoic volcano-tectonics in the southern Tyrrhenian Sea: Space-
684 time distribution and geodynamic significance. *J. Geodyn.* 27, 409 – 432.
- 685 Argnani A. and Bonazzi C., 2005. Tectonics of Eastern Sicily Offshore. *Tectonics* 24, TC4009,
686 doi:10.1029/2004TC001656
- 687 Argnani, A., Serpelloni, E., Bonazzi, C., 2007. Pattern of deformation around the central Aeolian
688 Islands: evidence from multichannel seismics and GPS data. *Terra Nova* 19, 317–323.
689 doi:10.1111/j.1365-3121.2007.00753.x
- 690 Baccheschi, P., Margheriti, L., Steckler, M.S., 2008. SKS splitting in Southern Italy: Anisotropy
691 variations in a fragmented subduction zone. *Tectonophysics* 462, 49–67.

692 doi:10.1016/j.tecto.2007.10.014

693 Barberi, F., Innocenti, F., Ferrara, G., Keller, J., Villari, L., 1974. Evolution of Eolian arc volcanism
694 (Southern Tyrrhenian Sea). *Earth and Planetary Science Letters* 21, 269–276.
695 doi:10.1016/0012-821X(74)90161-7

696 Bezada, M.J., Humphreys, E.D., Toomey, D.R., Harnafi, M., Dávila, J.M., Gallart, J., 2013.
697 Evidence for slab rollback in westernmost Mediterranean from improved upper mantle
698 imaging. *Earth and Planetary Science Letters* 368, 51–60. doi:10.1016/j.epsl.2013.02.024

699 Bigi, G., Cosentino, D., Parotto, M., Sartori, R., Scandone, P., 1990 Structural Model of Italy
700 1:500.000. CNR, Progetto Finalizzato Geodinamica.

701 Biju-Duval, B., Morel, Y., Baudrimont, A., Bizon, G., Bizon, J.J., 1982. Données nouvelles sur les
702 marges du Bassin Ionien profond (Méditerranée Orientale). Résultats des campagnes
703 Escarmed. *Oil & Gas Science and Technology - Rev. IFP* 37, 713–732.
704 doi:10.2516/ogst:1982036

705 Bijwaard, H., Spakman, W., 2000. Non-linear global P-wave tomography by iterated linearized
706 inversion. *Geophysical Journal International* 141, 71–82. doi:10.1046/j.1365-
707 246X.2000.00053.x

708 Blanco, M.J., Spakman, W., 1993. The P-wave velocity structure of the mantle below the Iberian
709 Peninsula: evidence for subducted lithosphere below southern Spain. *Tectonophysics* 221,
710 13–34. doi:10.1016/0040-1951(93)90025-F

711 Blankenship, C.L., 1992. Structure and palaeogeography of the External Betic Cordillera, southern
712 Spain. *Marine and Petroleum Geology* 9, 256–264. doi:10.1016/0264-8172(92)90074-O

713 Bonardi, G., Cavazza, W., Perrone, V., Rossi, S., 2001. Calabria-Peloritani terrane and northern
714 Ionian Sea, in: Vai, G.B., Martini, I.P. (Eds.), *Anatomy of an Orogen: The Apennines and*
715 *Adjacent Mediterranean Basins*. Springer Netherlands, pp. 287–306.

716 Bonnin, M., Nolet, G., Villaseñor, A., Gallart, J., Thomas, C., 2014. Multiple-frequency
717 tomography of the upper mantle beneath the African/Iberian collision zone, *Geophys. J. Int.*,
718 198(3), 1458-1473, doi:10.1093/gji/ggu214.

719 Booth-Rea, G., Ranero, C.R., Martínez-Martínez, J.M., Grevemeyer, I., 2007. Crustal types and
720 Tertiary tectonic evolution of the Alborán sea, western Mediterranean. *Geochem. Geophys.*
721 *Geosyst.* 8, Q10005. doi:10.1029/2007GC001639

722 Bordoni, P., Valensise, G., 1998. Deformation of the 125 ka marine terrace in Italy: Tectonic
723 implications, in: Stewart, I.S., Finzi, C.V. (Eds.), *Coastal Tectonics, Special Publications*.
724 The Geological Society, London, pp. 71 – 110.

725 Braga, J.C., Martín, J.M., Quesada, C., 2003. Patterns and average rates of late Neogene– recent
726 uplift of the Betic Cordillera, SE Spain. *Geomorphology* 50, 3–26, doi:10.1016/S0169-

727 555X(02)00205-2

728 Buform, E., Bezzeghoud, M., Udías, A., Pro, C., 2004. Seismic Sources on the Iberia-African Plate
729 Boundary and their Tectonic Implications. *Pure appl. geophys.* 161, 623–646.
730 doi:10.1007/s00024-003-2466-1

731 Buform, E., Pro, C., Cesca, S., Udias, A. S., del Fresno, C., 2011. The 2010 Granada, Spain, deep
732 earthquake, *Bull. Seism. Soc. Am.*, 101(5):2418-2430. doi: 10.1785/0120110022.

733 Burchfiel, B.C., Royden, L.H., 1991. Antler orogeny: A Mediterranean-type orogeny. *Geology*, 19,
734 66–69.

735 Butler, J.P., Beaumont, C., Jamieson, R.A., 2014. The Alps 2: Controls on crustal subduction and
736 (ultra)high-pressure rock exhumation in Alpine-type orogens, *J. Geophys. Res. Solid Earth*,
737 119, 5987–6022, doi:10.1002/2013JB010799.

738 Calvert, A., Sandvol, E., Seber, D., Barazangi, M., Vidal, F., Alguacil, G., Jabour, N., 2000.
739 Propagation of regional seismic phases (Lg and Sn) and Pn velocity structure along the
740 Africa–Iberia plate boundary zone: tectonic implications. *Geophysical Journal International*
741 142, 384–408. doi:10.1046/j.1365-246x.2000.00160.x

742 Carminati, E., Giunchi, C., Argnani, A., Sabadini, R., Fernandez, M., 1999. Plio-Quaternary vertical
743 motion of the Northern Apennines: Insights from dynamic modeling. *Tectonics* 18, 703–
744 718. doi:10.1029/1999TC900015

745 Carminati, E., Lustrino, M., Doglioni, C., 2012. Geodynamic evolution of the central and western
746 Mediterranean: Tectonics vs. igneous petrology constraints. *Tectonophysics, Orogenic*
747 *processes and structural heritage in Alpine-type mountain belts* 579, 173–192.
748 doi:10.1016/j.tecto.2012.01.026

749 Carminati, E., Wortel, M.J.R., Spakman, W., Sabadini, R., 1998. The role of slab detachment
750 processes in the opening of the western–central Mediterranean basins: some geological and
751 geophysical evidence. *Earth and Planetary Science Letters* 160, 651–665.
752 doi:10.1016/S0012-821X(98)00118-6

753 Carrara, G., NEAREST Team, 2008. NEAREST 2008 CRUISE PRELIMINARY REPORT R/V
754 URANIA, 1st Aug 2008- 04th Sept 2008, Technical Report. ISMAR CNR.

755 Chamot-Rooke, N., Jestin, F., 1997. Constraints on Moho Depth and Crustal Thickness in the
756 Liguro-Provençal Basin from a 3d Gravity Inversion: Geodynamic Implications. *REVUE*
757 *DE L' INSTITUT FRANCAIS DU PETROLE* 52, 557–583. doi:10.2516/ogst:1997060

758 Channell, J.E.T., Oldow, J.S., Catalano, R., D'Argenio, B., 1990. Paleomagnetically determined
759 rotations in the western Sicilian fold and thrust belt. *Tectonics* 9, 641–660.
760 doi:10.1029/TC009i004p00641

761 Chertova, M.V., Spakman, W., Geenen, T., van den Berg, A.P., van Hinsbergen, D.J.J., 2014.

762 Underpinning tectArgnani A. and Bonazzi C. (2005) - Tectonics of Eastern Sicily Offshore. *Tectonics*, 24,
763 TC4009, doi:10.1029/2004TC001656. onic reconstructions of the western Mediterranean region
764 with dynamic slab evolution from 3-D numerical modeling. *J. Geophys. Res. Solid Earth*
765 119, 2014JB011150. doi:10.1002/2014JB011150

766 Chiarabba, C., De Gori, P., Speranza, F., 2008. The southern Tyrrhenian subduction zone: Deep
767 geometry, magmatism and Plio-Pleistocene evolution. *Earth and Planetary Science Letters*
768 268, 408–423. doi:10.1016/j.epsl.2008.01.036

769 Cifelli, F., Mattei, M., Porreca, M., 2008. New paleomagnetic data from Oligocene–upper Miocene
770 sediments in the Rif chain (northern Morocco): Insights on the Neogene tectonic evolution
771 of the Gibraltar arc. *J. Geophys. Res.* 113, B02104. doi:10.1029/2007JB005271

772 Cifelli, F., Mattei, M., Rossetti, F., 2007. Tectonic evolution of arcuate mountain belts on top of a
773 retreating subduction slab: The example of the Calabrian Arc. *J. Geophys. Res.* 112,
774 B09101. doi:10.1029/2006JB004848

775 Cimini, G.B., 1999. P-wave deep velocity structure of the Southern Tyrrhenian Subduction Zone
776 from nonlinear teleseismic travelttime tomography. *Geophys. Res. Lett.* 26, 3709–3712.
777 doi:10.1029/1999GL010907

778 Cimini, G.B., De Gori, P., Frepoli, A., 2006. Passive seismology in southern Italy: the SAPTEX
779 array *Ann. Geophys.*, 49 (2/3), 825–840.

780 Cimini, G.B., Marchetti, A., 2006. Deep structure of peninsular Italy from seismic tomography and
781 subcrustal seismicity. *Ann. Geophys. Supplement - to - Vol - 49*, 331 – 345.

782 Cloos, M., 1993. Lithospheric buoyancy and collisional orogenesis: subduction of oceanic plateaus,
783 continental margins, island arcs, spreading ridges, and seamounts. *Bulletin of the Geological*
784 *Society of America* 105, 715–737.

785 D’Agostino, N., D’Anastasio, E., Gervasi, A., Guerra, I., Nedimović, M.R., Seeber, L., Steckler,
786 M., 2011. Forearc extension and slow rollback of the Calabrian Arc from GPS
787 measurements. *Geophys. Res. Lett.* 38, L17304. doi:10.1029/2011GL048270

788 Dahm, T., Thorwart, M., Flueh, E.R., Braun, T., Herber, R., Favali, P., Beranzoli, L., D’Anna, G.,
789 Frugoni, F., Smriglio, G., 2002. Ocean bottom seismometers deployed in Tyrrhenian Sea.
790 *Eos Trans. AGU* 83, 309–315. doi:10.1029/2002EO000221

791 De Astis, G., Ventura, G., Vilardo, G., 2003. Geodynamic significance of the Aeolian volcanism
792 (Southern Tyrrhenian Sea, Italy) in light of structural, seismological, and geochemical data.
793 *Tectonics* 22, 1040. doi:10.1029/2003TC001506

794 Dewey, J.F., 1988. Extensional collapse of orogens. *Tectonics* 7, 1123–1139.
795 doi:10.1029/TC007i006p01123

796 Dewey, J.F., Helman, M.L., Knott, S.D., Turco, E., Hutton, D.H.W., 1989. Kinematics of the

797 western Mediterranean. Geological Society, London, Special Publications 45, 265–283.
798 doi:10.1144/GSL.SP.1989.045.01.15

799 Dewey, J.F., Pitman, W.C., Ryan, W.B.F., Bonnin, J., 1973. Plate Tectonics and the Evolution of
800 the Alpine System. Geological Society of America Bulletin 84, 3137–3180.
801 doi:10.1130/0016-7606(1973)84<3137:PTATEO>2.0.CO;2

802 Duarte, J.C., Rosas, F.M., Terrinha, P., Schellart, W.P., Boutelier, D., Gutscher, M.-A., Ribeiro, A.,
803 2013. Are subduction zones invading the Atlantic? Evidence from the southwest Iberia
804 margin. *Geology* G34100.1. doi:10.1130/G34100.1

805 Duggen, S., Hoernle, K., Bogaard, P.V.D., Garbe-Schönberg, D., 2005. Post-Collisional Transition
806 from Subduction- to Intraplate-type Magmatism in the Westernmost Mediterranean:
807 Evidence for Continental-Edge Delamination of Subcontinental Lithosphere. *J. Petrology*
808 46, 1155–1201. doi:10.1093/petrology/egi013

809 Faccenna, C., Mattei, M., Funiciello, R., Jolivet, L., 1997. Styles of back-arc extension in the
810 Central Mediterranean. *Terra Nova* 9, 126–130. doi:10.1046/j.1365-3121.1997.d01-12.x

811 Faccenna, C., Molin, P., Orecchio, B., Olivetti, V., Bellier, O., Funiciello, F., Minelli, L., Piromallo,
812 C., Billi, A., 2011. Topography of the Calabria subduction zone (southern Italy): Clues for
813 the origin of Mt. Etna. *Tectonics* 30, TC1003. doi:10.1029/2010TC002694

814 Faccenna, C., Piromallo, C., Crespo-Blanc, A., Jolivet, L., Rossetti, F., 2004. Lateral slab
815 deformation and the origin of the western Mediterranean arcs. *Tectonics* 23, TC1012.
816 doi:10.1029/2002TC001488

817 Favali, P., Chierici, F., Marinaro, G., Giovanetti, G., Azzarone, A., Beranzoli, L., De Santis, A.,
818 Embriaco, D., Monna, S., Bue, N. Lo, Sgroi, T., Cianchini, G., Badiali, L., Qamili, E., De
819 Caro, M.G., Falcone, G., Montuori, C., Frugoni, F., Riccobene, G., Sedita, M., Barbagallo,
820 G., Cacopardo, G., Cali, C., Cocimano, R., Coniglione, R., Costa, M., D'Amico, A., Del
821 Tevere, F., Distefano, C., Ferrera, F., Giordano, V., Imbesi, M., Lattuada, D., Migneco, E.,
822 Musumeci, M., Orlando, A., Papaleo, R., Piattelli, P., Raia, G., Rovelli, A., Sapienza, P.,
823 Speziale, F., Trovato, A., Viola, S., Ameli, F., Bonori, M., Capone, A., Masullo, R.,
824 Simeone, F., Pignagnoli, L., Zitellini, N., Bruni, F., Gasparoni, F., Pavan, G., 2013. NEMO-
825 SN1 Abyssal Cabled Observatory in the Western Ionian Sea. *IEEE Journal of Oceanic*
826 *Engineering* 38, 358–374. doi:10.1109/JOE.2012.2224536

827 Fillerup, M.A., Knapp, J.H., Knapp, C.C., Raileanu, V. 2010. Mantle earthquakes in the absence of
828 subduction? Continental delamination in the Romanian Carpathians. *Lithosphere* 2. 333–
829 340, doi: 10.1130/L102.1

830 Frepoli, A., Maggi, C., Cimini, G.B., Marchetti, A., Chiappini, M., 2011. Seismotectonic of
831 Southern Apennines from recent passive seismic experiments. *Journal of Geodynamics*,

832 Active Tectonics of the Circum-Adriatic Region 51, 110–124.
833 doi:10.1016/j.jog.2010.02.007

834 Frepoli, A., Selvaggi, G., Chiarabba, C., Amato, A., 1996. State of stress in the Southern
835 Tyrrhenian subduction zone from fault-plane solutions. *Geophys. J. Int.* 125, 879–891.
836 doi:10.1111/j.1365-246X.1996.tb06031.x

837 Gattacceca, J., Speranza, F., 2002. Paleomagnetism of Jurassic to Miocene sediments from the
838 Apenninic carbonate platform (southern Apennines, Italy): evidence for a 60°
839 counterclockwise Miocene rotation. *Earth and Planetary Science Letters* 201, 19–34.
840 doi:10.1016/S0012-821.

841 Geissler, W.H., Matias, L., Stich, D., Carrilho, F., Jokat, W., Monna, S., IbenBrahim, A., Mancilla,
842 F., Gutscher, M.-A., Sallarès, V., Zitellini, N., 2010. Focal mechanisms for sub-crustal
843 earthquakes in the Gulf of Cadiz from a dense OBS deployment. *Geophys. Res. Lett.* 37,
844 L18309. doi:10.1029/2010GL044289

845 Giacomuzzi, G., Chiarabba, C., De Gori, P., 2011. Linking the Alps and Apennines subduction
846 systems: New constraints revealed by high-resolution teleseismic tomography. *Earth and*
847 *Planetary Science Letters* 301, 531–543. doi:10.1016/j.epsl.2010.11.033

848 Giacomuzzi, G., Civalleri, M., De Gori, P., Chiarabba, C., 2012. A 3D Vs model of the upper
849 mantle beneath Italy: Insight on the geodynamics of central Mediterranean. *Earth and*
850 *Planetary Science Letters* 335–336, 105–120. doi:10.1016/j.epsl.2012.05.004

851 Gil, A., Gallart, J., Diaz, J., Carbonell, R., Torne, M., Levander, A., Harnafi, M., 2014. Crustal
852 structure beneath the Rif Cordillera, North Morocco, from the RIFSIS wide-angle reflection
853 seismic experiment. *Geochem. Geophys. Geosyst.* 15, 4712–4733.
854 doi:10.1002/2014GC005485

855 Goes, S., Giardini, D., Jenny, S., Hollenstein, C., Kahle, H.-G., Geiger, A., 2004. A recent tectonic
856 reorganization in the south-central Mediterranean. *Earth and Planetary Science Letters* 226,
857 335–345. doi:10.1016/j.epsl.2004.07.038

858 Govers, R. & Wortel, M.J.R., 2005. Lithosphere tearing at STEP faults: Response to edges of
859 subduction zones. *Earth and Planetary Science Letters* 236 (1-2), 505-523.
860 doi:10.1016/j.epsl.2005.03.022

861 Grad, M., Tiira, T., ESC Working Group, 2009. The Moho depth map of the European Plate.
862 *Geophysical Journal International* 176, 279–292. doi:10.1111/j.1365-246X.2008.03919.x

863 Gutscher, M.-A., Dominguez, S., Westbrook, G.K., Le Roy, P., Rosas, F., Duarte, J.C., Terrinha, P.,
864 Miranda, J.M., Graindorge, D., Gailler, A., Sallares, V., Bartolome, R., 2012. The Gibraltar
865 subduction: A decade of new geophysical data. *Tectonophysics* 574–575, 72–91.
866 doi:10.1016/j.tecto.2012.08.038

867 Gutscher, M.-A., Malod, J., Rehault, J.-P., Contrucci, I., Klingelhoefer, F., Mendes-Victor, L.,
868 Spakman, W., 2002. Evidence for active subduction beneath Gibraltar. *Geology* 30, 1071–
869 1074. doi:10.1130/0091-7613.

870 Gvirtzman, Z., Nur, A., 1999. The formation of Mount Etna as the consequence of slab rollback.
871 *Nature* 401, 782–785. doi:10.1038/44555

872 Hacker, B.R., Peacock, S.M., Abers, G.A., Holloway, S.D., 2003. Subduction factory 2. Are
873 intermediate-depth earthquakes in subducting slabs linked to metamorphic dehydration
874 reactions? *J. Geophys. Res.* 108, 2030. doi:10.1029/2001JB001129

875 Hacker, B.R., Andersen, T.B., Johnston, S., Kylander-Clark, A.R.C., Peterman, E.M., Walsh, E.O.,
876 Young, D., 2010. High-temperature deformation during continental-margin subduction &
877 exhumation: The ultrahigh-pressure Western Gneiss Region of Norway. *Tectonophysics*
878 480: 149-171.

879 Horvath, F., Berckhemer, H., 1982. Mediterranean backarc basins, in: Berckhemer, H., Hsu, K.
880 (Eds.), *Alpine-Mediterranean Geodynamics*, AGU Geodynamic Series. pp. 141 – 173.

881 Jolivet, L., Faccenna, C., 2000. Mediterranean extension and the Africa-Eurasia collision. *Tectonics*
882 19, 1095–1106. doi:10.1029/2000TC900018

883 Jenny, S., Goes, S., Giardini, D., Kahle, H.-G., 2006. Seismic potential of Southern Italy,
884 *Tectonophysics.*, 415, 81–101. doi:10.1016/j.tecto.2005.12.003

885 Kastens, K., Mascle, J., Auroux, C., Bonatti, E., Broglia, C., Channell, J., Curzi, P., Emeis, K.-C.,
886 Glaçon, G., Hasegawa, S., Hieke, W., Mascle, G., McCOY, F., Mckenzie, J., Mendelson, J.,
887 Müller, C., Réhault, J.-P., Robertson, A., Sartori, R., Sprovieri, R., Torii, M., 1988. ODP
888 Leg 107 in the Tyrrhenian Sea: Insights into passive margin and back-arc basin evolution.
889 *Geological Society of America Bulletin* 100, 1140–1156. doi:10.1130/0016-7606

890 Kennett, B.L.N., Engdahl, E.R., Buland, R., 1995. Constraints on seismic velocities in the Earth
891 from traveltimes. *Geophysical Journal International* 122, 108–124. doi:10.1111/j.1365-
892 246X.1995.tb03540.x

893 Koulakov, I., Kaban, M.K., Tesauro, M., Cloetingh, S., 2009. P- and S-velocity anomalies in the
894 upper mantle beneath Europe from tomographic inversion of ISC data. *Geophysical Journal*
895 *International* 179, 345–366. doi:10.1111/j.1365-246X.2009.04279.x

896 Krijgsman, W., Garcés M., 2004. Paleomagnetic constraints on the geodynamic evolution of the
897 Gibraltar Arc. *Terra Nova* 281–287.

898 Le Pichon, X., 1982. Land-locked oceanic basins and continental collision: The Eastern
899 Mediterranean as a case example. In K.J. HSU (ed *Mountain Building Processes.*,
900 Academic Press, London, 201-211.

901 Le Pichon, X., Bergerat, F., Roulet, M.-J., 1988. Plate kinematics and tectonics leading to the

902 Alpine belt formation; A new analysis, in: Geological Society of America Special Papers.
903 Geological Society of America, pp. 111–132.

904 Levander, A., Bezada, M.J., Niu, F., Humphreys, E.D., Palomeras, I., Thurner, S.M., Masy, J.,
905 Schmitz, M., Gallart, J., Carbonell, R., Miller, M.S., 2014. Subduction-driven recycling of
906 continental margin lithosphere. *Nature* 515, 253–256. doi:10.1038/nature13878

907 Lindquist, K.G., Engle, K., Stahlke, D., Price, E., 2004. Global topography and bathymetry grid
908 improves research efforts. *Eos Trans. AGU* 85, 186–186. doi:10.1029/2004EO190003

909 Lonergan, L., White, N., 1997. Origin of the Betic-Rif mountain belt. *Tectonics* 16, 504–522.
910 doi:10.1029/96TC03937

911 Malinverno, A., Ryan, W.B.F., 1986. Extension in the Tyrrhenian Sea and shortening in the
912 Apennines as result of arc migration driven by sinking of the lithosphere. *Tectonics* 5, 227–
913 245. doi:10.1029/TC005i002p00227

914 Mancilla, F. de L., Stich, D., Berrocoso, M., Martín, R., Morales, J., Fernandez-Ros, A., Páez, R.,
915 Pérez-Peña, A., 2013. Delamination in the Betic Range: Deep structure, seismicity, and GPS
916 motion. *Geology* 41, 307–310. doi:10.1130/G33733.1

917 Mancilla, F. de L., Booth-Rea, G., Stich, D., Pérez-Peña, J.V., Morales, J., Azañón, J.M., Martín,
918 R., Giaconia, F., 2015. Slab rupture and delamination under the Betics and Rif constrained
919 from receiver functions. *Original Research Article Tectonophysics*, In Press.

920 Mascle, J., Kastens, K., Auroux, C., 1988. A land-locked back-arc basin: preliminary results from
921 ODP Leg 107 in the Tyrrhenian Sea. *Tectonophysics* 146, 149–162. doi:10.1016/0040-
922 1951(88)90088-1

923 Mauffret, A., Frizon de Lamotte, D., Lallemand, S., Gorini, C., Maillard, A., 2004. E–W opening of
924 the Algerian Basin (Western Mediterranean). *Terra Nova*, 16, 257–264.

925 Maury, R. C., R., Fourcade, S., Coulon, C., Azzouzi, M. El, Bellon, H., Coutelle, A., Ouabadi, A.,
926 Semroud, B., Megartsi, M., Cotten, J., Belanteur, O., Louni-Hacini, A., Piqué, A.,
927 Capdevila, R., Hernandez, J., Réhault, J.-P., 2000. Post-collisional Neogene magmatism of
928 the Mediterranean Maghreb margin: a consequence of slab breakoff. *Comptes Rendus de*
929 *l'Académie des Sciences - Series IIA - Earth and Planetary Science* 331, 159–173.
930 doi:10.1016/S1251-8050(00)01406-3

931 Medaouri, M., Déverchère, J., Graindorge, D., Bracene, R., Badji, R., Ouabadi, A., Yelles-
932 Chaouche, K., Bendiab, F., 2014. The transition from Alboran to Algerian basins (Western
933 Mediterranean Sea): Chronostratigraphy, deep crustal structure and tectonic evolution at the
934 rear of a narrow slab rollback system. *Journal of Geodynamics*, SI: Geodynamic evolution
935 of the Alboran domain 77, 186–205. doi:10.1016/j.jog.2014.01.003

936 Mele, G., Rovelli, A., Seber, D., Hearn, T.M., Barazangi, M., 1998. Compressional velocity

937 structure and anisotropy in the uppermost mantle beneath Italy and surrounding regions. *J.*
938 *Geophys. Res.* 103, 12529–12543. doi:10.1029/98JB00596

939 Molnar, P., England, P.C., Jones, C.H., 2015. Mantle dynamics, isostasy, and the support of high
940 terrain. *J. Geophys. Res. Solid Earth* 120, 2014JB011724. doi:10.1002/2014JB011724

941 Monna, S., Argnani, A., Cimini, G.B., Frugoni, F., Montuori, C., 2015. Constraints on the
942 geodynamic evolution of the Africa–Iberia plate margin across the Gibraltar Strait from
943 seismic tomography. *Geoscience Frontiers, Special Issue: Plate and plume tectonics:*
944 *Numerical simulation and seismic tomography* 6, 39–48. doi:10.1016/j.gsf.2014.02.003

945 Monna, S., Cimini, G.B., Montuori, C., Matias, L., Geissler, W.H., Favali, P., 2013a. New insights
946 from seismic tomography on the complex geodynamic evolution of two adjacent domains:
947 Gulf of Cadiz and Alboran Sea. *J. Geophys. Res. Solid Earth* 118, 1587–1601.
948 doi:10.1029/2012JB009607

949 Monna, S., Dahm, T., 2009. Three-dimensional P wave attenuation and velocity upper mantle
950 tomography of the southern Apennines–Calabrian Arc subduction zone. *J. Geophys. Res.*
951 114, B06304. doi:10.1029/2008JB005677

952 Monna, S., Frugoni, F., Montuori, C., Beranzoli, L., Favali, P., 2005. High quality seismological
953 recordings from the SN-1 deep seafloor observatory in the Mt. Etna region. *Geophys. Res.*
954 *Lett.* 32, L07303. doi:10.1029/2004GL021975

955 Monna, S., Sgroi, T., Dahm, T., 2013b. New insights on volcanic and tectonic structures of the
956 southern Tyrrhenian (Italy) from marine and land seismic data. *Geochem. Geophys.*
957 *Geosyst.* 14, 3703–3719. doi:10.1002/ggge.20227

958 Montuori, C., Cimini, G.B., Favali, P., 2007. Teleseismic tomography of the southern Tyrrhenian
959 subduction zone: New results from seafloor and land recordings. *J. Geophys. Res.* 112,
960 B03311. doi:10.1029/2005JB004114

961 Morais, I., Vinnik, L., Silveira, G., Kiselev, S., Matias, L., 2015. Mantle beneath the Gibraltar Arc
962 from receiver functions. *Geophys. J. Int.* 200, 1155–1171. doi:10.1093/gji/ggu456

963 Neri, G., Marotta, A.M., Orecchio, B., Presti, D., Totaro, C., Barzaghi, R., Borghi, A., 2012. How
964 lithospheric subduction changes along the Calabrian Arc in southern Italy: geophysical
965 evidences. *Int J Earth Sci (Geol Rundsch)* 101, 1949–1969. doi:10.1007/s00531-012-0762-7

966 Otsuki, K., 1989. Empirical relationships among the convergence rate of plates, rollback rate of
967 trench axis and island-arc tectonics: “laws of convergence rate of plates.” *Tectonophysics*
968 159, 73–94. doi:10.1016/0040-1951(89)90171-6

969 Palomeras, I., Thurner, S., Levander, A., Liu, K., Villasenor, A., Carbonell, R., Harnafi, M., 2014.
970 Finite-frequency Rayleigh wave tomography of the western Mediterranean: Mapping its
971 lithospheric structure. *Geochem. Geophys. Geosyst.* 15, 140–160.

972 doi:10.1002/2013GC004861

973 Patacca, E., Sartori, R., Scandone, P., 1993. Tyrrhenian Basin and Apennines. Kinematic Evolution
974 and Related Dynamic Constraints, in: Boschi, E., Mantovani, E., Morelli, A. (Eds.), Recent
975 Evolution and Seismicity of the Mediterranean Region, NATO ASI Series. Springer
976 Netherlands, pp. 161–171.

977 Pérez-Peña, J.V., Azor, A., Azañón, J.M., Keller, E.A., 2010. Active tectonics in the Sierra Nevada
978 (Betic Cordillera, SE Spain): insights from geomorphic indexes and drainage pattern
979 analysis. *Geomorphology* 119, 74–87.

980 Piromallo, C., Morelli, A., 2003. P wave tomography of the mantle under the Alpine-Mediterranean
981 area. *J. Geophys. Res.* 108, 2065. doi:10.1029/2002JB001757

982 Platt, J., Allerton, S., Kirker, A., Platzman, E., 1995. Origin of the western Subbetic arc (South
983 Spain): palaeomagnetic and structural evidence. *Journal of Structural Geology* 17, 765–775.
984 doi:10.1016/0191-8141(94)00110-L

985 Platt, J.P., Behr, W.M., Johanesen, K., Williams, J.R., 2013. The Betic-Rif Arc and Its Orogenic
986 Hinterland: A Review. *Annual Review of Earth and Planetary Sciences* 41, 313–357.
987 doi:10.1146/annurev-earth-050212-123951

988 Platt, J.P., Vissers, R.L.M., 1989. Extensional collapse of thickened continental lithosphere: A
989 working hypothesis for the Alboran Sea and Gibraltar arc. *Geology* 17, 540.
990 doi:10.1130/0091-7613

991 Platzman, E.S., Platt, J.P., Olivier, P., 1993. Palaeomagnetic rotations and fault kinematics in the
992 Rif arc of Morocco. *J. Geol. Soc. Lond.* 150:707–18

993 Pondrelli, S., Piromallo, C., Serpelloni, E., 2004. Convergence vs. retreat in Southern Tyrrhenian
994 Sea: Insights from kinematics. *Geophys. Res. Lett.* 31, L06611. doi:10.1029/2003GL019223

995 Prada, M., Sallares, V., Ranero, C.R., Vendrell, M.G., Grevemeyer, I., Zitellini, N., de Franco, R.,
996 2014. Seismic structure of the Central Tyrrhenian basin: Geophysical constraints on the
997 nature of the main crustal domains. *J. Geophys. Res. Solid Earth* 119, 2013JB010527.
998 doi:10.1002/2013JB010527

999 Rawlinson, N., Reading, A.M., Kennett, B.L.N., 2006. Lithospheric structure of Tasmania from a
1000 novel form of teleseismic tomography. *J. Geophys. Res.* 111, B02301.
1001 doi:10.1029/2005JB003803

1002 Rehault, J.-P., Boillot, G., Mauffret, A., 1984. The Western Mediterranean Basin geological
1003 evolution. *Marine Geology* 55, 447 – 477. doi:http://dx.doi.org/10.1016/0025-
1004 3227(84)90081-1

1005 Rosenbaum, G., Gasparon, M., Lucente, F.P., Peccerillo, A., Miller, M.S., 2008. Kinematics of slab
1006 tear faults during subduction segmentation and implications for Italian magmatism.

1007 Tectonics 27, TC2008. doi:10.1029/2007TC002143

1008 Rosenbaum, G., Lister, G.S., 2004. Formation of arcuate orogenic belts in the western
1009 Mediterranean region. Geological Society of America Special Papers 383, 41–56.
1010 doi:10.1130/0-8137-2383-3

1011 Rosenbaum, G., Lister, G.S., Duboz, C., 2002. Relative motions of Africa, Iberia and Europe during
1012 Alpine orogeny. Tectonophysics 359, 117–129. doi:10.1016/S0040-1951

1013 Royden, L.H., 1993. Evolution of retreating subduction boundaries formed during continental
1014 collision. Tectonics 12, 629–638. doi:10.1029/92TC02641

1015 Sallarès, V., Gailler, A., Gutscher, M.-A., Graindorge, D., Bartolomé, R., Gràcia, E., Díaz, J.,
1016 Dañobeitia, J., Zitellini, N., 2011. Seismic evidence for the presence of Jurassic oceanic
1017 crust in the central Gulf of Cadiz (SW Iberian margin). Earth and Planetary Science Letters
1018 311, 1–2, 1, 112–123, doi:10.1016/j.epsl.2011.09.003

1019 Schettino, A., Turco, E., 2006. Plate kinematics of the Western Mediterranean region during the
1020 Oligocene and Early Miocene. Geophysical Journal International 166, 1398–1423.
1021 doi:10.1111/j.1365-246X.2006.02997.x

1022 Seber, D., Barazangi, M., Ibenbrahim, A., Demnati, A., 1996. Geophysical evidence for lithospheric
1023 delamination beneath the Alboran Sea and Rif–Betic mountains. Nature 379, 785–790.
1024 doi:10.1038/379785a0

1025 Séranne, M., 1999. The Gulf of Lion continental margin (NW Mediterranean) revisited by IBS: an
1026 overview. Geological Society, London, Special Publications 156, 15–36.
1027 doi:10.1144/GSL.SP.1999.156.01.03

1028 Serpelloni, E., Vannucci, G., Pondrelli, S., Argnani, A., Casula, G., Anzidei, M., Baldi, P.,
1029 Gasperini, P., 2007. Kinematics of the Western Africa-Eurasia plate boundary from focal
1030 mechanisms and GPS data. Geophysical Journal International 169, 1180–1200.
1031 doi:10.1111/j.1365-246X.2007.03367.x

1032 Serri, G., 1990. Neogene-Quaternary magmatism of the Tyrrhenian region: Characterization of the
1033 magma sources and its geodynamic implications. Mem. Soc. Geol. It. 41, 219 – 242.

1034 Serri, G., Innocenti, F., Manetti, P., 1993. Geochemical and petrological evidence of the subduction
1035 of delaminated Adriatic continental lithosphere in the genesis of the Neogene-Quaternary
1036 magmatism of central Italy. Tectonophysics 223, 117 – 147.
1037 doi:http://dx.doi.org/10.1016/0040-1951(93)90161-C

1038 Sethian, J.A., Popovici, A.M., 1999. 3-D travelttime computation using the fast marching method.
1039 Geophysics 64, 516–523. doi:10.1190/1.1444558

1040 Spakman, W., Wortel, R., 2004. A Tomographic View on Western Mediterranean Geodynamics, in:
1041 Cavazza, P.D.W., Roure, D.F., Spakman, P.W., Stampfli, P.G.M., Ziegler, P.P.A. (Eds.),

1042 The TRANSMED Atlas. The Mediterranean Region from Crust to Mantle. Springer Berlin
1043 Heidelberg, pp. 31–52.

1044 Speranza, F., Maniscalco, R., Mattei, M., Di Stefano, A., Butler, R.W.H., Funicello, R., 1999.
1045 Timing and magnitude of rotations in the frontal thrust systems of southwestern Sicily.
1046 *Tectonics* 18, 1178–1197. doi:10.1029/1999TC900029

1047 Speranza, F., Minelli, L., Pignatelli, A., Chiappini, M., 2012. The Ionian Sea: The oldest in situ
1048 ocean fragment of the world? *J. Geophys. Res.* 117, B12101. doi:10.1029/2012JB009475

1049 Srivastava, S.P., Roest, W.R., Kovacs, L.C., Oakey, G., Lévesque, S., Verhoef, J., Macnab, R.,
1050 1990. Alpine Evolution of Iberia and its Continental Margins Motion of Iberia since the Late
1051 Jurassic: Results from detailed aeromagnetic measurements in the Newfoundland Basin.
1052 *Tectonophysics* 184, 229 – 260. doi:http://dx.doi.org/10.1016/0040-1951

1053 Stampfli, G.M., Borel, G.D., 2002. A plate tectonic model for the Paleozoic and Mesozoic
1054 constrained by dynamic plate boundaries and restored synthetic oceanic isochrons. *Earth and*
1055 *Planetary Science Letters* 196, 17–33. doi:10.1016/S0012-821X(01)00588-X

1056 Stich, D., R. Martin, and J. Morales (2010), Moment tensor inversion for Iberia–Maghreb
1057 earthquakes 2005–2008, *Tectonophysics.*, 483, 390-398

1058 Stich, D., Serpelloni, E., de Lis Mancilla, F., Morales, J., 2006. Kinematics of the Iberia–Maghreb
1059 plate contact from seismic moment tensors and GPS observations. *Tectonophysics* 426,
1060 295–317. doi:10.1016/j.tecto.2006.08.004

1061 Thurner, S. Palomeras, I., Levander, A., Carbonell, R., Lee, C. T., 2014. Ongoing lithospheric
1062 removal in the Western Mediterranean: Ps receiver function results from the PICASSO
1063 project. *Geochem. Geophys. Geosyst.* 15, 1113–1127.

1064 Tortorici, L., Monaco, C., Tansi, C., Cocina, O., 1995. Recent and active tectonics in the Calabrian
1065 arc (Southern Italy). *Tectonophysics, Kinematics of distributed deformation in plate*
1066 *boundary zones with emphasis on the Mediterranean, Anatolia and Eastern Asia* 243, 37–55.
1067 doi:10.1016/0040-1951(94)00190-K

1068 van Hinsbergen, D.J.J., Vissers, R.L.M., Spakman, W., 2014. Origin and consequences of western
1069 Mediterranean subduction, rollback, and slab segmentation. *Tectonics* 33, 2013TC003349.
1070 doi:10.1002/2013TC003349

1071 Vannucci, G., Pondrelli, S., Argnani, A., Morelli, A., Gasperini, P., Boschi, E., 2004. An atlas of
1072 Mediterranean seismicity. *Ann. Geophys.* 47. doi:10.4401/ag-3276

1073 Vergés, J., Fernández, M., 2012. Tethys–Atlantic interaction along the Iberia–Africa plate
1074 boundary: The Betic–Rif orogenic system. *Tectonophysics, Orogenic processes and*
1075 *structural heritage in Alpine-type mountain belts.* *Tectonophysics* 579, 144–172.
1076 doi:10.1016/j.tecto.2012.08.032.

1077 Villaseñor, A., Chevrot, S., Harnafi, M., Gallart, J., Pazos, A., Serrano, I., Córdoba, D., Pulgar, J.
1078 A., Ibarra, P., 2015. Subduction and volcanism in the Iberia-North Africa collision zone
1079 from tomographic images of the upper mantle. *Tectonophysics* 663, 238-249,
1080 doi:10.1016/j.tecto.2015.08.042.

1081 Vissers, R.L.M., Meijer, P. Th, 2012. Iberian plate kinematics and Alpine collision in the Pyrenees.
1082 *Earth Science Reviews* 114, 61e83, doi: 10.1016/j.earscirev.2012.05.001

1083 Watts, A.B., Platt, J.P., Buhl, P., 1993. Tectonic evolution of the Alboran Sea basin. *Basin Research*
1084 5, 153–177.

1085 Westaway, R., 1993. Quaternary uplift of southern Italy. *J. Geophys. Res.* 98, 21741–21772.
1086 doi:10.1029/93JB01566.

1087 Wessel, P., and W. H. Smith (1991), Free software helps map and display
1088 data, *Eos Trans. AGU*, 72(41), 441.

1089 Wildi, W., 1983. La Chaîne tello-rifaine (Algérie, Maroc, Tunisie): structure, stratigraphie et
1090 évolution du trias au miocène *Rev. Geol. Dyn. Geogr. Phys.*, 24, 201-297.

1091 Wortel, M.J.R., Spakman, W., 2000. Subduction and Slab Detachment in the Mediterranean-
1092 Carpathian Region. *Science* 290, 1910–1917. doi:10.1126/science.290.5498.1910

1093 Wortel, M.J.R., Spakman, W., 1992. Structure and dynamics of subducted lithosphere in the
1094 Mediterranean region. *Proc. Kon. Ned. Acad. Wetensch* 95, 325 – 347.

1095 Zeck, H.P., 1996. Betic-Rif orogeny: subduction of Mesozoic Tethys lithosphere under eastward
1096 drifting Iberia, slab detachment shortly before 22 Ma, and subsequent uplift and extensional
1097 tectonics. *Tectonophysics* 254, 1–16. doi:10.1016/0040-1951(95)00206-5

1098 Zitellini, N., Gràcia, E., Matias, L., Terrinha, P., Abreu, M.A., DeAlteriis, G., Henriot, J.P.,
1099 Dañobeitia, J.J., Masson, D.G., Mulder, T., Ramella, R., Somoza, L., Diez, S., 2009. The
1100 quest for the Africa–Eurasia plate boundary west of the Strait of Gibraltar. *Earth and*
1101 *Planetary Science Letters* 280, 13–50. doi:10.1016/j.epsl.2008.12.005

Figure 1

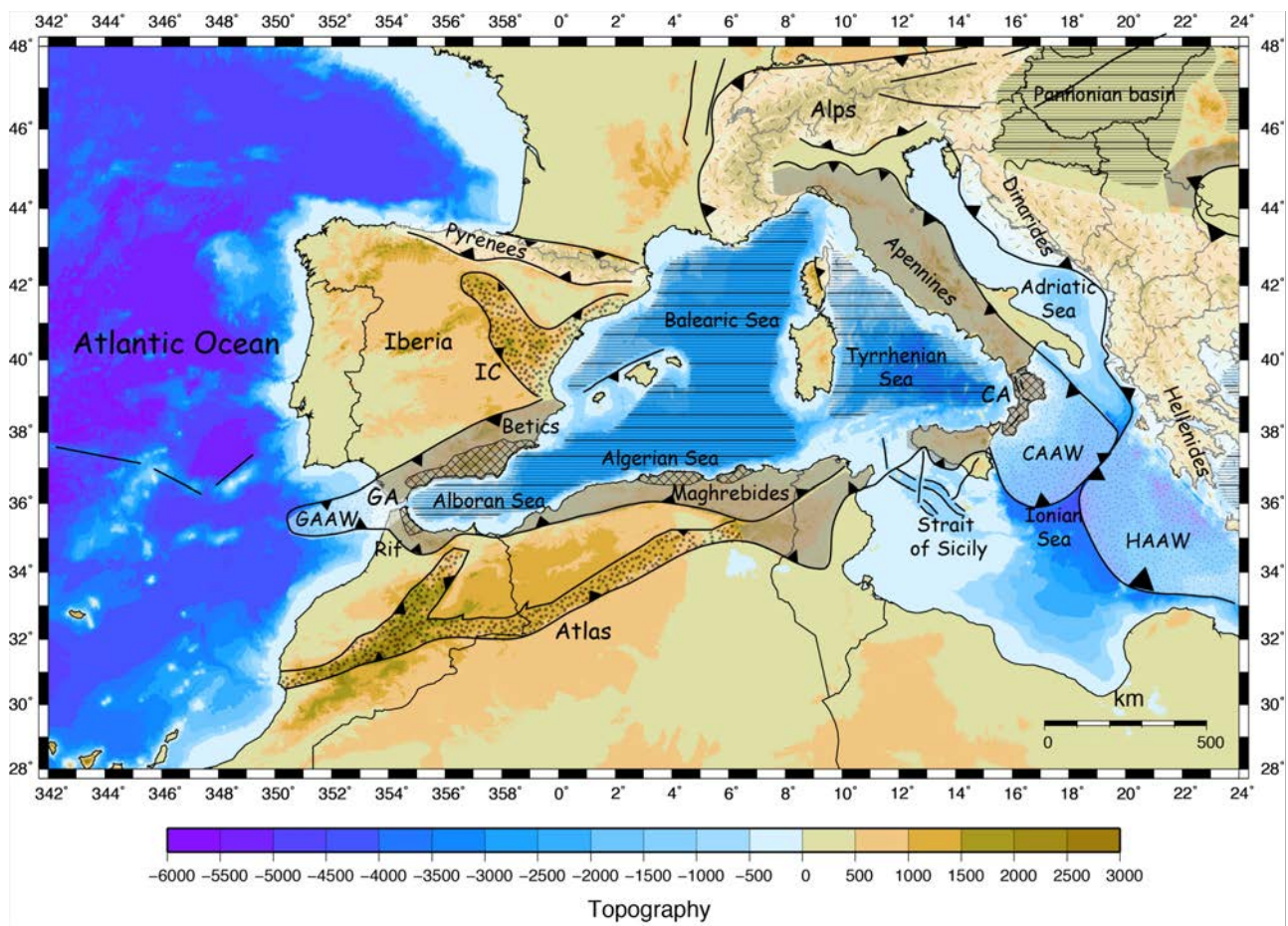


Fig. 1. Simplified geological map of the CWM region. The system of fold-and-thrust belts, indicated in gray, formed from Late Oligocene to Pliocene, during the opening of the backarc basins (horizontal rules; also including the volcanic arcs). The accretionary wedges related to oceanic subduction are indicated with fine dots (GAAW: Gibraltar Arc Accretionary Wedge; CAAW: Calabrian Arc Accretionary Wedge; HAAW: Hellenic Arc Accretionary Wedge). The units belonging to the internal domain are shown with cross hatching. The collisional belts are indicated with random dashes, whereas the Atlas and Iberian Chain (IC) intracontinental belts are indicated with coarse dots. BF: Bradanic foredeep basin; GCF: Gela-Catania foredeep basin.

Figure 2a

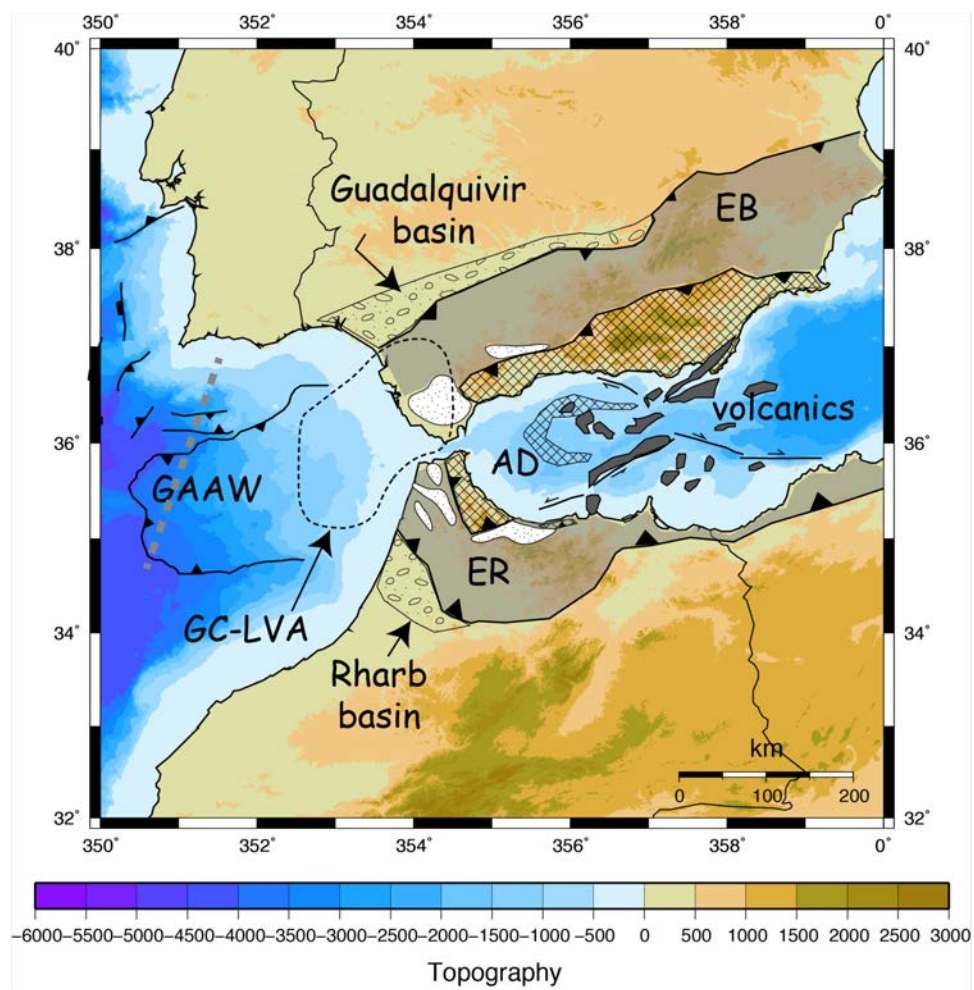


Figure 2b

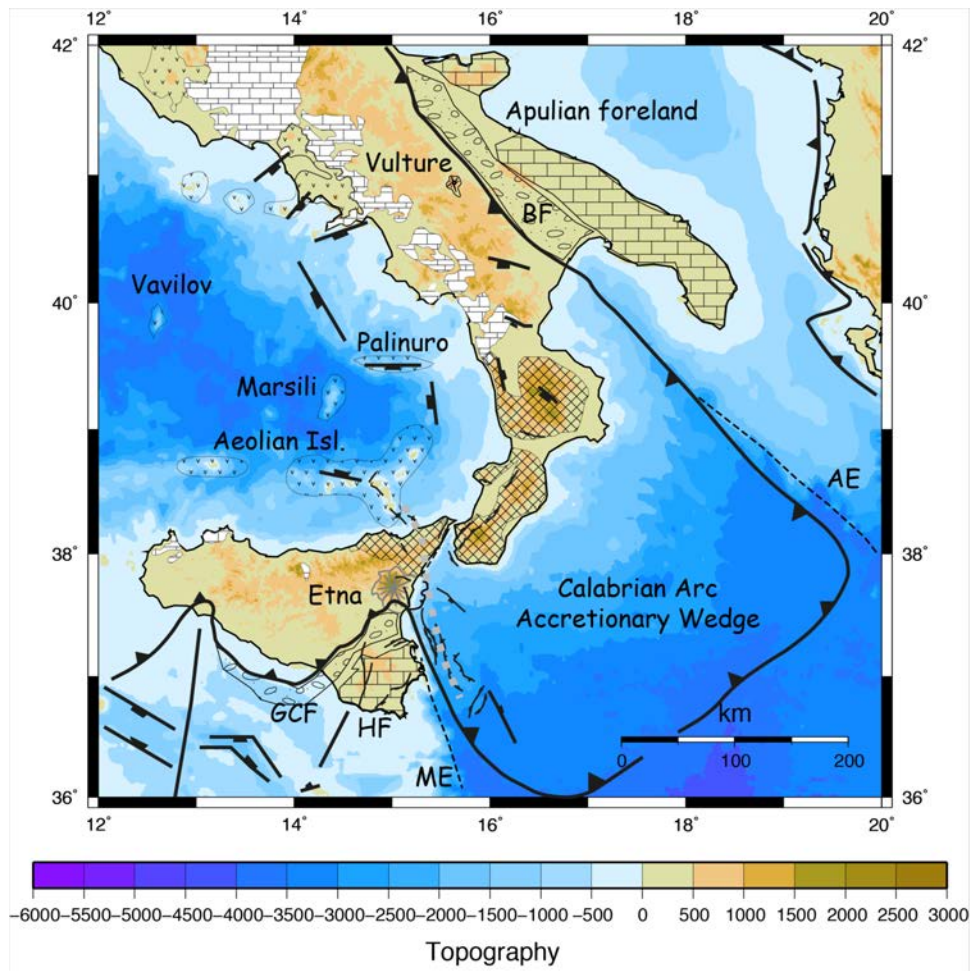


Fig. 2 Simplified geological maps of the two study regions. **a)** Gibraltar-Alboran region (after Alvarez-Marron, 1999; Platt et al., 2013; Gutscher et al., 2012; Duarte et al., 2013). The Alboran Domain (AD), that includes the Internal Betics and Internal Rif, is indicated by cross hatched pattern. The External Betics (EB in gray pattern) includes the Subbetic and Prebetic, and the External Rif (ER in gray pattern) includes the Intrarif and Mesorif. The white field with dotted pattern represents the Flysch belt, and the volcanics are indicated in dark gray. GAAW: Gibraltar Arc Accretionary Wedge; GC-LVA: approximate location of the low-velocity anomaly (from 100 to 200 km depth). Trace of seismic refraction profile (Sallares et al., 2011) indicated by thick gray dashed line. (After Monna et al., 2015).

Calabrian Arc-Southern Tyrrhenian region (after Bigi et al., 1990; Argnani, 2005). The outcrops of Apulian and Hyblean (HF) foreland are indicated with large brick pattern, whereas the carbonate

units encased within basinal units of the Southern Apennines-Maghrebides are indicated as white fields with brick pattern. The conglomerate pattern indicates the Bradanic (BF) and Gela-Catania (GCF) foreland basins. The mostly crystalline units of the Calabrian Arc are shown with cross hatching. The V pattern indicates Pliocene-Quaternary volcanics, including the Campania Magmatic Province. The Malta and Apulia Escarpments (ME and AE, respectively) are also indicated with a dashed line. The thick, gray dashed line offshore eastern Sicily marks the approximate location of the incipient lithospheric tear (after Argnani, 2009).

Figure 3

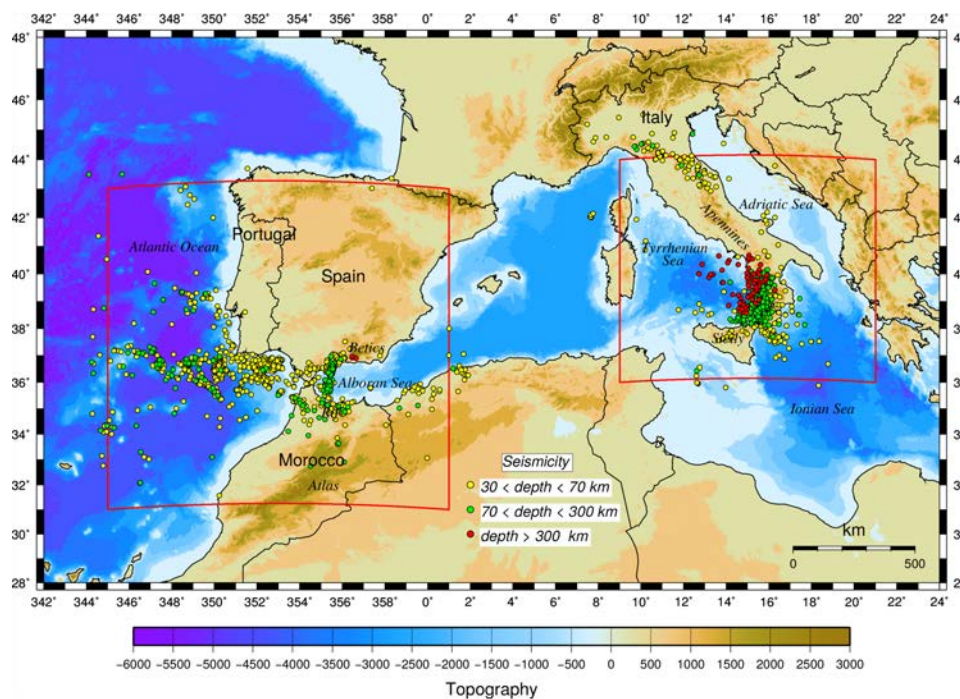


Fig. 3. Map of the CWM region with the two study areas. Colored circles show the sub-crustal seismicity ($M \geq 3$) which occurred in the years 1990-2013. Hypocentral parameters from IGN catalogue and INGV bulletins. Topography/bathymetric profiles are from the Global-Integrated-Topo/Bathymetry Grid (GINA) (Lindquist et al., 2004).

Figure 4

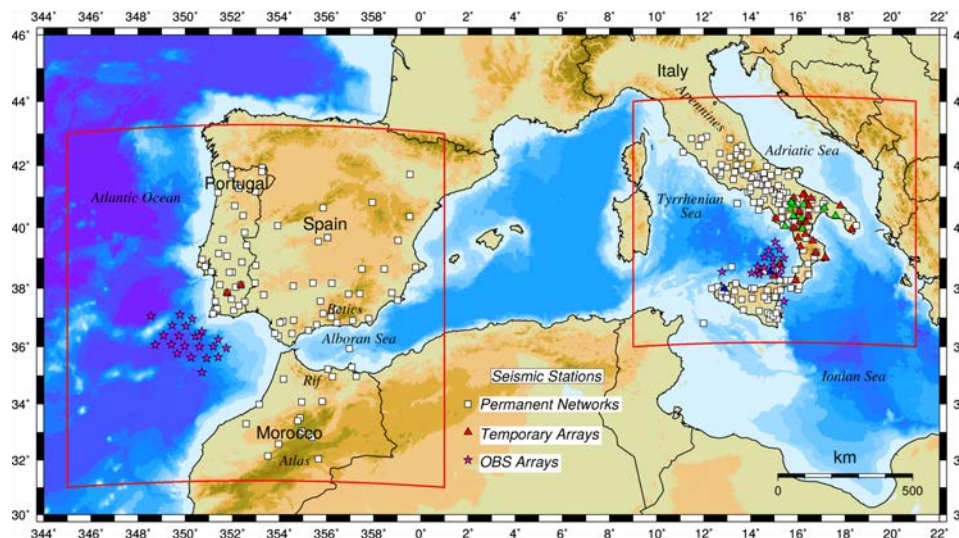


Fig. 4. Map of the seismic stations used in the two tomographic inversions. The OBS array in the Gulf of Cadiz was deployed during the NEAREST project (<http://nearest.bo.ismar.cnr.it>). The OBS in the Southern Tyrrhenian were deployed during the TYDE (Dahm et al., 2002) and SN1 (Monna et al., 2005) experiments. The temporary land arrays were deployed in Southern Italy during the SAPTEX (red triangles) (Cimini et al., 2006) and SeSCAL (green triangles) (Frepoli et al., 2011) experiments.

Figure 5

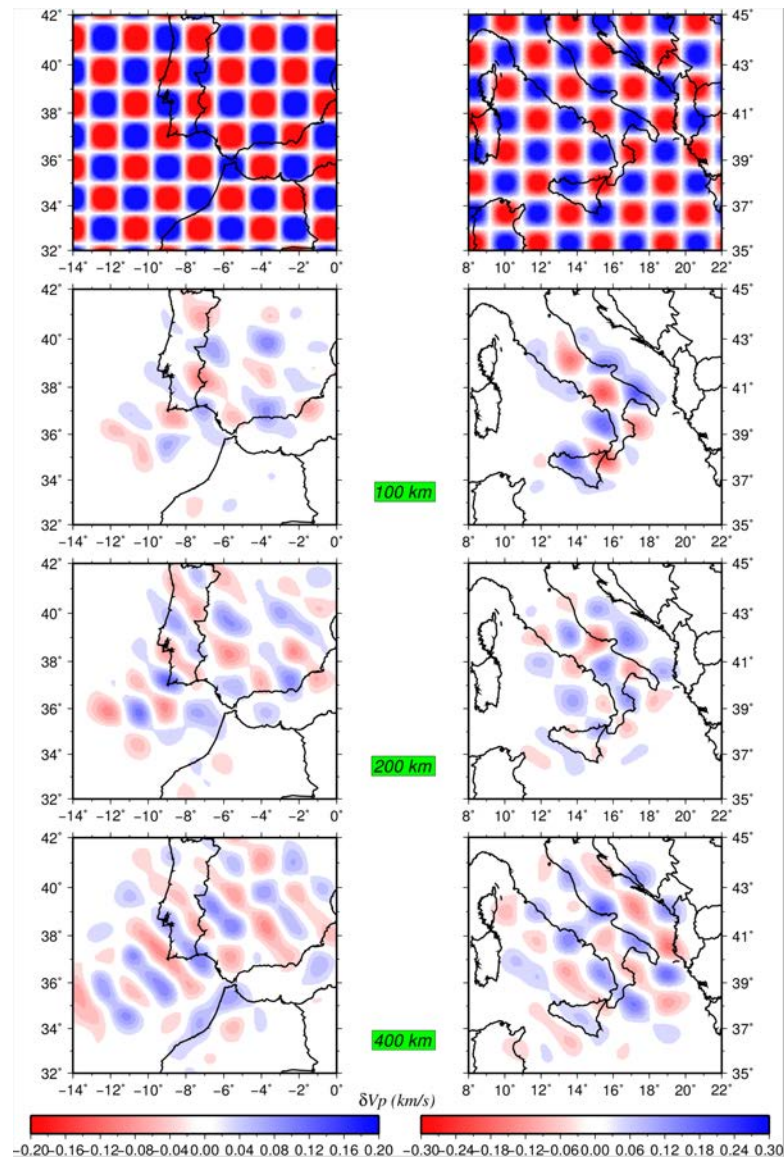


Fig. 5. Results of the checkerboard resolution test for three depth slices of the two tomographic models. Left panels are for the GA model, right panels for the CA model. Panels at the top are the input checkerboard velocity models. These patterns consist of alternating 100x100 km cells of fast and slow anomalies varying in latitude, longitude, and depth. The recovered patterns show wide areas of good resolution for both the models. The synthetic data sets, based on the source-receiver geometries of the GA and CA teleseismic inversions, include gaussian noise with standard deviations of 0.15s and 0.50s, respectively for picked and bulletin data.

Figure 6.

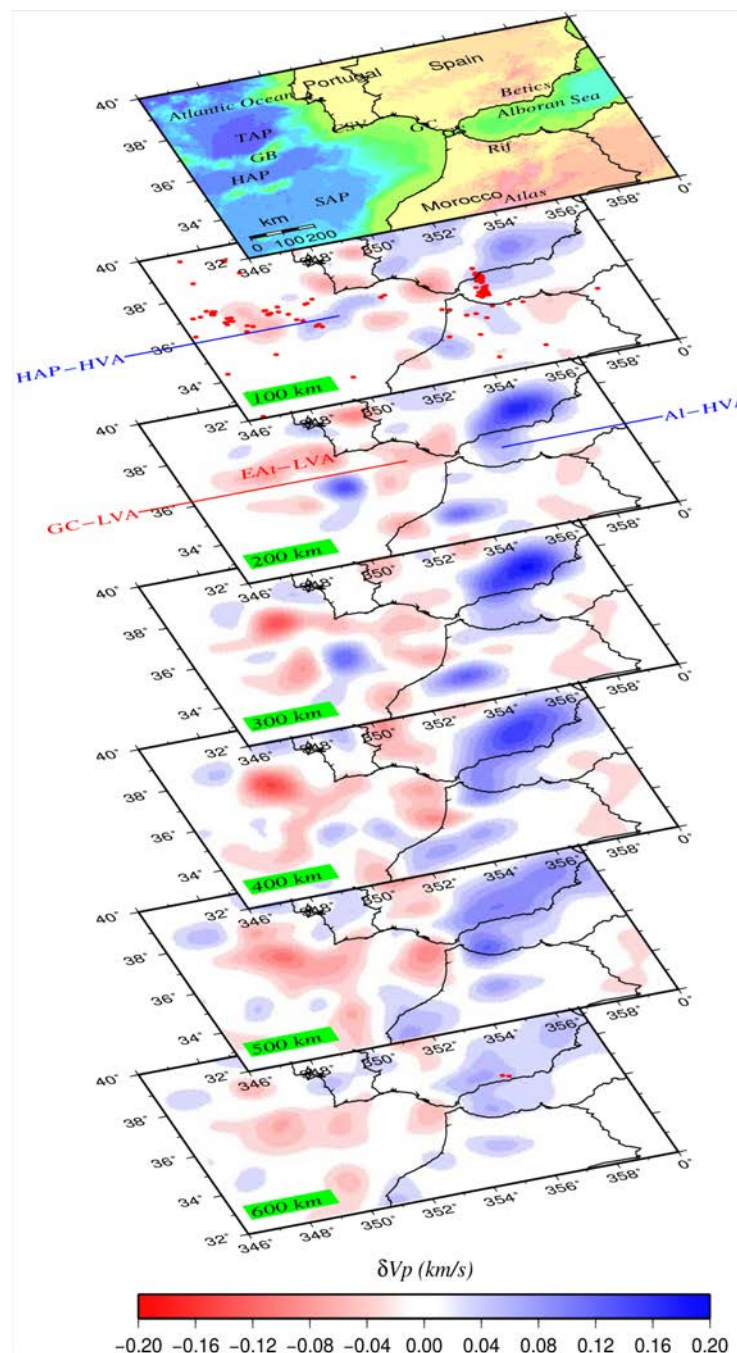


Fig. 6. Perspective view showing a series of horizontal slices extracted from the GA velocity model at depth intervals of 100 km. Blue colored areas indicate high velocity anomalies, present in the Betic-Alboran region (AI-HVA) and in the Atlantic SW Portugal (HAP-HVA). Red colored areas are zones of low velocity anomalies in the Eastern Atlantic (EAt-LVA) and the Gulf of Cadiz (GC-LVA). (After Monna et al., 2015).

Figure7

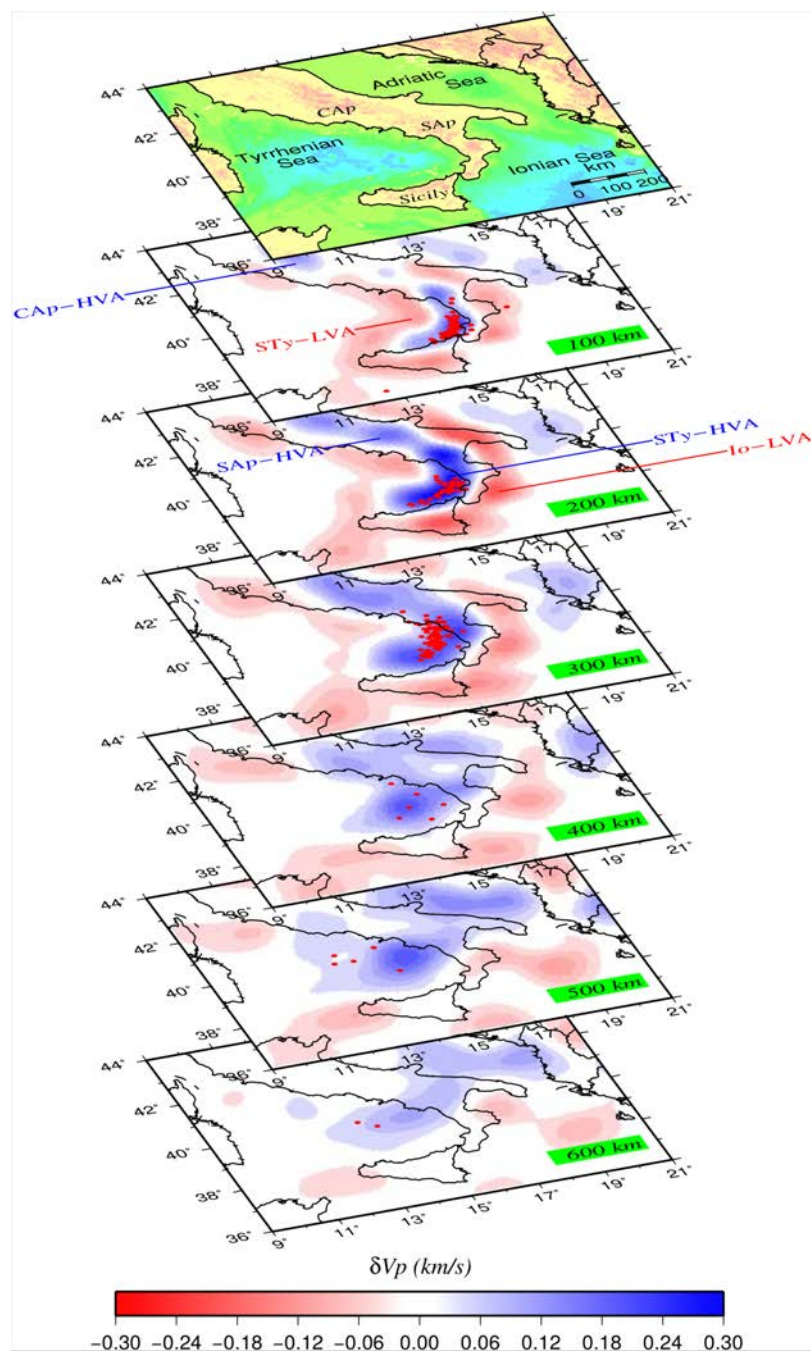


Fig. 7. Perspective view showing a series of horizontal slices extracted from the CA velocity model at depth intervals of 100 km. As in Fig. 6, blue colored areas indicate high velocity anomalies, present in the Southern Tyrrhenian region (STyHVA) and in the Southern Apennines (SAP-HVA). Red colored areas are zones of low velocity anomalies in the Tyrrhenian Sea (STy-LVA) and the Ionian Sea (Io-LVA).

Figure 8

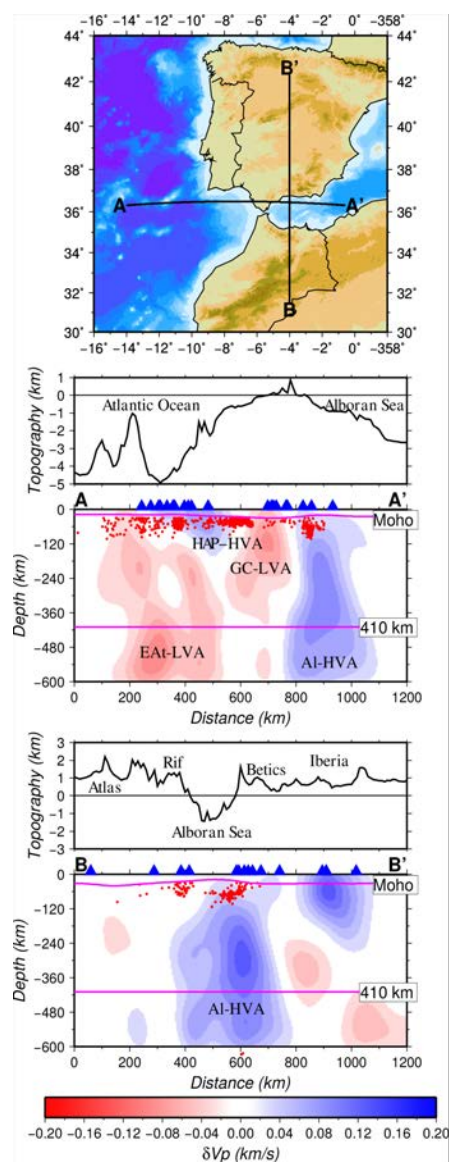


Fig. 8. Vertical slices displaying the velocity anomalies of the GA model along a west to east profile crossing the Gibraltar Arc (AA'), and along a south to north profile crossing the Alboran Sea (BB'). SAP = Seine Abyssal Plain; HAP = Horseshoe Abyssal Plain; TAP = Tagus Abyssal Plain. High velocity anomalies: Al-HVA=Betic-Alboran; HAP-HVA=Horseshoe Abyssal Plane. Low velocity anomalies: GC-LVA=Gulf of Cadiz; EAt-LVA=Eastern Atlantic. Blue triangles indicate the seismic stations and red dots the subcrustal seismicity, located within a 100 km wide zone centered on the profile. In profile BB', hypocenters deeper than 600 km represent the deep events below the Granada region. Moho topography is from the European Moho depth map (Grad et al., 2009). (After Monna et al., 2013a).

Figure9

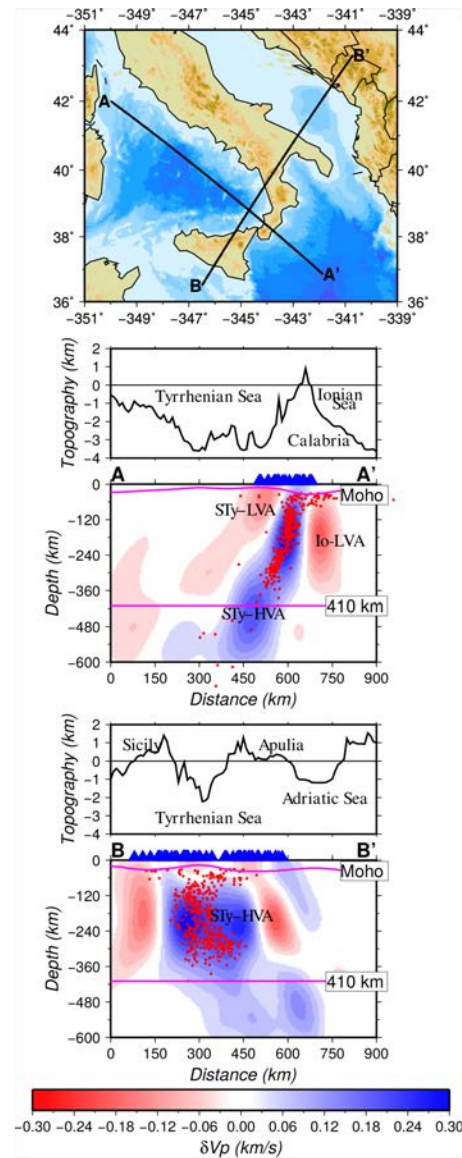


Fig. 9. Vertical slices displaying the velocity anomalies of the CA model along a northwest to southeast profile crossing the Calabrian Arc (AA'), and along a southwest-northeast profile crossing the southern Tyrrhenian basin (BB'). CAp = Central Apennines; SAp = Southern Apennines. High velocity anomalies: STy-HVA=Southern Tyrrhenian. Low velocity anomaly: STy-LVA=Southern Tyrrhenian. Blue triangles and red dots indicate the seismic stations and the subcrustal seismicity located within a 100 km wide zone centered on the profile. Moho topography is from the European Moho depth map (Grad et al., 2009).

Figure10

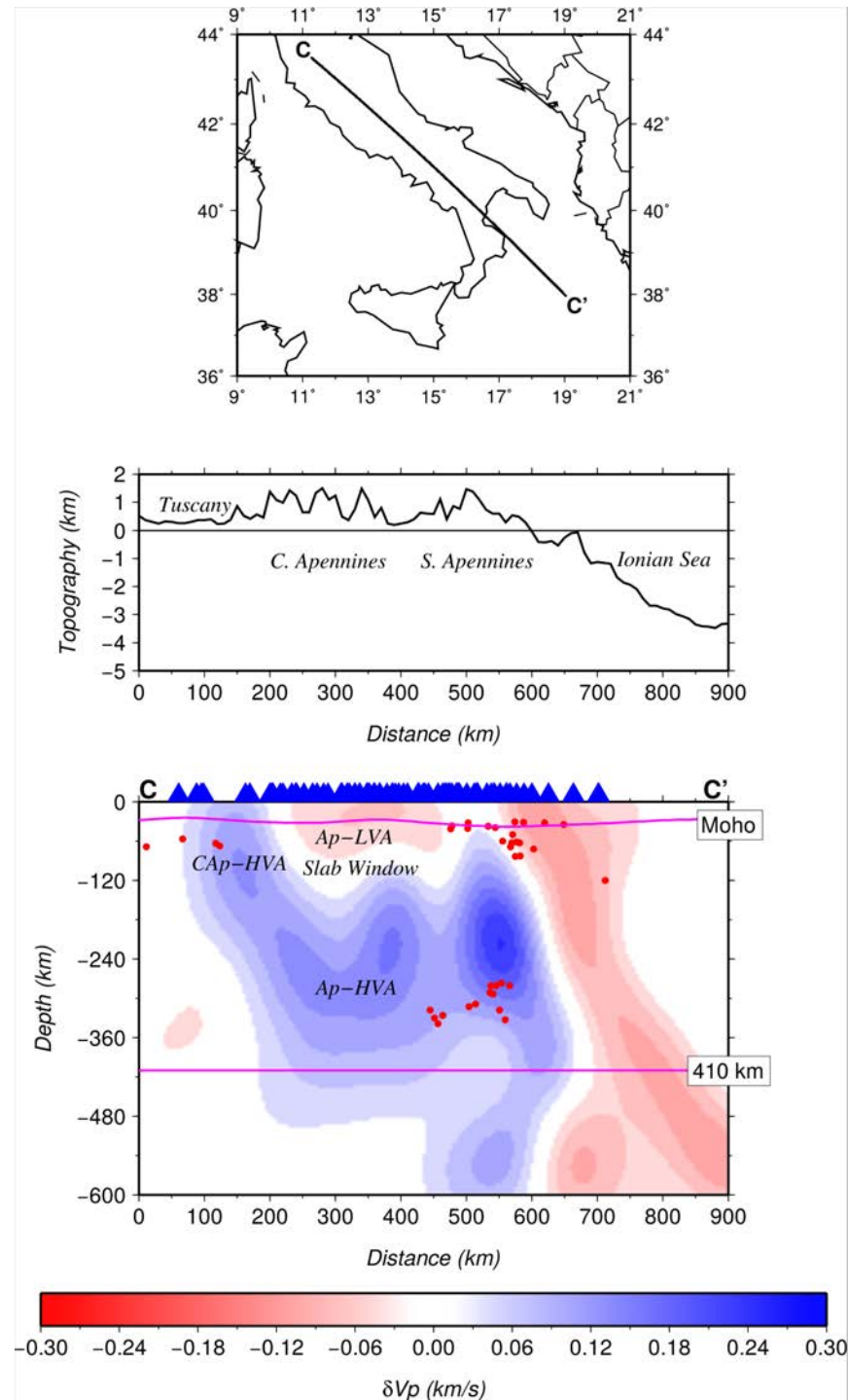


Fig. 10. Vertical slice displaying the velocity anomalies of the CA model along a northwest to southeast profile crossing the Southern Apennines (CC'). The trace and topographic profile are shown in the top and middle panels, respectively. A well defined slab window underneath the Southern Apennines is visible (lower panel). High velocity anomalies: CAp-HVA=Central Apennines; Ap-HVA=Apennines. Low velocity anomaly: Ap-LVA=Apennines-slab window.

Figure11

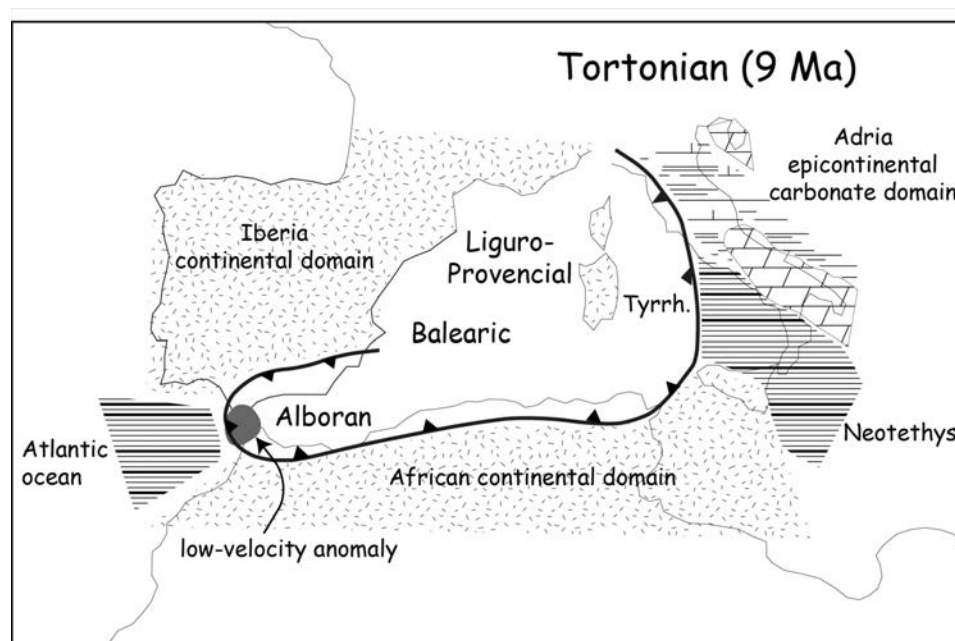


Fig. 11. Simplified tectonic reconstruction of the Mediterranean in Tortonian time. The African and Italian coasts are positioned with respect to stable Europe. Note that the Gibraltar arc was almost completely formed, whereas the Calabrian arc was still to be defined. During the Pliocene-Pleistocene the subduction and rollback of the narrow Neotethyan branch shaped the final arcuature of the Calabrian arc. The segment of African continental margin imaged just offshore Gibraltar (LVA, low-velocity anomaly) likely prevented any further development of the Gibraltar arc, favouring slab breakoff.

Figure12

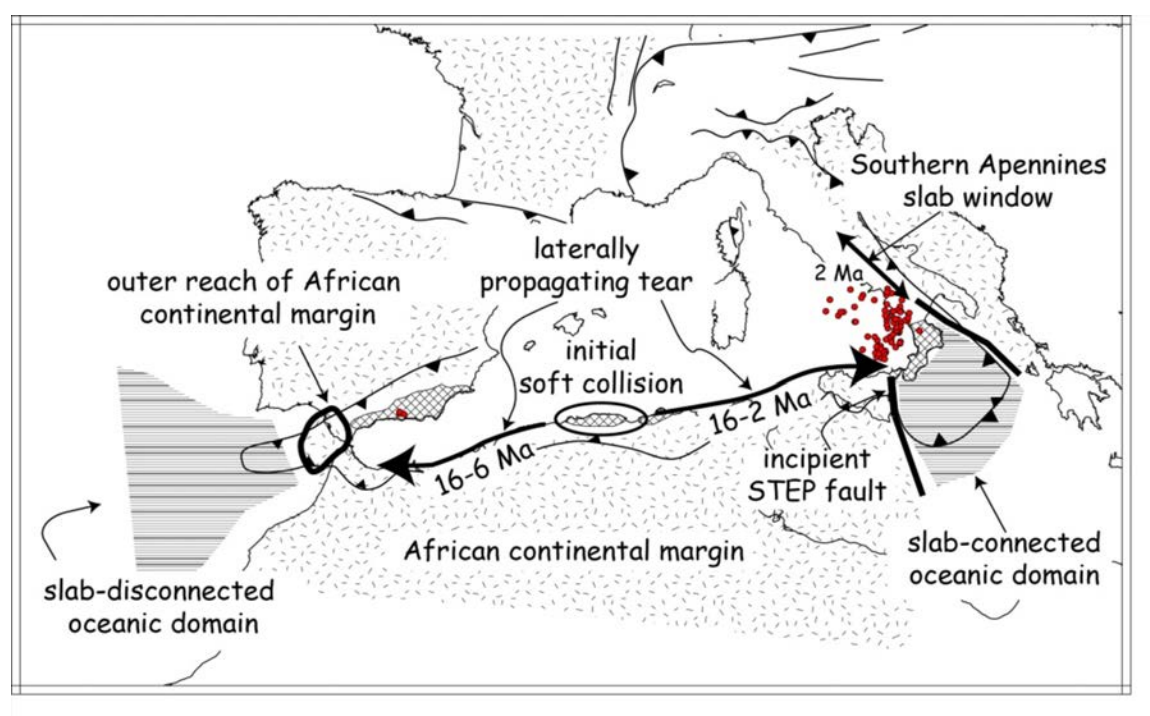


Fig. 12. Interpretation of the evolution of the CWM subduction system highlighting the main features which controlled arc formation. Slab tearing propagated laterally along the north African continental margin, following the initial soft collision in Algeria (ca. 16 Ma). Arc formation proceeded on either side, driven by slab sinking and trench retreat, but slab retreat was impeded in its westward motion by the segment of thinned continental margin imaged by the GA tomography underneath Gibraltar (GC-LVA). The eastward progression of arc formation, on the other hand, continued until very recently, with the opening of the Tyrrhenian basin, driven by the sinking Ionian slab. In its final stage the sinking also promoted the formation of a slab window underneath the Southern Apennines, which is responsible for the magmatism of the Campania Magmatic Province (Serri, 1990). Dots represent deep (depth > 300 km) $M \geq 3$ seismicity.